IMPACT OF HIGH PENETRATION OF PHOTOVOLTAICS ON LOW VOLTAGE SYSTEMS AND REMEDIAL ACTIONS

Reinaldo Tonkoski

A Thesis

In the Department

of

Electrical and Computer Engineering

Presented in Partial Fulfillment of the Requirements

for the Degree of

Doctor of Philosophy (Electrical and Computer Engineering) at

Concordia University

Montreal, Quebec, Canada

September 2011

CONCORDIA UNIVERSITY
SCHOOL OF GRADUATE STUDIES

This is to certify that the thesis prepared

By: Reinaldo Tonkoski

Entitled: Impact of High Penetration of Photovoltaics on Low Voltage Systems and Remedial Actions

and submitted in partial fulfillment of the requirements for the degree of

Doctor of Philosophy (Electrical and Computer Engineering)

complies with the regulations of the University and meets the accepted standards with respect to originality and quality.

Signed by the final examining committee:

Dr. C. Constantinides Chair

Dr. L. Chang External Examiner

Dr. A. Athienitis External to Program

Dr. A. G. Aghdam Examiner

Dr. S. Williamson Examiner

Dr. L. A. C. Lopes Thesis Supervisor

Approved by

Dr. W. E. Lynch
Chair of Department or Graduate Program Director

Date:_____ Dr. Robin A. L. Drew
Dean, Faculty of Engineering and Computer Science

ABSTRACT

Impact of High Penetration of Photovoltaics on Low Voltage Systems and Remedial Actions

Reinaldo Tonkoski, Ph.D.

Concordia University, 2011

Residential rooftop photovoltaics (PV) systems have great potential to supply part of the growing energy demand. However, its non-dispatchable, fluctuating, and intermittent characteristics may negatively impact the power quality and reliability (PQR) of low voltage (LV) distribution feeders. Large amounts of non-dispatchable PV sources, if integrated in a distributed way, can reverse the power flow in the feeder and lead to overvoltages. In diesel-based autonomous systems with high-penetration of PVs, the reduction in net load can significantly increase the wear and tear on the diesel genset(s). Therefore, connection of only a modest amount of PV is currently allowed at the LV level without a prior impact-assessment study.

This thesis focuses on the detrimental impact of high penetration of PVs on LV systems and on the remedial actions that can be taken to increase PQR and the displacement of fossil fuels in diesel-based autonomous systems. Two scenarios are considered.

First is the possibility of overvoltages in LV grid connected systems during periods of high PV generation and low load. The solutions used in medium-voltage feeders need to be revisited in light of the mostly resistive characteristics of LV feeders. An alternative is to use active power curtailment (APC) techniques. A droop-based APC approach, in

which all inverters use the same droop coefficients, is analyzed. However, this strategy results in more APC in the PV inverters located near the end of the feeder than in the ones in the beginning. A new approach is proposed that allows equal sharing of the APC. A one-year simulation study assessed the overvoltage occurrences, the sharing of the burden for overvoltage prevention per house, and the total energy yield of the feeder using a benchmark based on typical parameters of Canadian LV feeders.

The second scenario involves the impact of high-penetration PV systems in diesel-based autonomous LV systems, which are typical of remote communities. The use of APC of PV inverters is discussed, focusing on reducing the frequency variations and ensuring the diesel genset's minimum load, and can improve fuel consumption. This theoretical analysis is validated by simulations. Fuel consumption and yearly energy yields are estimated using statistical information about the load and solar irradiation.

ACKNOWLEDGMENTS

I would like to thank my supervisor Dr. Luiz Lopes for his trust and unconditional support during these five years. This work would not have been possible without his support and encouragement. I appreciate his critical thinking, amazing scientific knowledge, but essentially his extraordinary precision. I consider myself privileged to have been able to benefit from such training. Our discussions enabled me to develop my critical thinking and my analysis capacity. He has been an essential influence in my career.

During this period with the Power Electronics and Energy Research (PEER) team at Concordia University, I have learned a lot and I was lucky to work in a friendly and pleasant environment, which is very special. I am grateful to my colleagues and friends from the PEER group: Mr. Joseph Woods, Mr. Arbi Gharakhani, Mr. Khalid Elamari, Mr. Miguel Torres, Mr. Natheer Alatawneh, Mr. Nayeem Ahmed Ninad, Mr. Olivare Dzune Mipoung, Mrs. Rachel Namuli, Mr. Manu Jain, Mr. Nathan Curry, Mr. Peng Zhang, and Dr. Maged Fouad Barsom.

I thank professors Pragasen Pillay and Sheldon Williamson for allowing me to participate in a variety of activities during these five years in the Ph.D. program.

I am thankful to Dr. Lisa Dignard-Bailey, Dr. Tarek EL-Fouly, Mr. Dave Turcotte, Mr. David Beauvais and Mr. Jean-Claude Deslauriers from CanmetENERGY, Natural Resources Canada, for the opportunity to work with the Grid Integration of Renewable and Distributed Energy Resources team and for sharing valuable information with me.

I would like to thank the Government of Canada, through the Program on Energy Research and Development (PERD) and the Solar Buildings Research Network under the Strategic Network Grants Program of the Natural Sciences and Engineering Research Council (NSERC) of Canada, for the financial support that they provided for my studies.

Finally, my very special thanks go to my wife, Patricia Da Rosa, and her family. She always gave me words of encouragement and strong support from beginning to end. Her patience and friendship were always present even in the most difficult moments.

I would also like to thank my father, Reinaldo Tonkoski and my mother, Zuleica Tonkoski. I cannot end without thanking my trustful friends: Everton Luis, Ana Clara, and Amanda.

TABLE OF CONTENTS

LIST OF FIGURES

1. Introduction

2. Voltage Regulation in Radial Distribution Feeders with High-penetration of Distributed Generation

3. APC of Grid Connected PV Inverters for Overvoltage Prevention

4. Active Power Curtailment of PV Inverters in Diesel Hybrid Mini-grids

LIST OF TABLES

NOMENCLATURE

APC	Active Power Curtailment
APC-OPLS	Active Power Curtailment with Output Power Losses Sharing
DER	Distributed Energy Resource
DG	Distributed Generation
LDNO	Local Distribution Network Operator
LV	Low Voltage
MPPT	Maximum Power Point Tracking
MV	Medium Voltage
PCC	Point of Common Coupling
PQR	Power Quality and Reliability
PV	Photovoltaic
RET	Renewable Energy Technology
UPF	Unity Power Factor

LIST OF SYMBOLS

f	Electrical frequency
f_c	Center frequency of the droop function
f_{cri}	Frequency above which the power injected by the inverter is decreased with a droop factor
f_{nl}	No-load frequency of the generator
$K = R/X$	Feeder's resistance-reactance ratio or impedance characteristic
L	Feeder losses
m	Slope factor of the droop function
m_{EWH}	Slope factor of the electric water heater droop function
P	Active power
p	Number of poles of the synchronous machine
P_{gen}	Output power of the generator
P_{inv}	Active power injected by the inverter
P_{load}	Load active power consumption

P_{MPPT}	Maximum power available in the PV array for a given solar irradiance
$P_{pv\,max}$	Maximum power available from the PV system
P_{PVcap}	PV power capacity
Q	Reactive power
R	Resistance of the feeder
S_L	Loss sensitivity matrix
s_P	Slope of the generator's droop curve
S_V	Sensitivity matrix
Td	Reference temperature for the electric water heater
Td_b	Base set point temperature
T_H	Temperature of water in tank
V	Voltage at a certain bus
$V_{Ci/i+1}$	Voltage at each bus after curtailment
V_{cri}	Voltage above which the power injected by the inverter is decreased with a droop factor

$V_{i/i+1}$	The voltage in the bus $i/i+1$ without curtailment
Wd	Water draw for the electrical water heater
X	Reactance of the feeder
Z_L	Line impedance
δ	Voltage angle
ΔV	Voltage rise at the end of the line with respect to that in the beginning of the feeder
ω	Shaft speed of a synchronous machine

1. INTRODUCTION

The modernization of the utility grid gained worldwide media attention after US President Barack Obama signed a $787 billion stimulus bill in 2009, with the largest single investment in smart grid technology [1]. Essentially, investments in smart grids are being justified by governments as a way to provide a broader use of alternative/renewable energy and a better use of the available resources. Due to generation resource availability and economic barriers, most major production centers are built far from large centers of consumption, which necessitates the transport energy over long distances, in turn reducing system efficiency and reliability. Typically, 20% of the generation capacity is used only to meet peak demand that occurs only 5% of the time, and almost 8% of the generation output is lost along transmission lines [2]. In addition, the actual electricity grid is mostly unidirectional [2], which means that it was designed based on the fact that power would flow downstream from the large power plants to the consumers. However, if large amounts of renewable energy sources are now integrated in a distributed way, power may begin to flow upstream (reverse power flow) in some sections of the feeder. With today's technologies, power quality and reliability (PQR) cannot be ensured, given this scenario of a large amount of non-dispatchable renewable energy technologies.

The utilization of distributed energy sources supports the idea of having a smart self-healing grid that would be able to respond to a number of failures (due to diverse factors such as meteorological conditions and acts of terror) and still keep parts of the system running, adaptively creating islands with balanced generation and load.

Microgrids are locally controlled clusters of distributed energy sources that behave, from the grid's perspective, as single producers or loads (both electrically) that are also capable of islanding. They are semi-autonomous systems that use local generation and, sometimes, storage, and they can operate tied to a central grid or not [3, 4]. Microgrids allow the integration of high levels of distributed and renewable generation sources into the grid and increase grid reliability and power quality, as they provide backup power in case of failures in the main grid.

The impact of microgrid technology can be even more significant for stand-alone systems, which are a potential large market for renewable energy sources. For instance, more than 200,000 Canadians live in Canada's 310 remote communities [5]. These communities are not connected to the main electricity grid and usually depend on oil from the south for heating and electricity. Energy supply in these communities is thus characterized by high costs and a high degree of dependence on fossil fuels. Most communities rely on diesel generators for electricity production, at costs that vary between $0.15 and $1.50 per kWh. Given these prices, several renewable energy technologies (RETs) such as photovoltaic (PV) and wind would be cost effective in meeting part of the energy needs in many remote communities.

These local electricity networks that operate autonomously from the main grid are usually called mini-grids [6]. Many mini-grids are designed with a future expansion of the distribution system in mind that would allow the system to be connected to the main grid. In these remote communities, interconnected microgrids would be an important asset to improve reliability. This is because maintenance is costly and not immediately available in these areas, as technical resources are not concentrated there.

Given these facts, RETs will play an important role in supporting the stand-alone operation of microgrid systems and in supplying the growing demand for energy. Residential rooftop PV systems have a great potential to help fill this need; however, the benefits do not come without challenges.

The typical maximum capacity of residential rooftop PV systems is between 5 kW and 10 kW, and they are connected at low-voltage (LV) distribution feeders. These systems can usually be installed without the impact-assessment study that is required for larger units. During high PV generation and low load periods, the possibility exists for reverse power flow, and consequently voltage rise, in the LV feeder [7-14]. This is a serious issue, because protection equipment can trip sources and loads during large variations of voltage and frequency. As a result, relatively modest amounts of PV are currently allowed to be connected at the LV distribution level. Any increases in the allowed penetration level of non-dispatchable and stochastic RETs units that can be installed without an impact-assessment study will require new techniques to minimize their impact on the PQR of LV distribution feeders.

This thesis focuses on strategies for the prevention of overvoltages in grid-connected systems and for the part load operation of diesel-dominated mini-grids with LV feeders and high-penetration of PVs. Techniques for increasing a system's PQR, thereby increasing the displacement of energy and fossil fuels and reducing operational costs, are investigated and assessed.

With this aim, a brief background is first provided in this chapter to explain the operational aspects and the main issues related to high-penetration PVs in LV grid-

connected feeders and in diesel-dominated mini-grids. Possible solutions to a number of problems—including load management, power curtailment of non-dispatchable units, and energy-storage units—are discussed. The outline and contributions of this thesis are then presented.

1.1. High-penetration of PV in LV Utility Grid

The use of PV technology is accelerating in Canada. From 2008 to 2009, the installed PV power capacity almost tripled, reaching 94.6 MW in the 2009 Canadian PV status report [15]. A total of 11% of the PV systems installed on 2009 were for residential and building integrated grid-connected applications, with most of this growth fostered by the province of Ontario green energy police. These numbers promise to increase even more as a result of Ontario's successful feed-in tariff programs [16]. For instance, in February 2011, approximately 25,000 applications were submitted for small renewable projects with generating capacity of 10 kW or less, and 99% of these were PV systems. If all of these applications were accepted, suddenly about 234 MW of small PV systems would be connected to Ontario's power network. This brings about several advantages. First, generation of electricity closer to the consumers makes it possible to reduce distribution and transmission system congestion and power losses. This feature can be of pivotal importance for the deployment of electric and plug-in hybrid electric vehicles (EV and PHEV), which will put a significant stress on the transmission and distribution systems. For instance, the annual energy use in the US from electric vehicles could grow from the 146,000 MWh in 2010 to 2.6 million MWh by 2020 [17]. However, supplying this additional load with distributed generation (DG) at the distribution level does not come

without technical challenges. One of the main issues concerns voltage regulation in distribution feeders.

Distribution systems have been designed for many years to operate with unidirectional power flow. From the moment that DG units are integrated into the grid, the power no longer flows only from the distribution transformers to the costumers. In this context, during high generation and low load periods, the possibility of reverse power flow arises; consequently, the voltage at the end of the feeder can be higher than at the substation [7-13], instead of lower, when the DG production is higher than the local load consumption. This can lead to overvoltages in the feeder, and is one of the main reasons for limiting the capacity (active power) of non-dispatchable DG, such as PV, that can be connected to a low voltage (LV) distribution system [9]. For instance, Germany limits the maximum voltage increase to 2% of the rated voltage due to the integration of DGs on LV distribution systems [18].

Residential feeders with PV systems can be considered a critical case regarding overvoltage. The typical load profile of residential feeders presents a peak value during the night period, when there is little or no PV generation. On the other hand, the demand is relatively low when power generation peaks, leading to reverse power flow in the feeder and consequently overvoltage. Conversely, the typical load profiles of commercial and industrial feeders present a good correlation with the typical PV power profile [19], which tends to reduce the likelihood and magnitude of overvoltages for the same ratio of peak load and peak power generation.

1.1.1. Voltage Rise in LV Feeders with High Penetration of PV

CAN CSA C22.2 No. 257-06 [20] specifies the electrical requirements for the interconnection of inverter-based micro-distributed resource systems to LV grids in Canada. This standard recommends using the CSA CAN3-C235 [21] as guidance for appropriate steady-state voltage levels in a distribution system. Based on these standards, for single-phase connection, *normal operating conditions* (NR – Normal Range) occur when the voltage level is within 0.917 pu and 1.042 pu. *Extreme operation conditions* (ER) have steady-state voltage limits of 0.880 pu and 1.058 pu. It is worth mentioning that although networks are allowed to operate under *extreme conditions*, improvement or corrective action should be taken on a planned and programmed basis. In other words, if the voltage at a certain point in the feeder is beyond the NR and within the ER, the utility would need to take a corrective action; however, this action is not urgent. If the voltage is beyond the ER, a corrective action should be taken immediately. In general, the voltage limits established for inverter protection (0.880 pu and 1.1 pu of voltage [22, 23]) are mostly beyond the recommended voltage limits for distribution networks. Thus, the feeder may be experiencing overvoltage while the inverter protection does not reach its threshold value. In addition, CSA CAN3-C235 [21] offers no recommendation regarding whether a certain number of overvoltage occurrences might be acceptable in the feeder. This differs from European standards (i.e., EN 50160) where for 5% of a week occurrences of overvoltages up to a certain magnitude are acceptable.

The LV distribution feeders are conceived to supply a certain load at a certain distance without considering distributed generation. At the planning stage, they are designed to allow a maximum 5% voltage drop from the secondary side of the LV network

transformer to the customer meter. It is a common practice in certain weak feeders to adjust the tap of LV transformers, stepping-up the voltage in order to comply with voltage level requirements under peak load condition. This means that the voltage at the beginning of the feeder may be adjusted to operate at 3-4% above the rated value. This leaves little or no margin for reverse power flow in these feeders.

Another important aspect is that the voltage sensitivity to active power variations is typically higher in LV feeders than in MV feeders. Consider a simple 2-bus system where the voltage rise at the end of the line with respect to that in the beginning of the feeder (ΔV) can be approximated by [24]:

$$\Delta V \approx \frac{PR + QX}{V} \tag{1.1}$$

where P and Q are the active and reactive powers injected by a PV inverter and R and X are the resistance and reactance of the feeder, respectively. LV feeders are characterized as having large resistance-reactance ratios (R/X). This means that active power variations have a large influence in voltage variations in LV feeders. Along with the fact that the load could not necessarily correlate with generation, the main conditions for having overvoltages due to voltage rise caused by non-dispatchable DG units are related to the grid architecture and the load/generation profile.

1.1.1.1. Case Studies Regarding Voltage Rise Due to PV Systems

Several studies were conducted regarding voltage rise in LV distribution system in the presence of PVs [7, 9, 10, 13, 25-28]. Cases where the distribution feeders were conceived to cope with the integration of PV were presented in [7, 13]. Few studies

discuss the impact of PVs in overvoltages on feeders that were already built before considering the integration of PV systems [25, 27]. A simulation study on the impact on the feeder's voltage profile with 216 residences integrating grid-connected PV using typical Canadian feeders parameters is presented in [27]. Overvoltage was found more likely to occur in suburban and rural feeders, as opposed to urban. For instance, in one particular suburban feeder, if more than 2.5 kW per household of PV panels were installed, overvoltages could occur. Feeder impedance, feeder length, and transformer impedance also played important roles in determining the degree of voltage rise for residential feeders with high PV penetration levels.

A detailed US monitoring study investigated a neighborhood of 115 houses with 2 kW of PV for a total capacity of 230 kW connected to a 20 MVA substation [13]. Only a slight voltage rise of approximately 0.6% was observed on clear days, which is expected for a relatively low penetration level.

Several studies have considered urban real estate developments in Germany, Netherlands and France with high-penetration of distributed PV generation [7], with penetration capacity reaching up to 110% of LV transformer capacity (Germany). The voltage level increase in all cases was within the normal range (0.9 and 1.1 pu - EN 50160) according to European standards. However these standards are more relaxed than the North-American ones. The voltage reached about 1.06 pu in Freiburg, Germany and Heerhugowaard, Netherlands and 1.05 pu in Soleil-Marguerite, France. The level of penetration in these sites was significantly higher compared with the US case presented in [13]. However, as already mentioned, in both the US and European reports, the feeders were expected to receive PV systems in the design stage.

A current network in the city of Leicester in the UK, which originally did not include PV resources, was modeled using a stochastic approach and one-minute data information regarding house/load consumption and the solar irradiance data obtained for the region [25]. Overvoltages were found in this feeder in the case that included 1.8 kW PV systems in 50% of the 1262 houses.

1.1.2. Voltage Control Solutions for LV Feeders with High-penetration of PV

This Section discusses the main solutions reported in the literature regarding voltage control that can be applied to LV feeders with high-penetration of non-dispatchable DGs. The choice of the best strategy for prevention of overvoltages for a certain feeder is quite site dependent, as regulations and characteristics may differ from one case to another. In addition, a combination of approaches could be also used to plan for load and generation growth [29].

1.1.2.1. Demand Side Management

In general, a good match between local load and generation can reduce the likelihood and magnitude of overvoltages. A possible approach for reducing overvoltage occurrences in LV residential feeders is the utilization of demand side management. The availability of controllable residential loads that could shift the period of operation to moments of excess power generation can alleviate the overvoltage issue. The performance of a voltage control strategy using electric water heaters is presented in [30]. Often, the operation of this controllable load is combined with time-of-use pricing or other price differentiation dynamics in order to improve the load and generation correlation [31].

Although promising, demand side management, in general, requires significant investment in control and/or communication infrastructure.

1.1.2.2. Azimuth Diversification of PV Panels

Another way to reduce the magnitude of the voltage rise, and, consequently, the likelihood and magnitude of overvoltages, is to diversify the azimuth of the PV panels. The azimuth (solar orientation) is the angle clockwise from true north of the direction that the PV array faces. Usually, PV systems in the northern hemisphere are placed facing south, azimuth = 0°, to achieve the highest annual energy yield. However, having all houses in a PV feeder with panels due south, as presented in [28], brings the peak power generation time of all the PV panels to be around noon. This can create a large surplus of active power in the system, and consequently, higher probability of occurrence of overvoltage in a feeder than if the PV systems are installed with different azimuths. Increasing the azimuth angle favors afternoon energy production, while decreasing the azimuth angle favors morning energy production [32], as shown in Figure 1.1 (SW = 45° and SE = -45°).

Figure 1.2 shows the variation in yearly PV panel generation with the azimuth. Comparison of southwest and southeast orientation with south shows a loss of about 8% on the yearly energy yields.

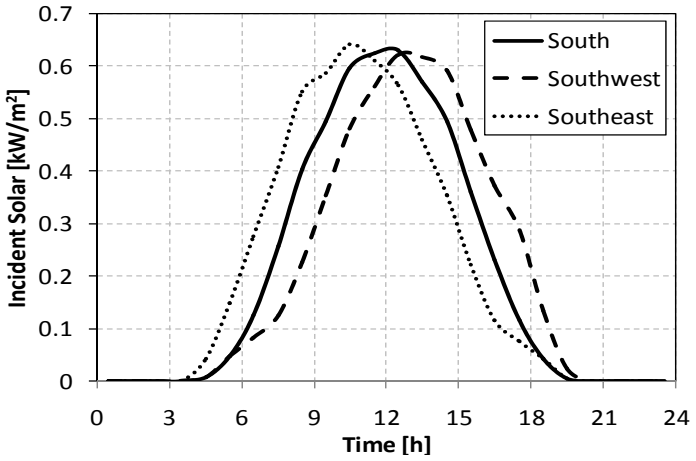

Figure 1.1. Average daily incident solar power profile in July for south (0° azimuth), southeast (-45° azimuth) and southwest (45° azimuth) facing panels mounted in Montreal with a slope of 45°.

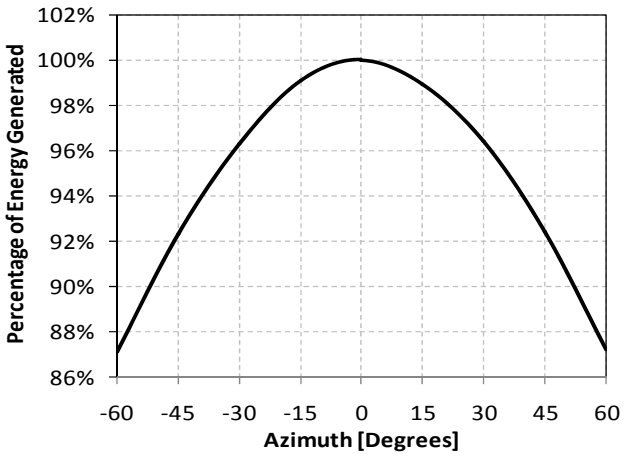

Figure 1.2. Percentage of yearly energy generation regarding energy yield of a south facing PV panel for Montreal with a slope equal to latitude and the effects of varying the PV panel azimuth (orientation).

As shown in [32], this will not drastically affect the yearly net energy generation level but can provide a smoother peak hour generation. This strategy, by itself, cannot guarantee that no overvoltages would occur, but it can reduce their magnitude and frequency.

1.1.2.3. Secondary LV Transformer Tap Adjustment and Conductor Section Increase

Simply readjusting the tap of the LV transformer at certain seasons can be very effective. The main challenge, assuming that the tap cannot be changed frequently without the addition of an on-load tap changer controller, is being able to find a setting that can be used for rated and no generation of PV without violating the voltage limits. A rule of thumb approach to define the appropriate voltage in the secondary of the transformer is presented in [33]. The idea is to adjust the voltage halfway between the upper and lower voltage limits. This ensures that the voltage rise/drop will have the same range of operation. If undervoltage limits are not reached during rated load and no generation, then, during rated generation and no load, the voltage limits will also not be reached. However, this is not possible for all feeders since, in some cases, decreasing the LV transformer voltage can lead to undervoltages.

Another passive approach is to upgrade the conductors [34]. Increasing the cross sectional area of the wires reduces their resistance and reduces the voltage rise/drop in the feeder. For instance, changing the cables of a particular feeder from a NS90 3/0 AWG to a 4/0 AWG cable (aluminum, XLPE) would lead to about a 20% reduction in the line equivalent resistance per kilometer. Consequently, the voltage rise/drop in this section of the feeder is reduced, as can be seen from equation (1.1). In addition, it reduces losses in

the feeder. However, this can be considered an expensive approach, especially for underground feeders.

1.1.2.4. Install Auto-transformers/Voltage Regulators

Auto-transformers/voltage regulators are already being widely used in distribution networks [34-36]. Basically, these consist of a transformer that has multiple taps in one of the sides, which are automatically changed according to a control algorithm by an on-load tap changer. Changing the tap that is connected to the grid modifies the turns ratio of the transformer so that the secondary voltage is stepped up or down from the actual value. The change in the tap is made by the on-load tap changer, according to the voltage variation downstream from the regulator. The control can include line-drop compensation or it can use some sort of communication link to monitor the voltage at a particular point [35]. The main issue regarding the use of a voltage regulator is that it introduces another unreliability factor into the system, which should be considered by local distribution network operators.

1.1.2.5. Allow the PV Inverters to Absorb Reactive Power

PV inverters usually inject all of the active power available from the PV systems to the grid. The main idea for local voltage control is to allow inverters to absorb reactive power together with active power [37-41]. From equation (1.1), one sees that the voltage decreases as the inverter draws reactive power. Therefore, to control the voltage, a certain amount of reactive power could be absorbed by the PV inverters when they inject active power, thereby reducing the voltage rise in the system.

In Canada, according to [20], small power producers should not interfere with the voltage control of the feeder using reactive power in LV systems, unless in agreement with the utility. However, the inverters may operate with power factor between ± 0.85. In some other countries, reactive power cannot be absorbed at all by inverters connected to the LV system [42, 43]. Thus, overvoltage prevention through reactive power control cannot be used in these cases.

In places where this practice is allowed, the extra stress added to the feeder should be considered, which would require an estimate of how much reactive power is needed for overvoltage prevention. This is due to the fact that increases in the reactive power flow in the feeder also increase the RMS value of the current and therefore feeder losses. A preliminary value can be obtained by considering the simple 2-bus system where the voltage rise at the end of the line with respect to that in the beginning of the feeder can be approximated by (1.1).

Let us consider the following strategy for preventing overvoltage while minimizing the amount of reactive power absorbed at the end of the feeder [40]: The PV inverter operates at unity power factor until the voltage at its terminals reaches the maximum allowed value. From this point on, any increases in the injected power has to be compensated with reactive power absorption.

For the PV inverter operating with maximum power with unity power factor (P_1) and maximum allowed voltage at the end of the feeder (V_{max}) one has

$$\Delta V_1 = \frac{P_1 R}{V_{\max}} \tag{1.2}$$

If one wishes to achieve further increases in the amount of injected active power in P_2 without increasing the voltage at the end of the feeder, one has to use a certain amount of reactive power (Q_2). Assuming that the grid voltage remains unchanged, $\Delta V_1 = \Delta V_2$. Therefore, from

$$\frac{P_1 R}{V_{\max}} = \frac{P_2 R + Q_2 X}{V_{\max}} \tag{1.3}$$

one can calculate the amount of reactive power required at the end of the feeder to keep the voltage there constant at the maximum voltage allowed for a certain increase in the injected active power ($\Delta P = P_2 - P_1$), as

$$Q = -\Delta P \frac{R}{X} \tag{1.4}$$

From (1.4), one sees that as the factor R/X increases, higher values of reactive power injection will be required to prevent overvoltage. This will demand inverter(s) with higher power capacity, will result in higher currents – and losses – in the feeder, and will also cause lower power factors at the input of the feeder. The definition of a typical R/X value above (in which the use of reactive power control to allow increased active power injection would be less attractive) is not straightforward since system characteristics and limits imposed by local standards can vary quite a bit.

1.1.2.6. Curtail the Power of DG Units

The option of active power curtailment (APC) seems very attractive because it requires only minor modifications in the PV's inverter control logic [8, 12, 28]. In addition, it is

only activated when needed, thereby minimizing the amount of curtailed active power, also known as output power losses [9].

The main issue regarding APC is in buses where overvoltages often happen. This creates a large amount of power being curtailed from the PV systems, thereby reducing the revenues of the customers.

1.1.2.7. Store the Power Surplus for Later Use

Another strategy that also considers active power management is the utilization of energy storage units to absorb the power that would be curtailed to prevent overvoltages and store it for later use.

A study in Japan, including more than 500 houses with PV systems, investigated the losses incurred from the PV inverter's overvoltage protection circuits [9, 26], including battery-integrated PV systems using lead acid batteries. The results showed that the additional losses in the battery-integrated system were larger than the amount of energy saved. One of the reasons pointed out was that overvoltages were rare in that system (0.3% of the year under study).

In addition, energy storage units are usually expensive and the cost benefit ratio can be low if they have to be sized to store the surplus of high-penetration of RETs.

1.2. High-penetration of PV in Diesel Dominated Autonomous Systems

Access to electricity is an important factor related to human health and wellbeing. However, its current generation and use is affecting the global climate; so that the way energy is produced and consumed needs to be reconciled with ways to reduce environmental effects related to local and global greenhouse gas emissions [44]. Energy supply in remote communities is based on diesel generator sets and is characterized by high costs and a high degree of dependence on fossil fuels. Several RETs such as PV and wind can be cost effective to meet part of the energy needs in many remote communities.

In principle, the integration of RETs into a diesel-based system is relatively simple and these integrated systems operate as passive generation units, with no participation in the control strategy of the mini-grid [45, 46]. They usually inject the maximum amount of energy that can be converted from the wind and sun using some sort of maximum power point tracking (MPPT) strategy. However, the stochastic and fluctuating characteristics of PV and wind can also affect the power quality and reliability of autonomous systems.

It should also be noted that many remote community systems are characterized by highly variable loads, with the peak load as high as 4 to 10 times the average load. Thus, the power-balancing task of the grid forming unit(s), usually one or more diesel gensets, is even more demanding in the presence of RETs. Mini-grids, by definition, represent weak grid conditions. Sudden variations in reasonable amounts of power generation/consumption may deteriorate the power quality and stability of the mini-grid [24]. Large variations in frequency and voltage can lead to tripping of sources and loads.

This problem is even more critical during high-penetration of RETs and with systems that operate with reduced amounts of rotating masses due to low combined generator inertia, which can significantly increase the wear and tear on the diesel genset [24]. It is worth mentioning that the operation of gensets at partial (light) load conditions can result in increased carbon build up in the diesel engine [47, 48], which can significantly affect the maintenance costs and even the lifetime of the genset. Diesel gensets should not operate below a certain minimum load for extended periods of time, according to the manufacturers; 40% is a common threshold [48], although 15-30% might be more common for newer sets. In case this cannot be avoided, the gensets should run close to full load for 1-2 hours to get rid of the carbon accumulated during the day. This leads to high costs in fuel and offsets part of the gains with the installation of renewable energy sources. Thus, when the PV system generation is high and the load in the feeder is low, the genset may be operating below its minimum required load, thereby requiring dissipation of this "excess" power to prevent carbon build-up in the diesel engine.

Figure 1.3 shows a typical PV-diesel hybrid mini-grid. Two or more diesel units, one for backup, are used to provide energy to multiple residential and commercial loads. Small wind turbines, and/or run-off river hydro power sources may also be used to supply part of the load [49]. One of the diesel generators operates continuously, while other gensets can be dispatched based on variations in load demand and DG availability.

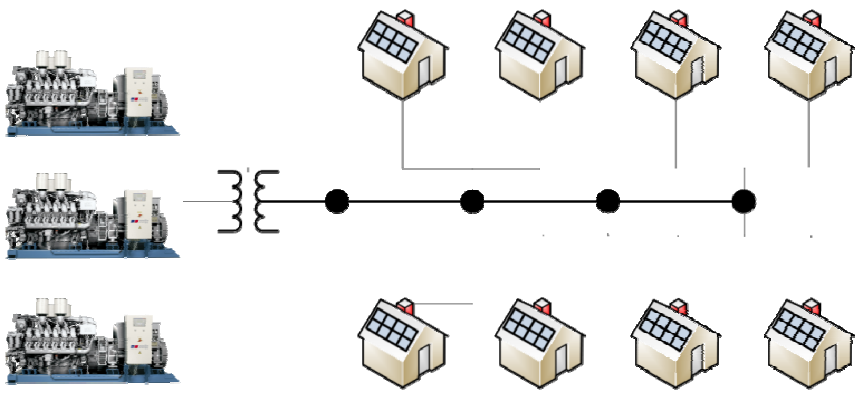

Figure 1.3. Typical PV-diesel hybrid mini-grid.

1.2.1. The Diesel Generator

The diesel generator set is essentially composed of a diesel engine that has its fuel intake controlled by a governor and that drives the shaft of a synchronous machine with an excitation system to control the output voltage of the genset. Figure 1.4 shows the basic diagram of a diesel genset.

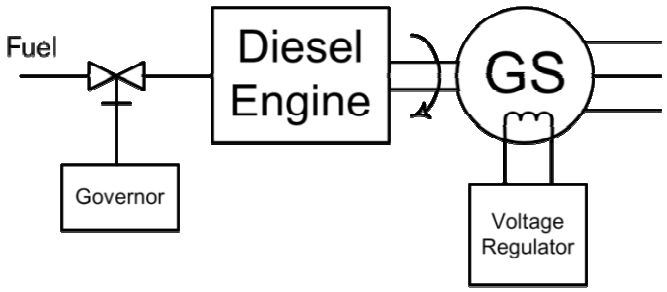

Figure 1.4. Basic diagram of a diesel genset.

The governor regulates the speed of the engine by controlling the fuel injection. Regulating the engine speed means that the output electrical frequency of the generator is also regulated, in steady state, as for synchronous machines the shaft speed (ω [RPM]) is

related with the electrical frequency (f [Hz]) and the number of poles of the machine (p) as:

$$\omega = \frac{120f}{p} \tag{1.5}$$

The governor may operate in two modes, isochronous or droop, depending mainly on the application. Figure 1.5 shows the frequency vs. load curve for isochronous operation. In this type of operation, the genset runs at constant speed/frequency, in steady state, regardless of the load. This method is ideal when the mini-grid uses a single genset, as it keeps the frequency constant. However, when multiple units are present, a communication link is required to avoid circulating currents and to allow appropriate power sharing among the units.

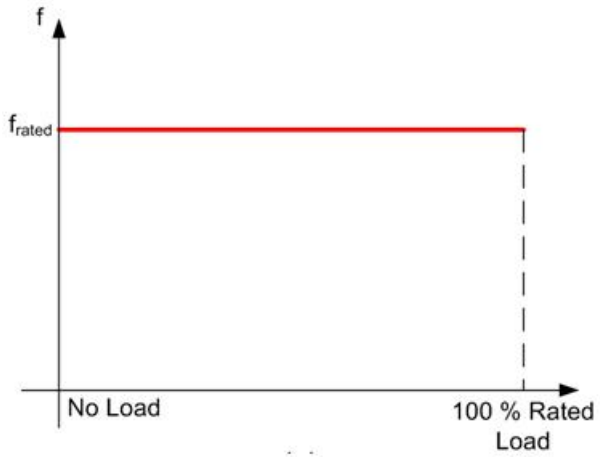

Figure 1.5. Isochronous operation of governor: steady state frequency vs. load operation.

In the droop operation mode, the genset speed/frequency varies according to the load. Figure 1.6 shows the frequency vs. load curve for droop operation. The frequency

decreases linearly when the load increases. The frequency/speed difference between the no load condition and the actual frequency is called droop.

Droop control is a well-known technique for operation and power sharing of power generators connected in parallel. The relationship between frequency and power can be described by:

$$P_{gen} = s_p \left(f_{nl} - f \right) \tag{1.6}$$

for $f \leq f_{nl}$. Here, P_{gen} is the output power of the generator (kW), s_P is the slope of the curve (kW/Hz), f_{nl} is the no-load frequency of the generator (Hz) and f is the operating frequency of the system (Hz). In case of two droop-controlled generators (sources) supplying a common load (P_{load}), the relationship with the frequency would be,

$$P_{load} = P_{gen\_1} + P_{gen\_2} = s_{p\_eq} \left(f_{nl\_eq} - f \right) \tag{1.7}$$

where,

$$s_{p\_eq} = s_{p\_1} + s_{p\_2} \tag{1.8}$$

$$f_{nl\_eq} = \frac{s_{p\_1} f_{nl\_1} + s_{p\_2} f_{nl\_2}}{s_{p\_1} + s_{p\_2}} \tag{1.9}$$

For a given value of load power, one can calculate first the system frequency with (1.7) and then the output power of each generator with (1.6).

The droop is usually set to a maximum of 5% at full load [50]. The droop-based governor is commonly used when several other generators are operating in parallel, as it provides load sharing among the units.

The frequency and voltage curves for a diesel genset rated at 75 kW for single-phase connection using a droop-based governor are shown in Figure 1.7 and Figure 1.8, respectively.

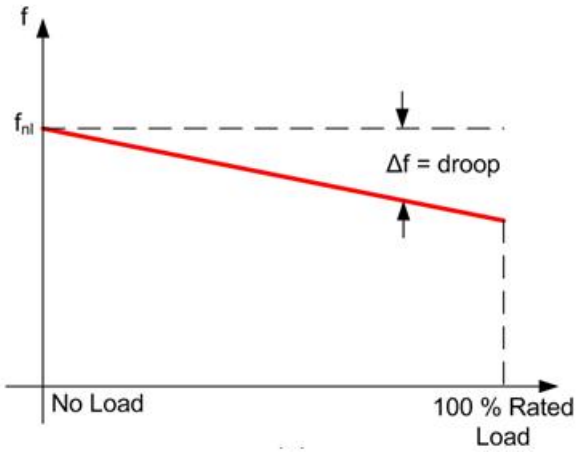

Figure 1.6. Droop operation of governor: steady state frequency vs. load operation.

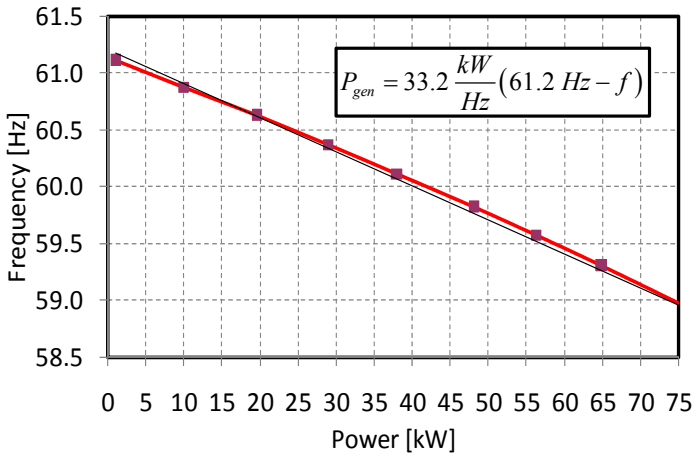

Figure 1.7. 75 kW diesel genset frequency droop characteristic.

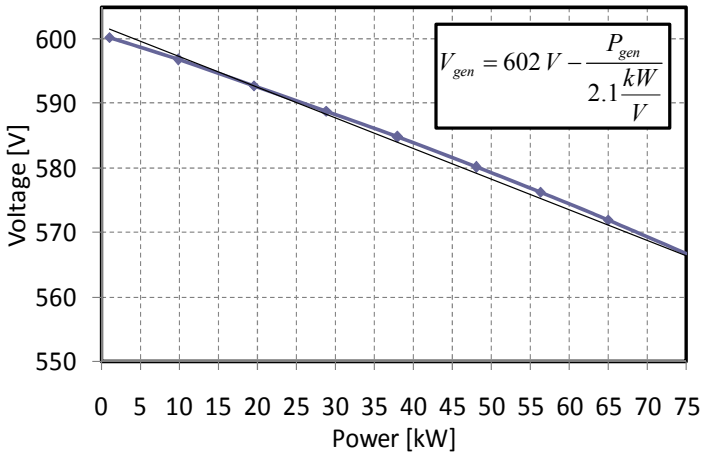

Figure 1.8. 75 kW diesel genset voltage variations with output power.

Sizing of diesel power plants is done based on a detailed analysis of daily and seasonal load fluctuations, annual load growth, and incorporation of practical constraints for feasible and reliable diesel operation [49]. Sizing based on peak and average load values, with some safety margins and additional capacity for future expansion, generally results in very oversized diesel power plants [49].

1.2.2. Operational Aspects of Diesel Generators

The diesel plant can have all of its units the same size, or it can operate with multiple size gensets, which is more efficient based on daily and seasonal variations of the mini-grid load. The generators can be dispatched according to the current state of load demand. One issue is that multiple instances of unit cycling should be avoided for maintenance and expected life considerations [49].

Considering fuel consumption characteristics and the load profile of remote communities, the use of multiple size gensets is very attractive. Figure 1.9 presents the fuel consumption for three 3-phase diesel gensets of different ratings. The fuel consumption

data provided by Simson-Maxwell [51] for full rated load, ¾ of rated load, ½ of rated load and ¼ of rated load were used to generate trendlines. The use of different genset ratings allows a reduction in the fuel consumption under low load conditions and an optimal dispatching of units to match load demand.

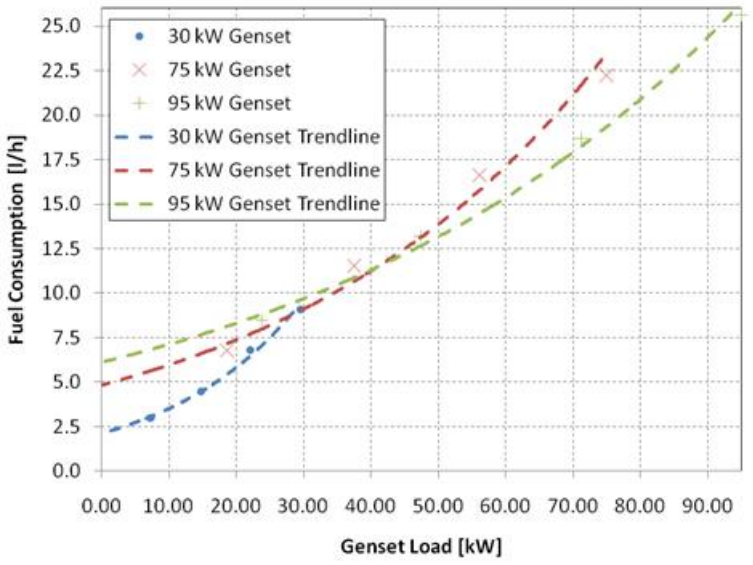

Figure 1.9. Fuel consumption for gensets with different rated power.

For sizing a multi-genset plant, some basic requirements should be followed [49]:

- The plant should have at least two gensets in case of a unit failure or maintenance,

- The suggested minimum loading of a single unit (15-40% of rated capacity) should not be larger than the average mini-grid load to reduce machines running under-loaded, as it can result in increased carbon build up in the diesel engine, thereby increasing the maintenance costs and reducing the lifetime of the genset.

- The largest unit of the plant and/or any combined capacity of two units out of service at all times should be capable of providing about 110% of the forecast peak load,

• For a spinning reserve, the units in operation should not be loaded more than 85%. The spinning reserve is the plant capacity to cover a sudden increase in the load or loss of generation.

Figure 1.10 presents a hypothetical cumulative load curve for a remote community, showing the number of hours that the load equaled or exceeded (x) the y-axis amount. The plant capacity is defined by a prediction of a future increase in the load demand based on the data available for the community [52]. The average load is defined by the amount of energy consumed in a year period divided by the total number of hours in a year.

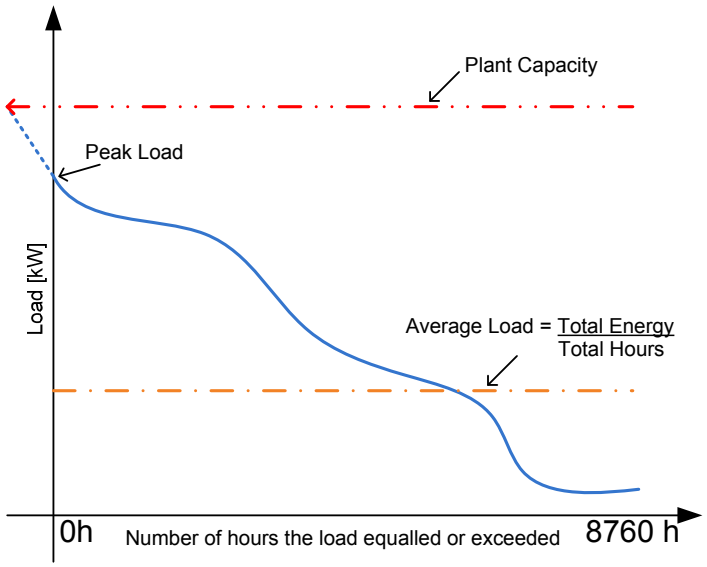

Figure 1.10. Hypothetical load characteristic for a remote community.

1.2.3. Integration of PV in Diesel-based Mini-grids

Today, PV technology is now being widely used in mini-grids. Since 1992, the off-grid PV market is growing at an average rate of 25% per year in Canada and the installation

capacity in 2009 reached 35.2 MW in systems that use PV arrays as a single generator or with a diesel genset or small wind turbine in hybrid systems [15]. For RETs to achieve significant market penetration in off-grid remote community energy markets, and to achieve the corresponding diesel fuel displacement, inclusion of effective means to compensate for their inherent fluctuating and intermittent power characteristics is also necessary.

The ideal remote community system can be foreseen as a hybrid system that combines one or more renewable energy technologies and a fossil fuelled system. Diesel gensets should not operate below a certain minimum load for extended periods of time. As the integration of non-dispatchable RETs in diesel-based mini-grids will reduce the load seen from the genset, it can increase the operation at low load conditions (part load operation). Thus, a scheme for active power sharing must be invoked, where controllable DGs would assist in balancing the system in the quasi-steady-state. These problems can be mitigated by local control of clusters of DGs [53]. Therefore, the control structure plays an important role in maintaining power system stability and also in avoiding unnecessary losses in electricity generators. The main solutions being used to reduce power fluctuations due to the addition of non-dispatchable RETs and part load operation of diesel gensets are discussed in the following Sub-Sections.

1.2.3.1. Dump Loads

Due to their simplicity and low capital cost, dump loads are being widely employed in hybrid mini-grids. These are resistors that are most of the time controlled by frequency or power sensitive relays. They can be switched in steps or turned ON/OFF as a single unit

[48, 54]. The main objective of the dump load is to absorb the excess power generated whenever the genset load is below a certain threshold value, thereby increasing the load in the system. However, dump loads incur a further waste of costly fuel, therefore reducing the gains of installing RETs [48, 55].

1.2.3.2. Active Power Curtailment in Autonomous Systems

Active power curtailment (APC) of RETs can be implemented based on locally measured variables that have the potential to address the low loading condition of the genset, overfrequencies [56, 57], and overvoltages [12, 28, 58, 59]. The new German grid code, for protection purposes, requires inverter-based systems connected into the MV network to curtail the output power according to a certain droop function when the frequency of the system is above 50.2 Hz [60, 61]. The curtailment rate is defined as 40%/Hz of the output power. If the droop function parameters could be adjusted in the PV inverter's control unit, this capability may be of particular interest as well for the interconnection of PV systems in mini-grids. Recall that diesel power plants in mini-grids are usually composed of a number of gensets operating with power vs. frequency droop control. If the parameters are readjusted so that the curtailment would happen when the genset is under low loading condition, the curtailment effect could substitute for the effect of a dump load, reducing the genset's operation under low load. This comes with several advantages. It is an active method, so the curtailment can vary linearly with the load variations, thereby avoiding load oscillations due to connection and disconnection of dump loads. It can also be adjusted to reduce fuel consumption under different low load conditions. An increase in the installed PV capacity in the feeder does not require upgrading of the dump load to avoid reverse power flow and low load [48].

1.2.3.3. Demand Side Management in Autonomous Systems

An alternative to curtailing or dumping the excess power is the activation/deactivation of some consumer loads using frequency sensitive relays. Due to their relatively large time constants, thermal loads such as electric water heaters (EWH) present energy storage characteristics and are good candidates for power balancing and frequency control [62, 63].

As the actual loading of the genset is proportional to the frequency, [64] proposes to modify the *Td* (reference temperature for the EWH) using a frequency versus temperature droop function shown in (1.10), so that the power consumed by the EWH could be controlled:

$$Td = Td_b + m_{EWH}(f - f_c) \tag{1.10}$$

where m_{EWH} is a slope factor and f_c is the center frequency (Hz). Td_b is the base set point temperature. Figure 1.11 (a) shows the frequency x temperature droop function with m_{EWH} = 20 °F/Hz, Td_b=120 °F, and f_c = 61 Hz. The value of T_H (the temperature of water in the tank) will vary within $Td \pm \Delta$, as shown with the dotted lines. The action of droop is limited to when *Td* is within acceptable limits of temperature; in this case, between 100 °F and 140 °F. In a frequency droop diesel genset, when the load increases, the frequency of the generator decreases. This frequency reduction will cause *Td* in the EWH to decrease, whereas when the generator load decreases, the frequency will increase, making *Td* increase. Varying *Td* during steady and transient conditions will affect the average power consumption, as can be seen on Figure 1.11 (b) for different values of *Wd* (water draw), for the EWH described in [64]. The results presented in [64] showed that

power variations in the mini-grid can be reduced with the proposed control strategy; however, the reduction is strongly dependent on the values of water draw from the houses.

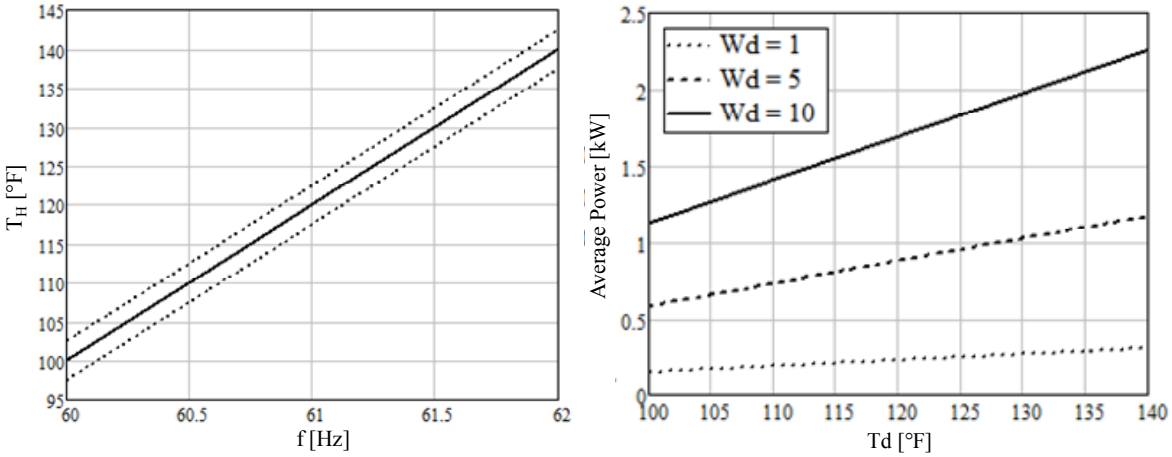

(a) (b)

Figure 1.11. (a) Frequency x temperature droop variation (b) Average power consumption variation with *Td* for different average water draw.

1.2.3.4. Storage Units in Autonomous Systems

In general, power smoothing in systems with RETs is achieved with energy storage devices [65-67]. Batteries have high capabilities for injecting power during small time intervals, but they have a finite capacity for storing energy [68, 69]. This makes them a rather costly solution for operation with high-penetration of RETs in remote communities. The economic aspects of using different methods for smoothing the output power of large PV systems (dump load, power curtailment, and batteries) were examined in [55]. Overall, if the limits of fluctuation are not strict, batteries alone incurred higher losses in terms of revenue. However, if a hybrid approach is considered, using batteries and power curtailment, the losses in revenue were the lowest in all cases studied, which

means that the size of the storage unit is quite a sensitive factor. Further investigation regarding design and optimization of the operation of battery-integrated systems is necessary, including the possibility of combining other functions with PV systems (i.e., peak shaving) in order to aggregate value and improve fuel displacement.

1.3. Thesis Outline and Contributions

The objective of this thesis is to investigate techniques that allow increased penetration of fluctuating RETs in low voltage microgrids and mini-grids, with good power quality and with reduced fuel consumption and maintenance costs of the grid forming gensets in mini-grids.

As previously discussed, overvoltages are one of the main reasons for limiting the installed capacity of PV systems, which reduces the amount of active power that can be injected into a certain LV distribution system. The well-known techniques used in medium voltage (MV) feeders to regulate voltage need to be revisited, considering the fact that the impedance of LV feeders is mostly resistive, with large *R/X* ratios. Chapter 2 investigates the impact of varying active power and reactive power on the voltage and losses of a radial LV distribution feeder with uniformly distributed loads and non-dispatchable (active power) sources, based on the sensitivity analysis of the feeder. This is the main contribution of this chapter. The feeder characteristics as well as the net active power of the buses are considered in the analysis. This method can be used to provide an insight about the best strategy for voltage control, as later explored in [70]. It also can be used to adjust controller parameters, as presented in [28, 71].

Prevention of overvoltages in LV feeders with high-penetration of PV is usually accomplished by limiting the size of PV systems to very conservative values, even if critical periods rarely occur. Alternatively, one can use APC techniques to reduce the amount of active power injected by the PV inverters, as the voltage at their buses increases above a certain value. In this way, the installed PV capacity and energy yield can be increased while preventing overvoltages. Chapter 3 investigates a number of approaches for sizing and controlling the PV power generated by 12 net-zero energy houses equipped with large rooftop PV systems. These are connected to a typical 240 V/75 kVA Canadian suburban radial distribution feeder benchmark, which is used to assess the overvoltage occurrences and losses in LV residential feeders. Two droop-based APC techniques for overvoltage prevention in radial LV feeders are also presented as a means of increasing the installed PV capacity and energy yield. In the first scheme, all PV inverters have the same droop coefficients. A design approach for the droop coefficients is proposed. Using this scheme, PV houses downstream from the LV transformer incurred higher generation losses than the ones located upstream. The main contribution of this chapter is the design of a droop-based APC scheme that shares the power curtailment among the PV units in a certain feeder. The proposed droop coefficients are different so that they share the total active power curtailed among all PV inverters/houses and, consequently, share the household losses in revenue. Simulation results using PSCAD demonstrate the effectiveness of the proposed schemes and show that the option of sharing the power curtailment among all customers comes at the cost of an overall higher amount of power curtailment. The reduction in the installed PV capacity and the diversification of the azimuth angle (PV panel orientation) are analyzed as

candidate solutions for overvoltage prevention. One contribution is the evaluation of the performance of the different approaches presented in terms of overvoltage occurrence. This is done by examining the sharing of the burden for overvoltage prevention per house and total energy yield of the residential PV feeder in a one-year period simulation study, with typical solar irradiance and load profiles. This study provides quantitative values to support the assessment of the overvoltage prevention solutions.

As discussed previously, renewable energy sources such as PV have great potential for reducing fuel consumption in diesel-based autonomous systems. However, the fluctuating and intermittent nature of these sources can give rise to a number of problems in autonomous systems (mini-grids) with high-penetration of non-dispatchable renewable that have reduced or non-existent storage units. Chapter 4 discusses the use of a frequency x power droop control strategy for curtailing the output power of PV inverters during periods of excess of power in a diesel-dominated mini-grid. This approach reduces the operation of the diesel genset under part (low) load conditions, thereby reducing frequency variations in the mini-grid and it can also reduce fuel consumption. In addition, if an increase in the PV installed capacity occurs in the feeder, the dump load(s) does not need upgrading to avoid reverse power flow and low load operation of the genset. A benchmark is used for the evaluation of part load operation of LV residential diesel-based mini-grid and the impact on fuel consumption. The effectiveness of using the frequency x power droop-based APC scheme is also assessed for reducing part load operation of diesel-based mini-grids. The theoretical analysis is verified by means of digital simulations with PSCAD. The main contribution of this chapter is the use of statistical information about the load and PV power generation profile to provide an estimation of

part load operation, yearly energy yields, and fuel consumption for different protection schemes to reduce part load operation using the PV-diesel mini-grid benchmark. Chapter 5 presents a summary, with the main conclusions from this study.

2. VOLTAGE REGULATION IN RADIAL DISTRIBUTION FEEDERS WITH HIGH-PENETRATION OF DISTRIBUTED GENERATION

This chapter focuses on the impact of the resistance-reactance ratio ($K = R/X$) of LV and MV feeders, as well as on the net power factor and reactive power of the feeder buses, on the effectiveness of using active and reactive power for regulating the voltage profile of a radial feeder with high-penetration of PV. This can influence the choice of PV units with overrated inverters for additional capacity of reactive power control, as presented in [40], or power curtailment of RETs to minimize overvoltages during peak power production.

2.1. Voltage Variation in Radial Distribution Feeders with High-penetration of PV

The proposed analysis is carried out with the simple 5-bus feeder shown in Figure 2.1. Bus 1 is the substation (slack/reference bus) where the voltage magnitude can be regulated by means of taps. The total feeder impedance is equal to 0.02 pu, which would represent an approximately 100 (200) m feeder in a LV (MV) system, where four sources/loads would be connected. The resistance-reactance ratio of the feeder impedance varies between 0.25 and 5 to represent MV and LV feeders [72]. The loads are assumed to be uniformly distributed through the feeder buses. Identical PV inverters are placed at the last four buses to represent a solar neighborhood. The total load (active power) of the system under study varies from 1 pu net load to – 1 pu, where 1 pu is the substation or transformer capacity. Negative load means that the feeder is producing power. It is

assumed that the net reactive power of each node can be changed by means of the reactive power supplied/absorbed by the PV inverter. Figure 2.2 shows how the voltage at bus 5 varies with the net active power in the unity power factor buses, for feeders with different resistance-reactance ratios, using a Newton-Raphson load flow algorithm written in Matlab©. Note that the feeder impedance per meter, in this case, is constant and that the feeder power is uniformly distributed through the 4 nodes. One sees that feeders with large resistance-reactance ratios (same impedance) yield larger voltage variations as the net active power varies.

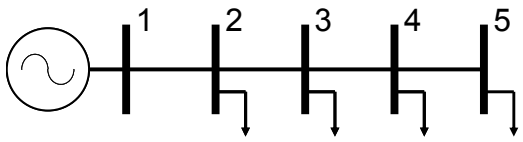

Figure 2.1. 5-bus system.

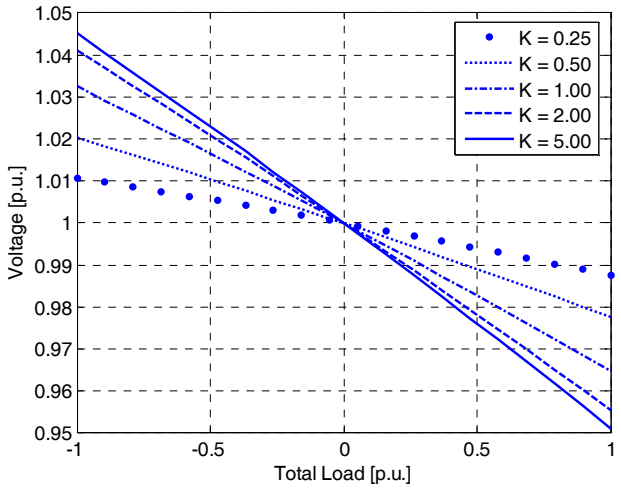

Figure 2.2. Voltage in bus 5 for different feeder resistance-reactance ratio (K) and UPF.

The same happens with the total feeder losses, as noted in Figure 2.3 (the transformer losses have been neglected for simplicity). As the resistance-reactance ratio of the feeder increases, so do the losses, since the losses are proportional to I^2R, where I is the RMS value of the current and R the feeder resistance. Figure 2.3 shows asymmetry, which can be explained as follows: If the power consumed/generated by the buses is assumed constant when the feeder is behaving as a net producer, the voltage in the feeder rises, thereby reducing the current circulating in the feeder, and consequently the losses for a given bus power level.

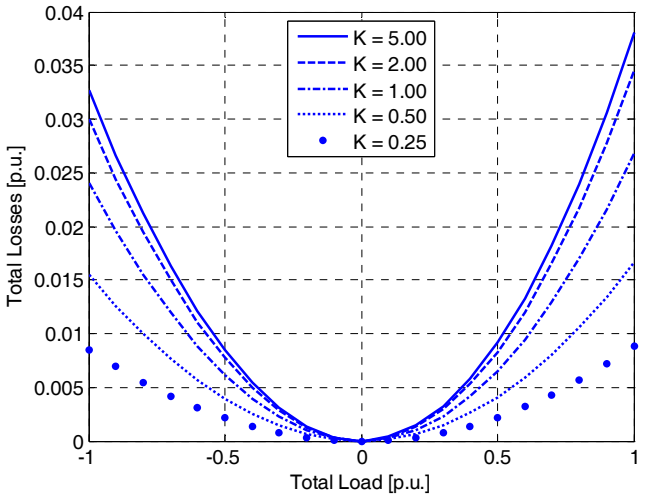

Figure 2.3. Total losses for different feeder resistance-reactance ratio (K) and UPF.

2.2. Voltage Sensitivity to Active and Reactive Power

The first order sensitivity analysis method is used to obtain a quantitative measure of the impact of the variation of the active and reactive power of the inverters on the variation of the magnitude of the voltage at the radial distribution feeder. The impedance characteristic ($K = R/X$) of the feeder is varied, as is the total net load/source power

factor. From power (load) flow analysis, one obtains the sensitivity matrix shown in equation (2.1):

$$S_V = \begin{bmatrix} 1 & 0 \\ 0 & |V| \end{bmatrix} \begin{bmatrix} \frac{\partial P}{\partial \delta} & |V|\frac{\partial P}{\partial V} \\ \frac{\partial Q}{\partial \delta} & |V|\frac{\partial Q}{\partial V} \end{bmatrix}^{-1} = \begin{bmatrix} \frac{\partial \delta}{\partial P} & \frac{\partial \delta}{\partial Q} \\ \frac{\partial V}{\partial P} & \frac{\partial V}{\partial Q} \end{bmatrix} \tag{2.1}$$

The voltage sensitivity matrix is composed of 4 sub matrices (S_{Vmn}, $m = 1, 2$, $n = 1, 2$) with partial derivatives that portray the variation in the voltage magnitude and angle of the buses due to variations in active and reactive power at each bus. Sub-matrices S_{V21} and S_{V22} are used for the analysis of voltage variation. Theoretical validation of the results obtained from the sensitivity analysis is obtained for the load flows of two cases for the system with $K = 5$ shown in Figure 2.1. In the first case, the system is fully loaded, with total load of the feeder equal to 1 pu. The second case considers that all buses behave as energy suppliers, from the PVs, with UPF. The sensitivity matrices for the first and second cases are presented in (2.2) and (2.3), respectively. The sign of each element indicates whether injecting P or Q should generate a voltage rise (drop) if positive (negative). This chapter focuses on the variation in voltage due to active and reactive power injection; therefore, the sub matrices of particular interest are S_{V21} and S_{V22}. Sub-matrices S_{V11} and S_{V12} will be used along with S_{V21} and S_{V22} to investigate the impact of the net active and reactive power at the buses on the losses of the distribution system.

The meaning of each element in these sub matrices is to be interpreted as the variation that would happen in the voltage profile in a certain bus in the case of a hypothetical injection of 1 pu of active power for S_{V21} or 1 pu of reactive power for S_{V22} at a certain operating point. These matrices also provide information regarding the amount of energy

that would be necessary to regulate the buses to a certain value. Figure 2.4 presents the voltage profile in each bus for the two discussed cases. In case 1, where the buses behave as loads, the voltage in bus 5 reaches 0.95 pu. It is 1.045 pu for case 2, where the buses behave as generation. For voltage regulation in bus 5 (to 1 pu), using active power, the amount to be injected can be calculated from S_{V21}, line 4 row 4, 0.0725 pu (0.0780 pu for case 2). Consequently, (1-0.95 pu)/0.0725 pu = 0.68 pu of active power needs to be injected into bus 5 to bring it to 1 pu voltage (- 0.58 pu of active power for case 2). In the same figure, the new voltage profile regulating the voltage to 1 pu is plotted in order to validate the results. For the sake of comparison, in case 1, if reactive power is used to regulate the voltage, the amount to be injected could be calculated from S_{V22}, line 4 row 4, 0.0150 pu (for cases 1 and 2). Therefore, (1-0.95 pu)/0.0150 pu = 3.3 pu (3.0 pu for case 2) of reactive power would be needed in bus 5 to bring it to 1 pu voltage. Thus, for this feeder, adjusting the active power flow is more *effective* in regulating the voltage magnitude the system than is reactive power control.

$$\left[\begin{array}{cccc|cccc} 0.0036 & 0.0036 & 0.0036 & 0.0036 & -0.0184 & -0.0184 & -0.0184 & -0.0184 \\ 0.0035 & 0.0070 & 0.0070 & 0.0070 & -0.0184 & -0.0363 & -0.0363 & -0.0363 \\ 0.0035 & 0.0069 & 0.0104 & 0.0104 & -0.0184 & -0.0363 & -0.0537 & -0.0537 \\ 0.0034 & 0.0069 & 0.0103 & 0.0137 & -0.0184 & -0.0363 & -0.0537 & -0.0710 \\ \hline 0.0184 & 0.0179 & 0.0176 & 0.0174 & 0.0038 & 0.0038 & 0.0038 & 0.0038 \\ 0.0184 & 0.0364 & 0.0357 & 0.0354 & 0.0038 & 0.0075 & 0.0075 & 0.0075 \\ 0.0184 & 0.0364 & 0.0543 & 0.0538 & 0.0038 & 0.0075 & 0.0113 & 0.0113 \\ 0.0184 & 0.0364 & 0.0543 & 0.0725 & 0.0038 & 0.0075 & 0.0113 & 0.0150 \end{array}\right] \quad (2.2)$$

$$\left[\begin{array}{cccc|cccc} 0.0039 & 0.0039 & 0.0039 & 0.0039 & -0.0191 & -0.0191 & -0.0191 & -0.0191 \\ 0.0040 & 0.0080 & 0.0080 & 0.0080 & -0.0191 & -0.0388 & -0.0388 & -0.0388 \\ 0.0041 & 0.0082 & 0.0123 & 0.0123 & -0.0190 & -0.0388 & -0.0591 & -0.0591 \\ 0.0041 & 0.0083 & 0.0124 & 0.0166 & -0.0190 & -0.0388 & -0.0590 & -0.0796 \\ \hline 0.0191 & 0.0198 & 0.0202 & 0.0204 & 0.0038 & 0.0038 & 0.0038 & 0.0038 \\ 0.0191 & 0.0388 & 0.0396 & 0.0401 & 0.0038 & 0.0075 & 0.0075 & 0.0075 \\ 0.0192 & 0.0388 & 0.0586 & 0.0592 & 0.0038 & 0.0075 & 0.0113 & 0.0113 \\ 0.0192 & 0.0388 & 0.0586 & 0.0780 & 0.0038 & 0.0075 & 0.0113 & 0.0150 \end{array}\right] \quad (2.3)$$

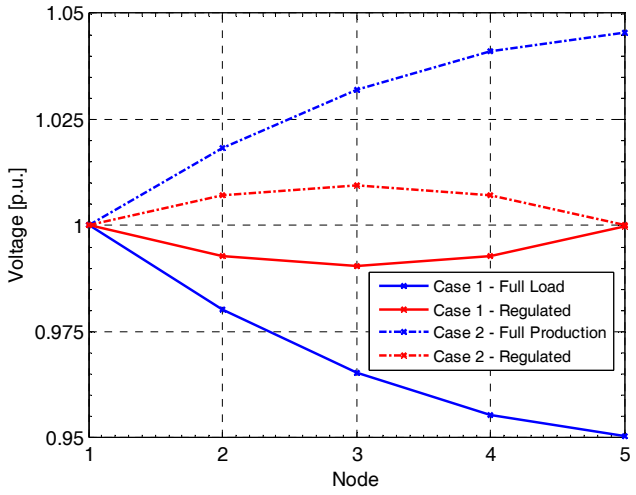

Figure 2.4. Voltage profile for two cases. 1 – Buses fully loaded and 2 – Buses in full production and the regulation of voltage in bus 5 to 1 pu in both cases, using the sensitivity results for the last node.

The determinants of sub-matrices S_{V21} and S_{V22} are used as a means of comparing the effectiveness of varying active and reactive power uniformly in all buses, on the bus voltages. The determinant of the sensitivity matrix at a given load point gives important information about the behavior of voltage near that point. The absolute value of the determinant gives the factor by which the voltage expands or shrinks volumes near the operation point [73]. Figure 2.5 and Figure 2.6 present the variation in the determinant of the sub matrices regarding voltage magnitude variation as a result of active power and reactive power variations for different net load levels, still with UPF, and for different feeder characteristics. LV feeders, with larger K ratios, show a higher value of the determinant of the sensitivity matrices due to active power injection variation (S_{V21} in Figure 2.5) than is seen for the reactive power injection case (S_{V22} in Figure 2.6). The trend is the opposite for MV feeders. This means that for the same amount of active and

reactive power variations, a larger variation in the voltage magnitude is achieved with active power injection for LV feeders. In addition, the voltage sensitivity to active power variation (gain) increases as the load level rises, as the sensitivity terms are dependent of the voltage level. The rate of variation of gain also increases in the same fashion. The opposite effect is seen for voltage sensitivity to reactive power variations. MV feeders, with smaller K ratios and more reactive characteristics, present higher voltage sensitivity, which decreases (gain) as more active power is absorbed.

Figure 2.7, Figure 2.8, Figure 2.9 and Figure 2.10 present the variations of the determinant of the sub matrices with respect to voltage magnitude variation due to active power injection and reactive power injection. The relationship is shown with the total load level of this system for different lagging PFs. In Figure 2.7 and Figure 2.8, the feeder is assumed to have an impedance ratio $K = 5$. For the sub matrix related to active power variation, in Figure 2.7, one sees that the power factor of the bus has a relatively small impact on the gain for $S > 0$, where S is the apparent power ($S = P+jQ$). The gain tends to increase as the load consumes more apparent power, $S > 0$. The gain variation with PF variation is larger for loads with $S < 0$, reaching a 5% difference for S = -1 pu. Loads operating with UPF present the larger variation of gain (10%) as the bus power varies from -1 to 1 pu. In contrast, in Figure 2.8, where the sub matrix is related to reactive power variations, the absolute value of the gain increases when the power factor decreases. It is lowest at no-load and highest at -1 and 1 pu power. However, it is still three orders of magnitude lower than the sensitivity to active power variations and is therefore negligible for voltage regulation purposes.

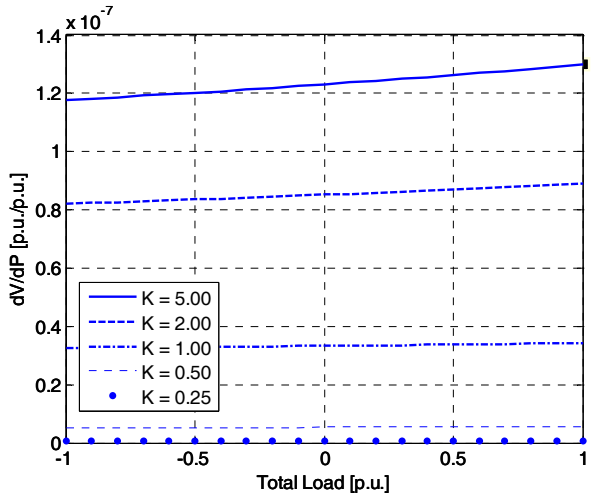

Figure 2.5. Voltage magnitude sensitivity with respect to variations in P for different net load levels with UPF and for different feeder impedances characteristics.

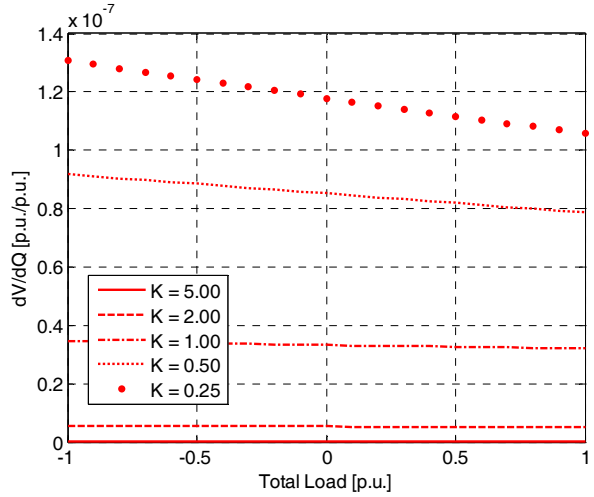

Figure 2.6. Voltage magnitude sensitivity with respect to variations in Q, for different net load levels with UPF and for different feeder impedances characteristics.

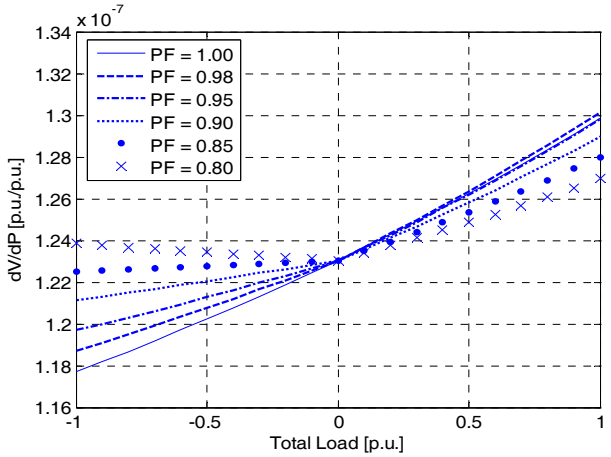

Figure 2.7. Voltage magnitude sensitivity with respect to variations in P, for different net load levels with variable PF and for a typical LV feeder (K = 5).

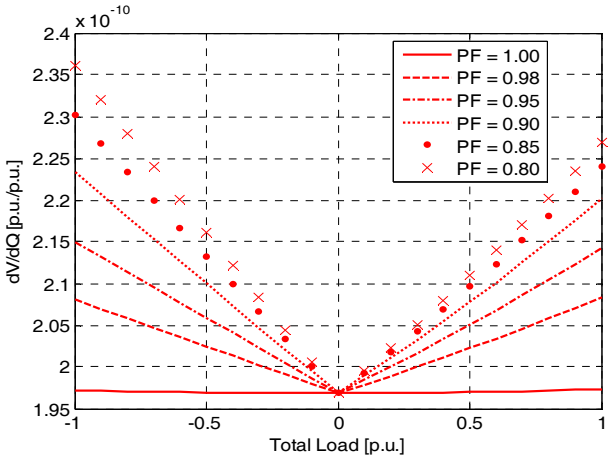

Figure 2.8. Voltage magnitude sensitivity with respect to variations in Q, for different net load levels with variable PF and for a typical LV feeder (K= 5).

For buses with a leading power factor, not shown, the results are quite similar to the lagging power factor load for the active power sub matrix. Nevertheless, for the reactive power sub matrix, the relationship changes. The sensitivity to *Q* decreases with the power factor. Figure 2.9 and Figure 2.10 show the curves of variation of sensitivity for different

PFs for K = 1. Note that the determinant values of both matrices regarding active and reactive power are now similar. Note also that the gains for both sensitivities increase for loads with lower PF (lagging). As for the previous value of K (large), for buses with leading power factor (not shown), the results are also quite similar to the lagging power factor load for the active power sub matrix.

However, for the reactive power sub matrix, the relationship again changes. The sensitivity to Q decreases with the power factor. In this case, the voltage rise can be obtained for all loads PFs by increasing the amount of active and reactive powers supplied at each bus. The gain of sensitivity, however, would change with the power factor, being the largest for lagging reactive power and smallest for leading reactive power.

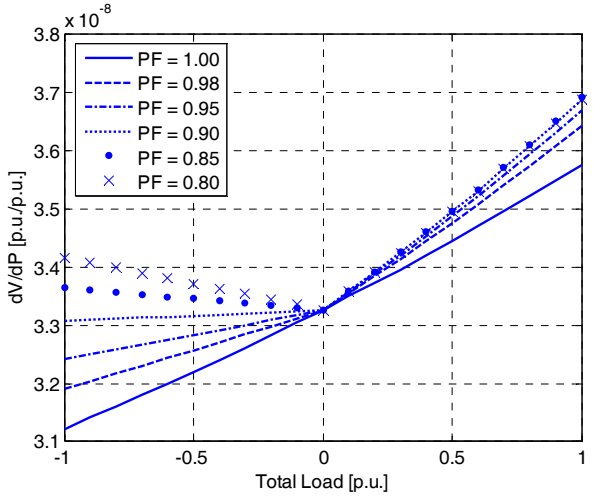

Figure 2.9. Voltage magnitude sensitivity with respect to variations in P, for different net load levels with variable PF and for a feeder with K = 1.

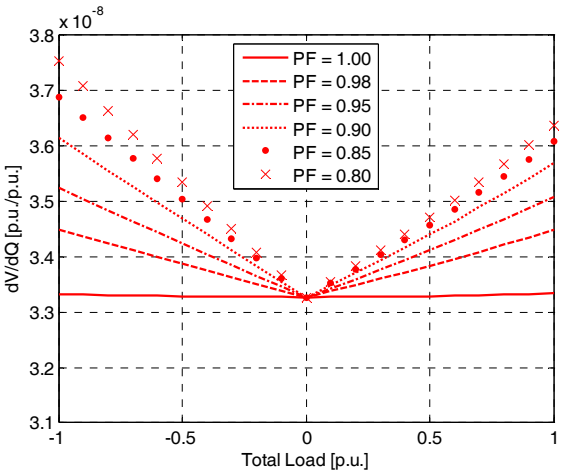

Figure 2.10. Voltage magnitude sensitivity with respect to variations in Q, for different net load levels with variable PF and for a feeder with K = 1.

The sensitivity analysis showed that active power variation has a greater impact in voltage variation than did reactive power variation for feeders with large *R/X* ratios. The sensitivity of voltage magnitude to active power variation is also larger for net load buses than for net generator buses, which are more relevant for the limitation of voltage rises for systems high-penetration of PV. Thus, reactive power injection in LV systems had a lower impact in voltage regulation than did active power; however, for MV systems, this strategy becomes more attractive since the sensitivity matrix for reactive power variation results in gains comparable to those of active power variation.

2.3. Feeder Impedance Loss Sensitivity to Active and Reactive Power

A first order sensitivity analysis was used to obtain a quantitative measure of the impact of the variation of the active and reactive power of the inverters on the variation of the feeder impedance losses at the radial distribution feeder. Let us consider the losses

referred to in the first line segment of the feeder of Figure 2.1. Equation (2.4) presents the losses in this part of the feeder:

$$L_{12} = \mathrm{Re}\left(\frac{\left(\vec{V}_1 - \vec{V}_2\right)^2}{\vec{Z}_{L12}} \right) \tag{2.4}$$

where,

$\vec{V}_1 = \hat{V}_1\left(\cos(\delta_1) + j\sin(\delta_1)\right)$

$\vec{V}_2 = \hat{V}_2\left(\cos(\delta_2) + j\sin(\delta_2)\right)$

$\vec{Z}_{L12} = R + jX_L = \left|\vec{Z}_{L12}\right|\left(\cos\left(tg^{-1}\left(\frac{1}{K}\right)\right) + j\sin\left(tg^{-1}\left(\frac{1}{K}\right)\right)\right)$

$\hat{V}_{1,2}$ are the voltage amplitudes in buses 1 and 2, respectively,

$\vec{V}_{1,2}$ are the complex voltage vectors in buses 1 and 2 respectively,

$\delta_{1,2}$ are the voltage angles in buses 1 and 2, respectively,

$\vec{Z}_{L12}$ is the complex line impedance connecting buses 1 and 2.

Expanding this expression, one obtains the feeder impedance losses between bus 1 and bus 2:

$$L_{12} = \frac{\hat{V}_1^{\,2}\left(K\cos(2\delta_1) + \sin(2\delta_1)\right) + \hat{V}_2^{\,2}\left(K\cos(2\delta_2) + \sin(2\delta_2)\right) - 2\hat{V}_1\hat{V}_2\left(k\cos(\delta_1 + \delta_2) + \sin(\delta_1 + \delta_2)\right)}{\left|z_{L12}\right|\sqrt{K^2 + 1}} \tag{2.5}$$

Using the chain rule and the voltage sensitivity data obtained previously, the derivative of losses in relationship to active and reactive power variations may be expressed in equations (2.6) and (2.7), respectively:

$$\frac{\partial L}{\partial P} = \frac{\partial L}{\partial V_1}\frac{\partial V_1}{\partial P} + \frac{\partial L}{\partial \delta_1}\frac{\partial \delta_1}{\partial P} + \frac{\partial L}{\partial V_2}\frac{\partial V_2}{\partial P} + \frac{\partial L}{\partial \delta_2}\frac{\partial \delta_2}{\partial P} \tag{2.6}$$

$$\frac{\partial L}{\partial Q} = \frac{\partial L}{\partial V_1}\frac{\partial V_1}{\partial Q} + \frac{\partial L}{\partial \delta_1}\frac{\partial \delta_1}{\partial Q} + \frac{\partial L}{\partial V_2}\frac{\partial V_2}{\partial Q} + \frac{\partial L}{\partial \delta_2}\frac{\partial \delta_2}{\partial Q} \tag{2.7}$$

where,

$$\frac{\partial L}{\partial V_1} = \frac{2V_1\left(\sin\left(2\delta_1\right) + K\cos\left(2\delta_1\right)\right) - 2V_2\left(\sin\left(\delta_1+\delta_2\right) + K\cos\left(\delta_1+\delta_2\right)\right)}{\left|z_{L12}\right|\sqrt{K^2+1}} \tag{2.8}$$

$$\frac{\partial L}{\partial \delta_1} = \frac{2V_1^2\left(\cos\left(2\delta_1\right) - K\sin\left(2\delta_1\right)\right) - 2V_1V_2\left(\cos\left(\delta_1+\delta_2\right) - K\sin\left(\delta_1+\delta_2\right)\right)}{\left|z_{L12}\right|\sqrt{K^2+1}} \tag{2.9}$$

$$\frac{\partial L}{\partial V_2} = \frac{2V_2\left(\sin\left(2\delta_2\right) + K\cos\left(2\delta_2\right)\right) - 2V_1\left(\sin\left(\delta_1+\delta_2\right) + K\cos\left(\delta_1+\delta_2\right)\right)}{\left|z_{L12}\right|\sqrt{K^2+1}} \tag{2.10}$$

$$\frac{\partial L}{\partial \delta_2} = \frac{2V_2^2\left(\cos\left(2\delta_2\right) - K\sin\left(2\delta_2\right)\right) - 2V_1V_2\left(\cos\left(\delta_1+\delta_2\right) - K\sin\left(\delta_1+\delta_2\right)\right)}{\left|z_{L12}\right|\sqrt{K^2+1}} \tag{2.11}$$

Note that the voltage sensitivity matrix is used to obtain the loss sensitivity as well as the partial derivatives of equation (2.5), as seen in equations (2.6) and (2.7).

The loss sensitivity matrix is composed of 2 sub matrices (S_{Lmn}, $m = 1, 2$) with partial derivatives that portray the variation of the losses in the feeder due to variations in active and reactive power at each bus:

$$S_L = \begin{bmatrix} \frac{\partial L}{\partial P} & \frac{\partial L}{\partial Q} \end{bmatrix} \tag{2.12}$$

Figure 2.11 and Figure 2.12 present the variation of the determinant of the sub matrices regarding loss variation as a result of active power and reactive power variations respectively for different net load levels (S), still with UPF, and for different feeder characteristics for the feeder configuration presented in Figure 2.1. The effect on losses of varying active and reactive power is increased for higher net load level. As the voltage decreases when the bus loading increases, variations in terms of active and reactive power leads to larger variations in current. Since losses are proportional to I^2R, where R is the resistive portion of the line impedance, an asymmetry shows in the curve. For feeders with higher resistance-reactance ratios (LV), this effect is increased with regards to active power. Note also that, in LV feeders, the injection of reactive power does not produce as great a loss variation than if active power is injected. This is due to the fact that the losses are a function of the RMS value of the current circulating in the feeder, which is dependent on the voltage sensitivity, as shown in (2.6) and (2.7).

Figure 2.13 and Figure 2.14 present the effect of lagging net power factor on losses due to active and reactive power respectively in a typical LV feeder. When the net power factor is decreased, it reduces the active power variation effect in the losses. However, the reactive power variation effect would be increased. This means that if a strategy of

voltage regulation based on reactive power variation is used, when the feeder is behaving as a net producer, the effect on losses of reactive power injection is increased as the net power factor will be decreased and, consequently, the loss variation should be increased.

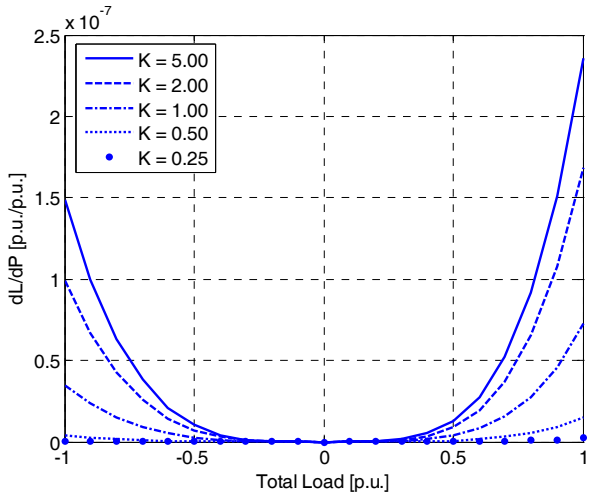

Figure 2.11. Loss sensitivity with respect to variations in P, for different net load levels (UPF) and for different feeder impedances characteristics.

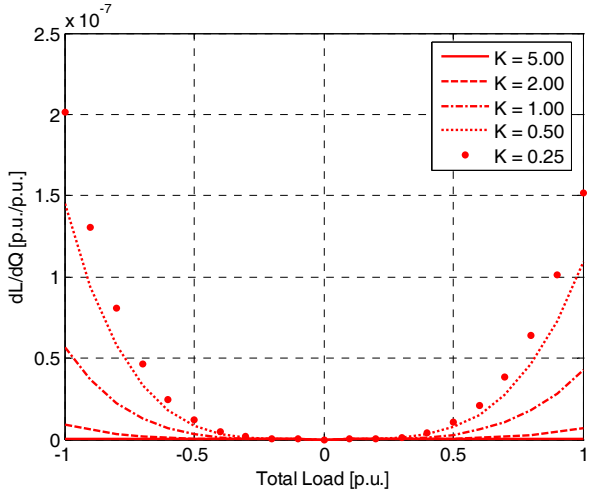

Figure 2.12. Loss sensitivity with respect to variations in Q, for different net load levels (UPF) and for different feeder impedances characteristics.

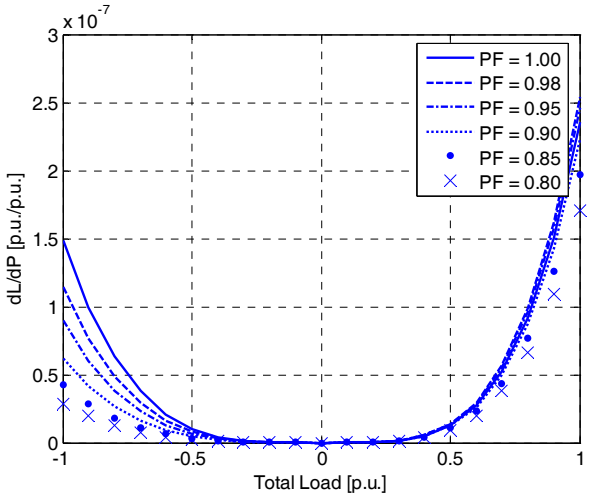

Figure 2.13. Loss sensitivity with respect to variations in P, for different net load levels with variable PF and for a typical LV feeder (K = 5).

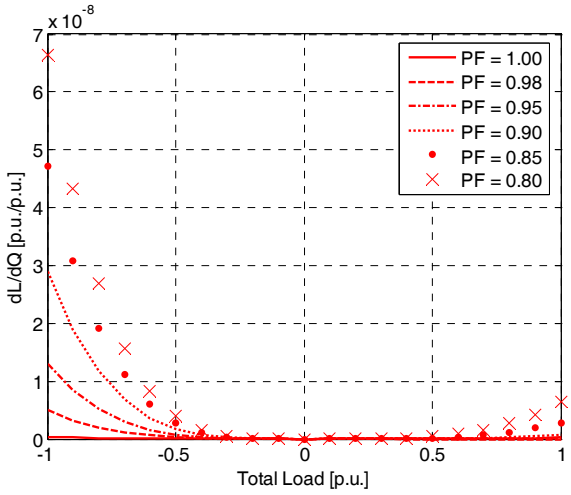

Figure 2.14. Loss sensitivity with respect to variations in Q, for different net load levels with variable PF and for a typical LV feeder (K= 5).

2.4. Effect of Voltage Regulation with Active Power Curtailment and Reactive Power Injection in Feeder Losses.

Figure 2.15 presents the ratio of reactive power vs. active power necessary to vary the voltage for a certain amount in bus 5, based on the sensitivity values for different kinds of feeders. For a LV feeder with K = 5, as 5 (K) times as much reactive power than active power is necessary to regulate the voltage at the same bus. This rule of thumb may also be applied for different K values.

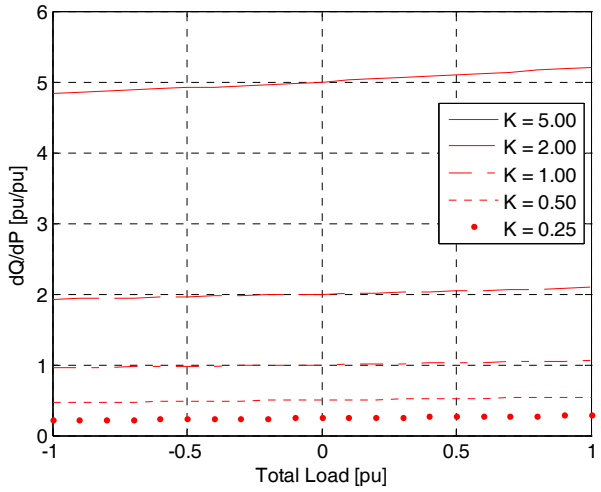

Figure 2.15. Proportion of reactive power per active power needed to vary the voltage the same amount.

Regarding feeder losses, using the voltage and loss sensitivity values allows the impact of using active power or reactive power to be demonstrated in the voltage regulation task in the feeders. The variations in losses for a given variation in voltage, achieved with different variations of active and reactive power, are presented in (2.13) and (2.14) respectively. As an example, if one wishes to increase the voltage at that bus by 5% (ΔV)

by means of active power, and knowing the sensitivity to losses and voltage in that node, equation (2.13) could be used to estimate the effect on the losses. The same is valid for reactive power using equation (2.14).

$$\Delta L_P = \Delta P \frac{\partial L}{\partial P} = \Delta V \frac{\partial P}{\partial V} \frac{\partial L}{\partial P} \tag{2.13}$$

$$\Delta L_Q = \Delta Q \frac{\partial L}{\partial Q} = \Delta V \frac{\partial Q}{\partial V} \frac{\partial L}{\partial Q} \tag{2.14}$$

Figure 2.16 and Figure 2.17 show the effect of varying the voltage in bus 5 on losses using active and reactive power, respectively. Considering the loss variations, both strategies behave similarly. However, when active power is curtailed, feeder current is reduced, so there will be a reduction in the feeder losses. With reactive power control, the RMS value of the current is increased, and so are the feeder losses.

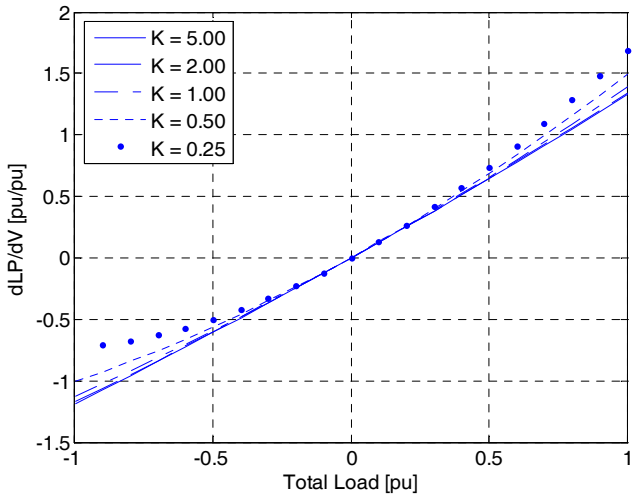

Figure 2.16. Loss variation given a voltage variation in bus 5 using active power as regulation means.

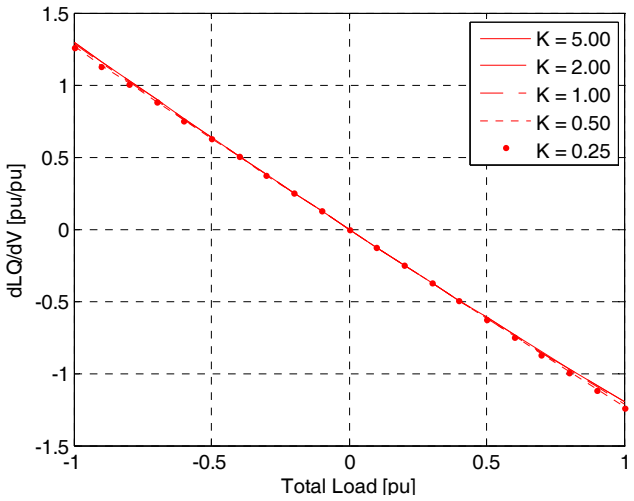

Figure 2.17. Loss variation given a voltage variation in bus 5 using reactive power as regulation means.

2.5. Conclusions

This chapter discussed the use of active and reactive power control for preventing overvoltages in systems with a high penetration of RETs. A method is proposed for the analysis of the impact of varying active power and reactive power on the voltage and losses of a radial LV distribution feeder with uniformly distributed loads and non-dispatchable (active power) sources based on the sensitivity analysis of the feeder. A simple radial feeder with 5 buses and with PV generation and local loads distributed uniformly was used in this study. The feeder impedance characteristic plays an important role in the choice of the most effective approach. The voltage in feeders with large ratios *R/X*, common in LV feeders, can be regulated with lower variation of active power than with reactive power. In other words, voltage regulation with reactive power is less effective in LV feeders than in MV ones. Next, a method was developed to obtain the feeder loss sensitivity to prevent overvoltage by means of active and reactive power

control. The use of reactive power control results in more losses in the feeder, which can possibly offset the additional active power injected by the PV inverters, if no active power is curtailed. On the other hand, with active power control, one can achieve both voltage regulation and feeder loss reduction. Reactive power control is indicated more for MV feeders, which typically present a smaller ratio *R/X*. The net power factor of the buses was also shown to change the behavior of the sensitivity matrix, but the effect of line characteristics is stronger in the definition of the voltage regulation strategy. Inductive buses (load plus reactive power of the inverter) decrease the sensitivity of the voltage magnitude to active power injection variation in LV feeders when the feeder is a net load. However, they increase the sensitivity when the buses are net producers of active power.

3. APC OF GRID CONNECTED PV INVERTERS FOR OVERVOLTAGE PREVENTION

In this chapter, the effectiveness of four techniques are assessed and compared for LV residential feeders with high-penetration of PV. Two passive methods are used as reference for performance assessment of two active methods, where the first one is to reduce the installed PV capacity to prevent overvoltage. The second method is based on the use of residential rooftop PV systems with different values of azimuth, which should reduce the peak and widen the shoulders of the PV generation curve for the feeder [74]. The third and fourth are active methods that are easily implemented in the PV inverter, and that curtail the active power injected into the feeder as a function of the local voltage [8, 12, 58, 59]. The main advantages of these APC techniques are that they allow the installation of relatively larger PV systems without the risk of overvoltage. The reduction in active power injection only happens when, and if, overvoltage is about to occur. In one of the active methods, the same coefficients are used in all PV inverters. One issue worth discussing is the contribution, in terms of active power curtailed, of each inverter so as to prevent overvoltage in the feeder. PV inverters located further from the low voltage transformer will have higher local voltages and therefore will have more power curtailment than those closer to the transformer. This will certainly have a negative impact on their revenues from PV power injection. To overcome this problem, a new approach that allows the equal sharing of the APC required to prevent overvoltage among all inverters is presented. In such a case, the inverters will present different APC

parameters, chosen as a function of the feeder characteristics and position of the inverters in the feeder.

As discussed in Section 1.1.1, CAN CSA C22.2 No. 257-06 [20] specifies the electrical requirements for inverter-based micro-distributed resource system interconnection to LV grids in Canada. This standard recommends using the CSA CAN3-C235 [21] as guidance for appropriate distribution system steady-state voltage levels. Based on these standards, for single-phase connection, normal operating conditions (NR – Normal Range) occurs when the voltage level is within 0.917 and 1.042 pu. During extreme operation conditions, the steady-state voltage limits are 0.88 pu and 1.058 pu. As most Canadian utilities adopt the CAN3-C235 [21] limits, these will be adopted in this study.

Section 3.1 presents the candidate techniques for overvoltage prevention. Section 3.2 introduces the benchmark. Section 3.3 presents the design considerations for the droop-based APC schemes and shows how the system's voltage profile changes with the net power generated/consumed for different voltage prevention schemes. The system's voltage profile for a 24-hour period with typical PV generation and load profiles is shown in Section 3.4. Section 3.5 presents a one-year simulation study using PSCAD to estimate the energy yields and overvoltage occurrences for the feeder under study. Section 3.6 presents an estimation of yearly energy yields to evaluate the performance of the APC schemes with azimuth diversification of the PV panels. Finally, the conclusions are stated in Section 3.7.

3.1. Candidate Techniques for Overvoltage Prevention in LV PV Residential Feeders

Section 1.1.2 discussed the voltage control solutions available for LV feeders with high-penetration of PVs. The azimuth diversification of PV panels can support the voltage control task reducing the PV power generation peaks. The main limitation of reducing the secondary LV transformer voltage, namely adjusting the tap (assuming that the tap cannot be changed frequently), is being able to find a setting that can be used for rated and no generation of PV without violating the voltage limits. Upgrading the conductors is a very effective but expensive approach, especially for underground feeders. The addition of voltage regulators introduces another unreliability factor into the system, which should be considered by LDNOs. Reactive power control may result in higher currents, and losses, in the feeder and also in lower power factors at the input of the feeder. This is especially true in LV systems, where voltages are less sensitive to reactive power due to a "more resistive" feeder characteristic. The apparent power of the inverters might also have to be increased. Demand side management requires significant investments in control and communication infrastructure. Energy storage units are usually expensive and the cost benefit ratio can be low if they have to be sized to store the surplus of high penetration RETs.

Three techniques are considered in this thesis that do not require communication infrastructure and do not need investments from the utility. First, the reduction of the installed PV capacity is discussed, which is the main approach used. This is followed by looking at the impact of diversifying the solar panel orientation (azimuth). The third

technique involves the APC of PV inverters. The option of APC seems very attractive because it requires minor modifications in the RET inverter control logic. It is also only activated when needed, thereby minimizing the amount of curtailed active power, also known as output power losses (OPL). In addition, no communication infrastructure is required. APC still allows the deployment of larger amounts of PV without the need for impact assessment studies.

3.1.1. Reducing Installed PV Capacity

Overvoltage happens mainly when the net generation in the feeder exceeds a certain amount, causing the voltage rise in the feeder to exceed the operational limits. As discussed in Section 1.1, residential loads cannot be correlated with PV generation. Thus, a maximum installed PV capacity can be defined based on typical characteristics of the feeder in order to prevent the voltage rise in the feeder from being sufficient to be considered a case of overvoltage. This would reduce the maximum instantaneous active power generation and, consequently, the yearly energy yields of the feeder.

3.1.2. Diversifying the Azimuth of the Rooftop PV Systems

As presented in Section 1.1.2.2, if one varies the azimuth angle of the PV systems around the ideal value, one can reduce the total peak net generation in the feeder and increase the generation at non-peak times and, consequently, reduce the probability of incurring overvoltages. This will not drastically affect the yearly net energy generation level, but can provide a smoother peak hour generation.

3.1.3. Droop-based APC

Droop control is a well-known technique used for operation and power sharing among generators connected in parallel. It primarily relates active power with frequency. In LV systems, the relationship of voltage with active power is stronger than with reactive power, given the highly resistive line characteristics [8, 14].

Grid-tie inverters are typically controlled as current sources with maximum power point tracking (MPPT) algorithms. In this chapter, the actual power injected by the inverter is proposed as a function of the bus voltage (V) according to:

$$P_{inv} = P_{MPPT} - m\left(V - V_{cri}\right) \tag{3.1}$$

for $V \geq V_{cri}$ and $P_{\text{inv}} \geq 0$. Here, P_{MPPT} is the maximum power available in the PV array for a given solar irradiance (kW), m is a slope factor (kW/V) and V_{cri} is the voltage (V) above which the power injected by the inverter is decreased with a droop factor. For $V < V_{cri}$, the inverter injects P_{MPPT}, as most PV inverters do. It uses local voltage to define how much power should be curtailed from each PV inverter. The droop coefficients of the inverters (m and V_{cri}) can be selected in order for the inverters to comply with the voltage limits at their connection buses. The logic used to implement (3.1) is shown in Figure 3.1.

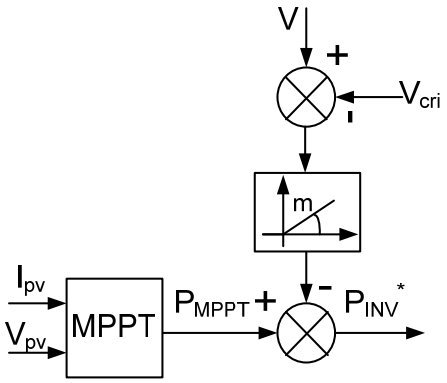

Figure 3.1. Droop-based APC of the PV inverter.

3.2. Net-zero Energy PV Benchmark

This Section describes the model of an overhead residential sub-urban feeder used in this study. The system was modeled based in [75], using a section of the LV part of the feeder with a total of 12 net-zero energy houses from the residential neighborhood.

The neighborhood under investigation, presented in Figure 3.2, has a 75 kVA, single-phase transformer, 14.4 kV - 120/240 V and the feeder has a total length of 120 m. This transformer does not present an on-load tap-changer and the voltage regulation is done in the MV side substation. The backbone of the feeder is 100 m long with 2 live wires twisted around a grounded neutral cable (NS 90 3/0 AWG). Along this circuit, 12 customers are connected in pairs to a splice every 20 m. The service entrance consists of 2 wires supported by a grounded neutral steel cable (NS 90 1/0 AWG) and has a length of drop of 20 m.

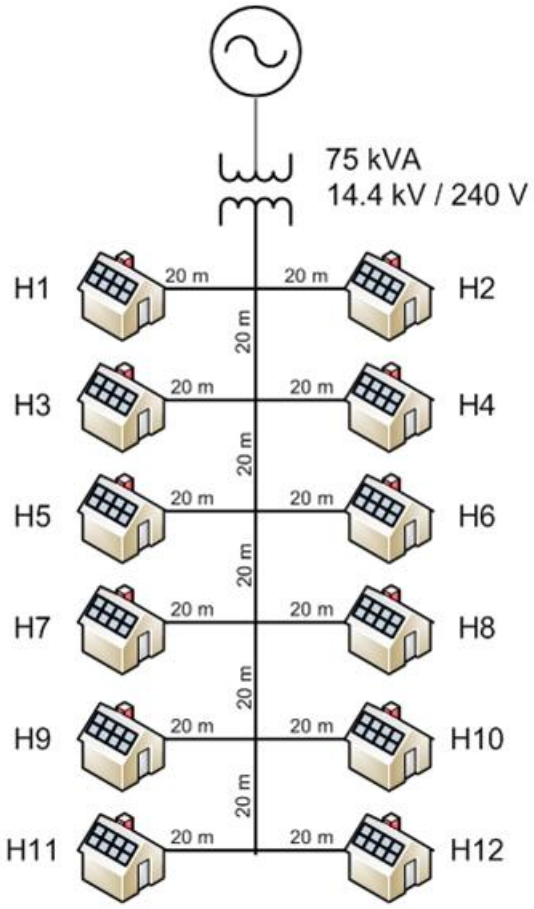

Figure 3.2. Overhead residential test feeder configuration.

The house characteristics for the voltage profile studies is based on the Alstonvale net-zero energy solar house (ANZH) [76, 77]. It is able to generate as much energy as it consumes in one year and was one of the winners of the EQuilibrium Initiative, a Canadian competition of sustainable houses that took place in 2006-2007. The ANZH presents a building integrated photovoltaic thermal (BIPV/T) rooftop system, which is capable of generating 22 kWp of thermal energy and 8.4 kWp of electrical power. The annual electricity generation expected from this house is about 10,000 kWh, which is estimated to match the annual consumption of the ANZH with a plug-in hybrid electric vehicle (PHEV) [76, 77]. The PV inverter and the house load models both use a voltage

dependent current source to represent the instantaneous active and reactive power load/generation of the houses/PVs. A basic inverter protection for voltage trip limits was modeled following Canadian standards [22, 23]. The voltage disconnection thresholds are 0.88 and 1.1 pu and the reconnection thresholds are 0.89 and 1.09 pu for undervoltage and overvoltage, respectively.

PSCAD© was chosen as the simulation platform in this study. The transformer, PI section lines, loads, and branches are implemented using standard library models. The single-phase line parameters are given in Table I. Figure 3.3 shows the configuration of the transformer model. Table II provides the low voltage transformer parameters.

TABLE I - SINGLE-PHASE PI SECTION LINES PARAMETERS (PER LINE CONDUCTOR)

	Drop Lines	*Pole-Pole Lines*
R	0.549 Ω/km	0.346 Ω/km
L	0.23 mH/km	0.24 mH/km
C	0.055 μF	0.072 μF/km

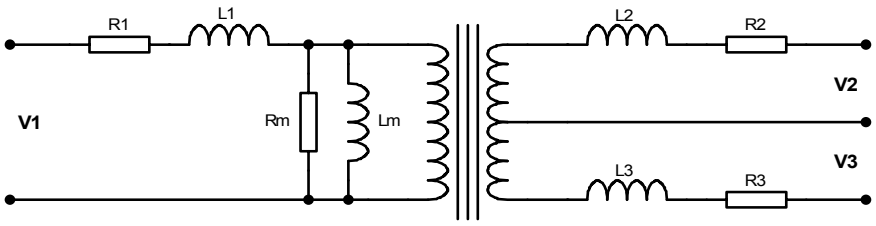

Figure 3.3. Transformer model.

TABLE II - LV TRANSFORMER PARAMETERS

S	75 kVA	L_1	0.02 pu	$L_{2,3}$	0.025 pu
V_1	14.4 kV	$V_{2,3}$	120 V	R_m	500 pu
R_1	0.006 pu	$R_{2,3}$	0.012 pu	L_m	500 pu

3.3. Basic System Operation and APC Design Approaches

Three case studies are investigated to verify how the system's voltage profile changes with the net power generated/consumed, without an overvoltage prevention scheme and with the proposed droop-based APCs. For the sake of simplicity, all houses are assumed to present identical load characteristics. A study with the houses presenting different load profiles is shown in the following Section. The loading/generation of the 12 houses is assumed to vary between 75 kW net load (transformer capacity) to 75 kW net generation at a unity power factor. Although the total PV capacity installed in the system is 100.8 kW, a minimum load is considered to be always present in this system, resulting in a maximum net generation of 75 kW during peak generation and low loading period in the feeder. The voltage in the secondary of the transformer was set at 1.02 pu, in order to allow a maximum 5% voltage drop in the last customer meter when the 12 houses consume 75 kW.

3.3.1. Base Case

The first case corresponds to the standard approach where the PV inverters operate with MPPT until, if ever, the voltage at their point of connection reaches 1.1 pu, when they would shut down. Results for this scenario are presented in Figure 3.4. One sees that the voltage in the last two houses (H 11/12) reaches the CSA CAN3-C235 limits for normal operation (NR) (1.042 pu) only for net generation above 27 kW (2.25 kW/house, ~36% of the LV transformer capacity). The limit for extreme operation (1.058 pu) is violated starting at 47 kW (3.92 kW/house, ~63% of the LV transformer capacity), which is well below the inverter's overvoltage protection (trip) threshold of 1.1 pu in all parts of the feeder. One can take this value as the maximum amount of PV that can be installed in the feeder without overvoltage prevention measures, as the minimum load considered in this study is not necessarily present in the system at all times.

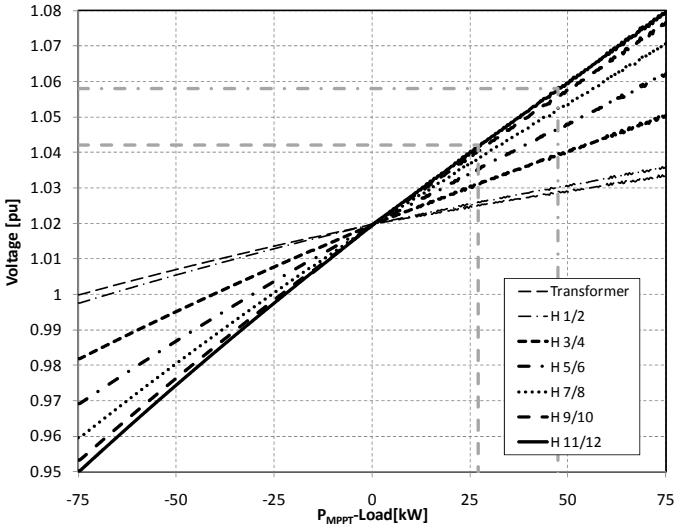

Figure 3.4. Voltage profile in the LV feeder at the point of connection of each house.

3.3.2. Droop-based APC Design and Results

The second case considers that all PV inverters are controlled with droop-based APC and present the same droop coefficients. The droop parameters should be selected so that APC only occurs for local voltages between 1.042 pu (maximum voltage level in NR) and 1.058 pu (extreme operation conditions). V_{cri} is defined as the voltage where the curtailment starts: 1.042 pu. In a 240 V rated system, it is 250 V.

The droop coefficient m is obtained by (3.2). The PV inverters' active power is curtailed linearly with the local voltage (V), starting at V_{cri} up to the voltage limit of 1.058 pu, or 254 V, when the PV inverters should not inject any power. The m coefficient is obtained dividing the power to be curtailed in this period by the voltage variation. For a 8.4 kW PV system, it is:

$$m = \frac{P_{pv\max}}{V_{1.058\,pu} - V_{1.042\,pu}} = 2.1\frac{kW}{V} \tag{3.2}$$

Figure 3.5 presents the feeder voltage profile with the droop-based APC. In this case, the maximum voltage found was ~1.052 pu at the end of the feeder, well below the 1.058 pu limit for extreme operation, because of the minimum local load considered in the system.

The houses downstream inject less power than the ones closer to the transformer, as can be seen in Figure 3.6. The houses closer to the transformer were able to export full PV power available even at maximum net power generation (P_{MPPT}-*Load = 75 kW*). The last customers were able to export just around 2.2 kW or 35% of the net power available (6.25 kW). Thus, the PV revenues for these customers are lower than for the other customers.

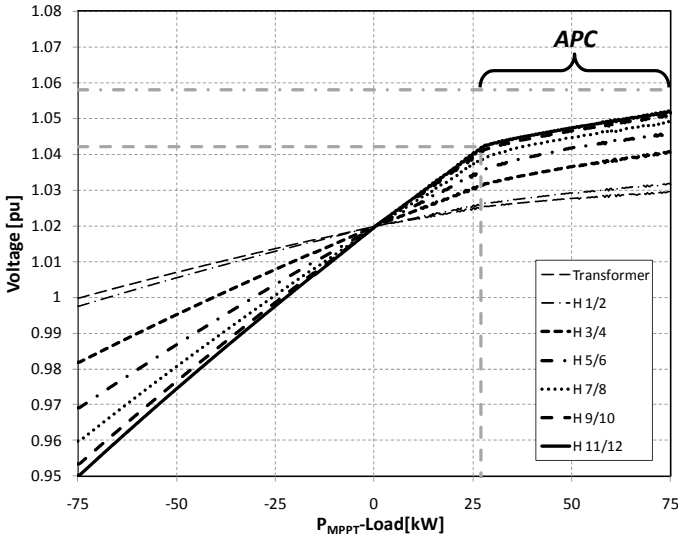

Figure 3.5. Voltage profile in the LV feeder at the point of connection of each house in the presence of droop-based APC.

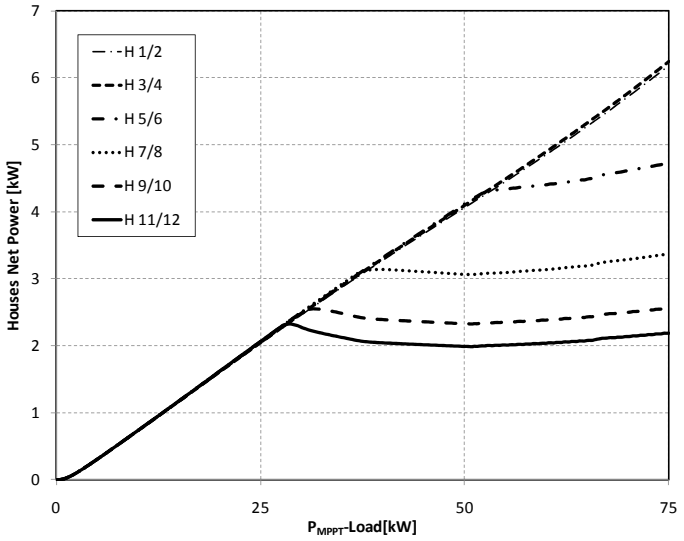

Figure 3.6. Power exported by each house with droop-based APC.

3.3.3. Droop-based APC Designed for Output Power Losses Sharing

In this last case, the inverters are also controlled with droop-based APC, but the droop parameters are different so that the output power losses (OPL) can be equally shared

among all inverters. The design of the droop coefficients for APC with OPL sharing (APC-OPLS) is based on the voltage sensitivity of the system, obtained running a Newton-Raphson load flow in Matlab for the backbone of the LV feeder, as presented in the previous chapter.

For the feeder under consideration, operating at 75 kW net generation, and disregarding the drop lines, for simplicity, sub-matrix S_{V21} is obtained as presented in (3.3):

$$\frac{\Delta V_{Hi/Hi+1}}{\Delta P_{Hj/Hj+1}} = \begin{bmatrix} 0.0509 & 0.0486 & 0.0468 & 0.0455 & 0.0447 & 0.0442 \\ 0.0510 & 0.1055 & 0.1025 & 0.1002 & 0.0988 & 0.0981 \\ 0.0510 & 0.1056 & 0.1595 & 0.1564 & 0.1543 & 0.1532 \\ 0.0510 & 0.1056 & 0.1596 & 0.2136 & 0.2109 & 0.2095 \\ 0.0510 & 0.1056 & 0.1596 & 0.2136 & 0.2682 & 0.2666 \\ 0.0510 & 0.1056 & 0.1596 & 0.2136 & 0.2682 & 0.3241 \end{bmatrix} \left[\frac{V}{kW}\right] \tag{3.3}$$

where i = 1,3,5…11 and j = 1,3,5…11.

The meaning of each element in this sub-matrix should be interpreted as the variation that would happen in the voltage profile in a certain bus (i) in the case of a hypothetical 1 pu variation in the injection of active power in bus j. The positive signs of all elements indicate that by decreasing *P*, the bus voltages would also decrease.

The droop-based APC coefficients are designed to operate between 1.042 pu and 1.058 pu of the grid voltage. As in the basic APC scheme, V_{cri} is defined as the voltage where the curtailment starts. Thus, to obtain V_{cri}, the voltage in the inverter bus is taken from Figure 3.4, when the last (critical) bus reaches 1.042 pu (maximum value in the NR).

The maximum voltage expected at full generation, without APC, is 1.08 pu at the last two houses as per Figure 3.4. The active power injected into the LV feeder must be curtailed so as to keep the voltage at the last house within the extreme operation limit (1.058 pu).

This corresponds to a ΔV of 0.022 pu (5.2 V). Considering that the ΔP should be the same in all buses:

$$\Delta P = \frac{\Delta P_{Hi/Hi+1}}{\Delta V_{H11/12}} \Delta V_{H11/12,i} \tag{3.4}$$

and that the total ΔV in the last two houses should be 0.022 pu, considering the effect of curtailing all the inverters equally, this means:

$$\Delta V = \sum_{i=1,3...11} \Delta V_{H11/H12,i} = 5.2\,V \tag{3.5}$$

Therefore, the active power to be curtailed per bus with 2 houses is,

$$\Delta P = \frac{\Delta V_{H11/H12,i}}{\sum_{i=1,3...11} \frac{\Delta V_{H11/12}}{\Delta P_{Hi/Hi+1}}} = \frac{5.2\,[V]}{1.096\left[\frac{V}{kW}\right]} = 4.75kW \tag{3.6}$$

This means that each inverter should curtail $\Delta P/2 = 2.375\ kW$, when the feeder has the potential to operate with net generation of 75 kW.

Using the sensitivity matrix, (3.3), the voltage at each bus after curtailment ($V_{Ci/i+1}$) can be estimated using:

$$V_{Ci/i+1} = V_{i/i+1} - \Delta P \sum_{j=1,3...11} \frac{\Delta V_{Hi/i+1}}{\Delta P_{Hj/Hj+1}} \tag{3.7}$$

where $V_{i/i+1}$ is the voltage in the bus $i/i+1$ without APC.

For each bus, the droop coefficient m is obtained knowing ΔP and the voltage in each bus using:

$$m_{i/i+1} = \frac{\Delta P}{V_{Ci/i+1} - V_{cri}} \tag{3.8}$$

As an example, for the last two inverters:

$$m_{11/12} = \frac{2.375[kW]}{254[V] - 250[V]} = 0.59\frac{kW}{V} \tag{3.9}$$

The coefficients obtained using this procedure and used in the simulation are presented in Table III.

TABLE III - DROOP COEFFICIENTS FOR EACH INVERTER

PV House	V_{cri}*[pu]*	*m [kW/V]*	*PV House*	V_{cri}*[pu]*	*m [kW/V]*
1/2	1.026	2.54	*7/8*	1.039	0.72
3/4	1.031	1.26	*9/10*	1.041	0.64
5/6	1.036	0.89	*11/12*	1.042	0.59

Figure 3.7 presents the feeder voltage profile with the APC-OPLS scheme. In this case, the maximum voltage was ~1.058 pu, at the end of the feeder, validating one of the design specifications. The sharing of the OPL among all inverters is demonstrated in Figure 3.8. There, one sees that all the houses have approximately the same amount of power being exported, in the region of active power curtailment, P_{MPPT} - P_{Load} > 26 kW. The small difference in exported power occurs because only the backbone of the LV feeder was considered to generate the voltage sensitivity matrix.

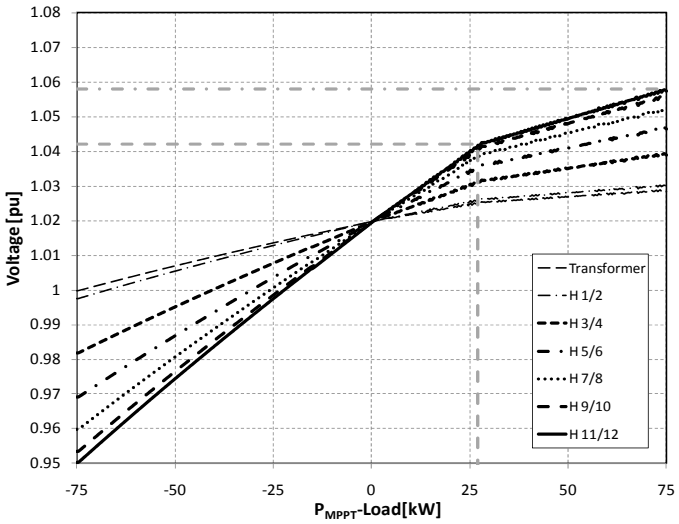

Figure 3.7. Voltage profile in the LV feeder at the point of connection of each house in the presence of droop-based APC-OPLS.

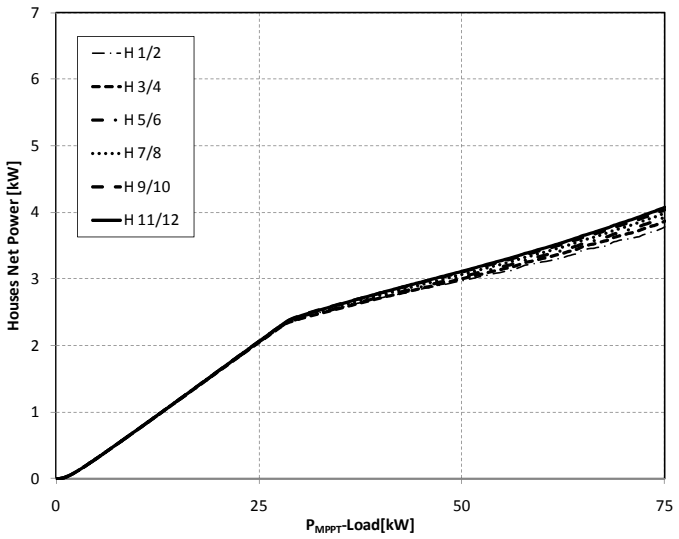

Figure 3.8. Power exported by each house with droop-based APC-OPLS.

3.4. Performance with Different House Loads

Verification of the voltage profile and amount of active power curtailed with the proposed schemes is important for the suburban residential feeder considering typical PV

power generation and load profiles. In this Section, a 24 hour period is considered. The 24 h PV inverter output was estimated for Montreal (Latitude 45°55' N and Longitude 73° W) using HOMER and data taken from NASA weather information center [78] for a clear, mild summer day. A residential load profile (type 1) based on [19] was also used in houses 1, 4, 7, and 10. To account for load diversity, load profile type 1 was time-shifted by two hours later to create load profile type 2, used in houses 2, 5 8, and 11, and time-shifted by two hours earlier to create load profile 3, used in houses 3, 6, 9, and 12.

The loads and PV profiles are presented in Figure 3.9. The values represent a 10 min average energy consumption /production, which is appropriate for a study focused on steady state conditions. There, one sees that for about an 11-hour period (6-17 h), more energy is being produced in the PV systems than is consumed by the loads. In this case, the feeder would be exporting active power to the grid (transformer) which could result in overvoltages.

Figure 3.10 presents the voltage profile at the various buses for the base case, without any APC based overvoltage prevention scheme. Only one house connected per feeder bus is presented, since the results are similar for the other house. The maximum voltage in the system (1.066 pu) occurs at noon, in houses 11 and 12, at the end of the feeder. There, the voltage exceeds the extreme operation condition from 9:40 h to 14:10 h (19% of the day). Houses 7 to 12 experience overvoltages (above 1.058 pu) for at least a small period of time during the day. Based on this result, and using the sensitivity information from (3.7), the PV capacity should be limited to about 7.5 kWp per house to prevent overvoltage on this specific day. If the conditions on this day do not correspond to the day of the year

with maximum net power generation in the feeder, the PV capacity should be further reduced to prevent overvoltages.

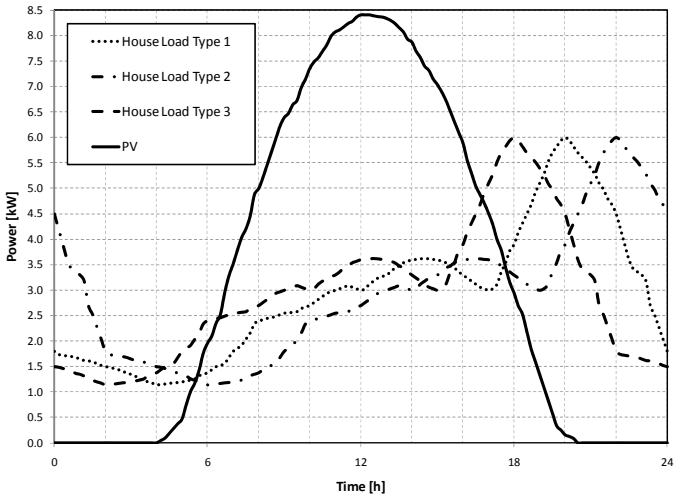

Figure 3.9. House load profile and PV production for a 24 h period.

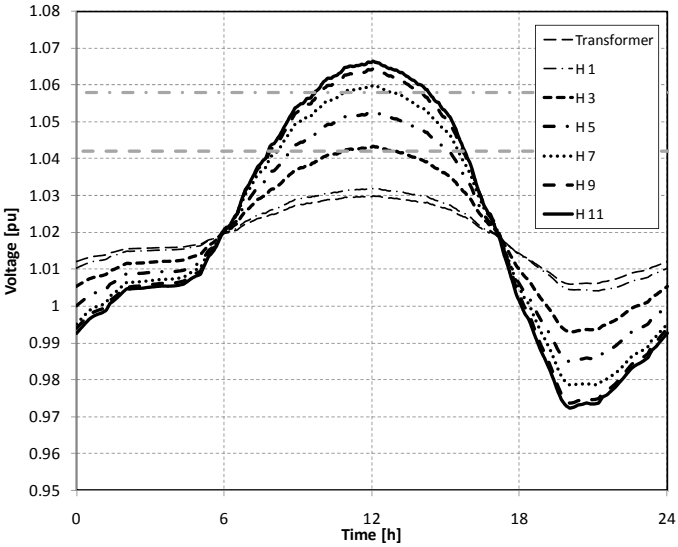

Figure 3.10. 24 h voltage profile without droop-based overvoltage prevention.

Figure 3.11 presents the voltage profile with the inverters using the droop-based APC. None of the houses experienced voltages above 1.058 pu. The maximum voltage in the

system (1.049 pu) occurs at noon, in houses 11 and 12. The total feeder load at this time is 37 kW. Subtracting this from the PV power that can be obtained with the inverters operating with MPPT (12 x 8.4 kWp) results in 63 kW. Using this value in the horizontal axis of Figure 3.5, which was created assuming uniform load distribution in the feeder, one obtains a voltage magnitude of 1.050 pu at the last bus of the feeder. This is very close to the value obtained in Figure 3.11, showing that, in this case, the characteristic of the load diversification did not have a significant impact on the magnitude of the voltage at the last bus, the most susceptible to overvoltage in this feeder.

The power curtailed in each house by the PV inverters is presented in Figure 3.12. The last house had almost 3 kW curtailed at noon. This amount was smaller for houses closer to the LV transformer. On the other hand, houses 1 to 4 did not have any power curtailed at any moment.

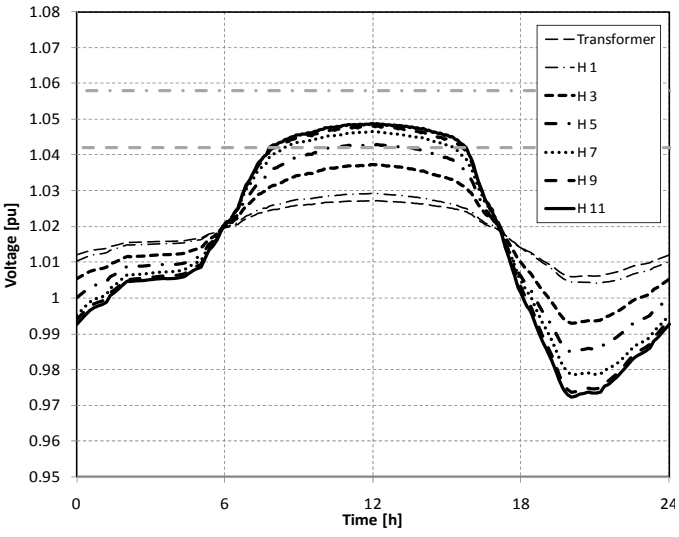

Figure 3.11. 24 h voltage profile with APC.

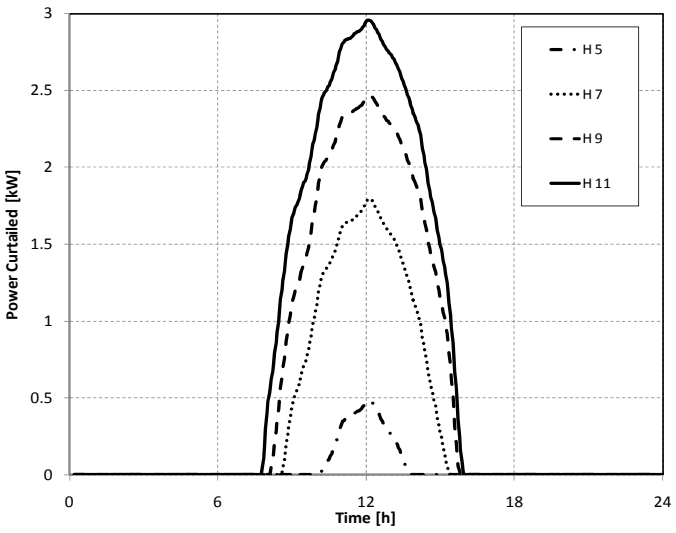

Figure 3.12. Power curtailed by APC in each house.

Figure 3.13 presents the voltage profile with the inverters using the APC-OPLS scheme. As seen for the previous APC, none of the houses experienced voltages above 1.058 pu. The maximum voltage in the system (1.052 pu) occurs at noon, in houses 11 and 12. Knowing that the net value of P_{MPPT}-*Load* is 63 kW, and using this value in the horizontal axis of Figure 3.7, which was created assuming uniform load distribution in the feeder, one obtains a voltage magnitude of 1.054 pu at the last bus of the feeder. This is very close to the value obtained in Figure 3.13, showing that, in this case, the characteristic of the load diversification also did not have a significant impact on the magnitude of the voltage at the last bus, the most susceptible to overvoltage in this feeder.

Figure 3.14 presents the active power curtailed in each house. At peak generation time, this varied between 1.3 kW and 1.6 kW, which is not significant if compared to the standard APC. The differences in the amount of APC can be justified by the different

house load conditions and because only the backbone of the LV feeder was considered in generating the voltage sensitivity matrix and in calculating the droop coefficients.

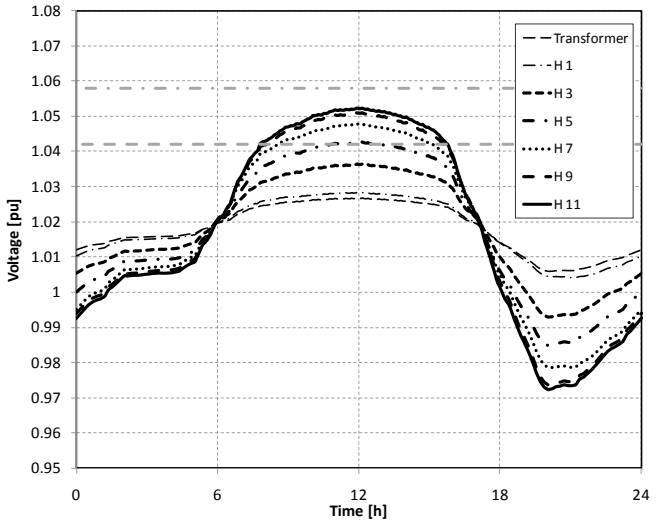

Figure 3.13. 24 h voltage profile with APC-OPLS.

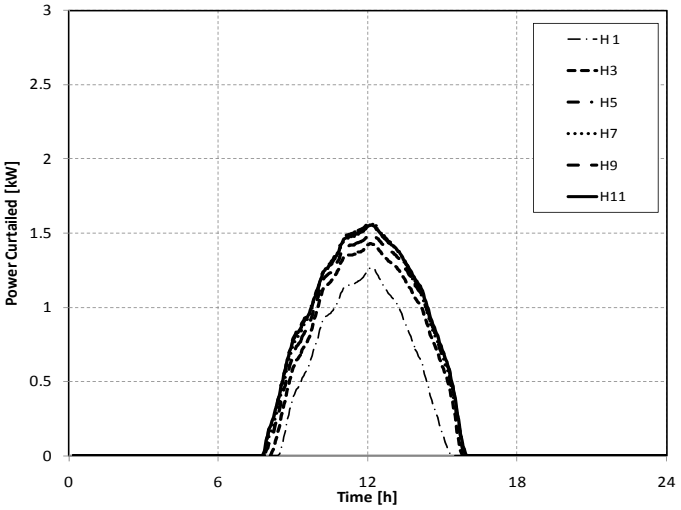

Figure 3.14. Power curtailed by APC-OPLS in each house.

Figure 3.15 shows the power exported to the grid (primary of transformer) considering APC and APC-OPLS. There, one sees that inverter operation with APC resulted in a maximum exported power that was 2.6 kW larger than with APC-OPLS.

Note that the amount of APC required for preventing overvoltage depends significantly on the net power produced in the feeder. For a given PV generation profile, the amount of APC decreases as the power demanded by the residential loads increases. However, this relationship is not "one to one," since the PV inverters do not attempt to regulate the ac bus voltages at a fixed value by means of active power curtailment in any of the methods discussed in this Section.

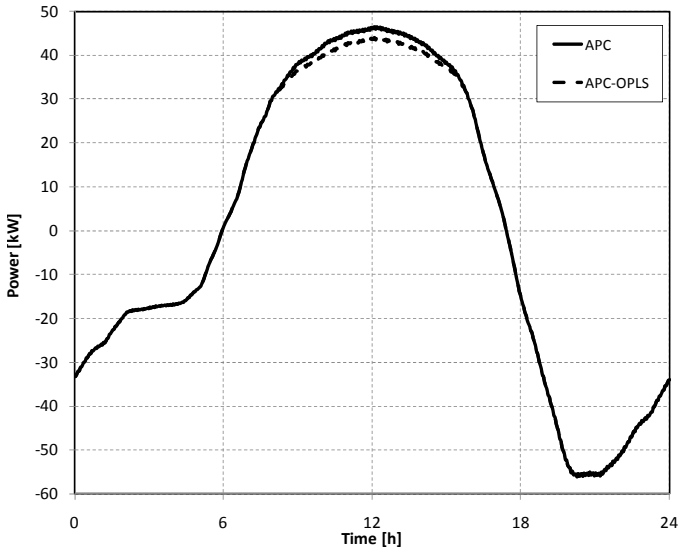

Figure 3.15. Power exported to the grid (transformer's primary) with APC and with APC-OPLS.

3.5. Estimation of Yearly Energy Yields in a Feeder with High-penetration of PV

PV system owners are particularly interested in the energy yield (revenue) they will get from their systems, which will be affected by the overvoltage prevention schemes. Considering the stochastic nature of residential load and PV generation, a fair assessment of the impact of these schemes on the PV revenues requires a long term study with typical load and solar irradiance profiles. This is done in this Sub-Section for the LV residential feeder benchmark with net-zero energy houses implemented in PSCAD, considering both the APC schemes investigated in [58], as well as a passive method where overvoltage is prevented by limiting the installed PV capacity to an appropriate value.

3.5.1. Yearly Load and PV Generation Profiles

The software HOMER is used to estimate the load profiles and the PV inverter's power output for each hour of one year. Two yearly load profiles were generated, in order to consider some level of variation in the load profiles in the houses. Average daily non-electric heated residential load data from [28] for different seasons, which also considered weekday and weekends (Figure 3.16 and Figure 3.17, respectively), were used as reference for HOMER to generate the yearly load data sets. December until February was considered winter, March–May was Spring, June–August was Summer and September–November was Fall.

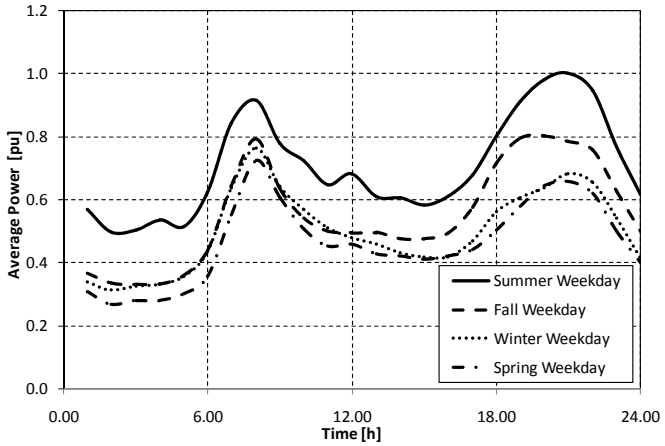

Figure 3.16. Weekday average load profiles.

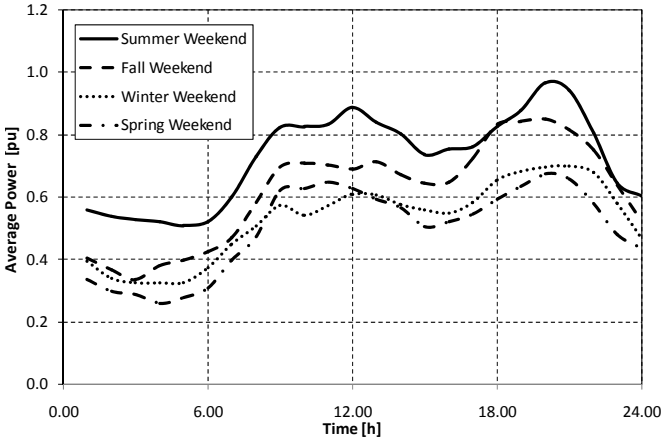

Figure 3.17. Weekend average load profiles.

The seasonal data were then scaled in HOMER to have an annual average energy demand of 30 kWh/day. The day-by-day and hour-by-hour random variability factors of 35% and 20%, respectively, were considered to represent the high variability characteristic of residential loads. The houses located on the left side of the feeder were given this load profile. The load profile box plot obtained from HOMER is presented in Figure 3.18. It shows the mean, the maximum, and minimum average power as well as the average daily max and min power for each month. The second load data set, attributed to the houses in

the right side of the feeder, was generated using the same procedure, this time using the data from [28] time shifted one hour later.

The one year hourly PV inverter output was estimated for Montreal (Latitude 45°55' N and Longitude 73° W) using HOMER and data taken from the NASA weather information center [78]. All of the 8.4 kWp PV arrays are considered to be south faced, placed with a slope of 45° and having a derating factor of 0.8. The efficiency of the inverter was assumed as 96%. Figure 3.19 shows a PV inverter average power output box plot generated by HOMER.

The hourly data content of the load datasets and PV inverter output power were exported monthly in CSV files and adapted to be used in PSCAD as input for the one-year study.

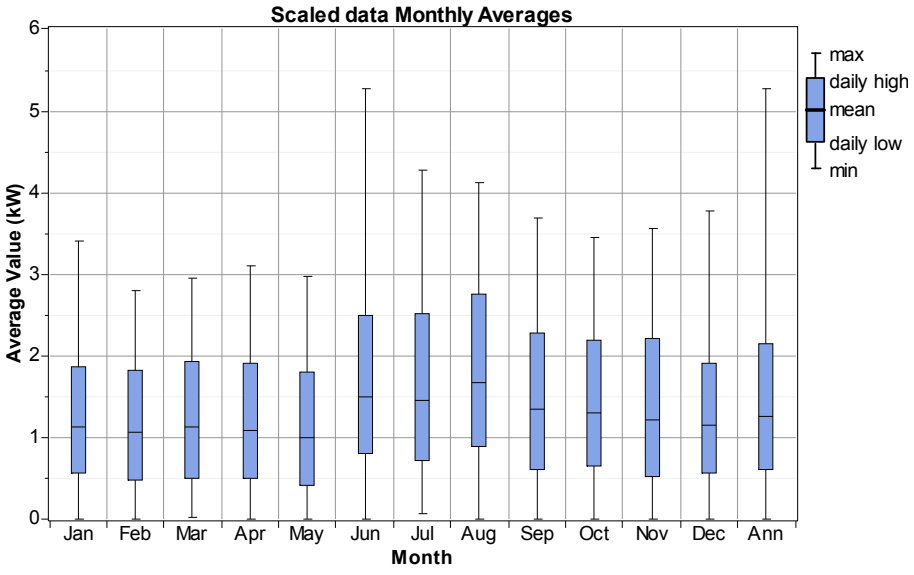

Figure 3.18. Scaled load profile monthly averages for load dataset 1.

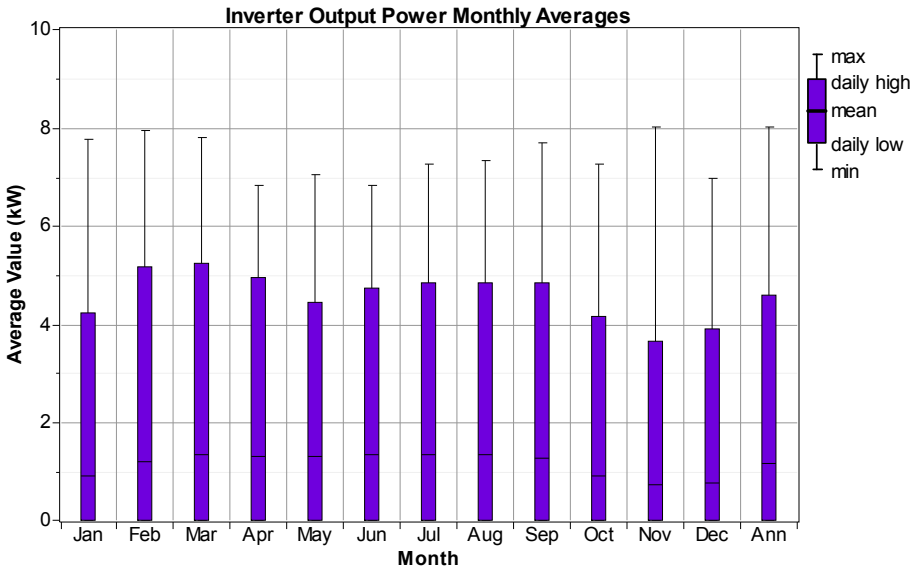

Figure 3.19. Monthly averages for PV power generation.

3.5.2. Simulation Results

An XY table is used in PSCAD to apply the load and generation active power references. For each of the cases studied, the simulation generated 35052 samples taken along the 8760 hours of the year, obtained through the interpolation of the input data, to give a sampling time of about 15 min. This sampling time step was chosen considering the compromise with simulation time. The results are exported from PSCAD and analyzed using IBM PASW© Statistics (Predictive Analytics SoftWare).

Four case studies are investigated to verify the system's voltage and energy yields for the original net-zero energy PV neighborhood, using reduced installed PV capacity to prevent overvoltage and with the proposed droop-based APC schemes.

3.5.2.1. Base Case

The first case corresponds to the standard approach where the PV inverters operate with MPPT until, if ever, the voltage at their point of connection reaches 1.1 pu, when the basic inverter protection for voltage trip limits [22, 23] shuts down the PV inverters.

Figure 3.20 presents the histogram of the voltage in the last house. It shows the number of occurrences at a certain voltage level. The vertical line indicates the 1.058 pu threshold where overvoltage occurs. There, one sees that a number of cases of overvoltage occur in this bus. The maximum voltage found was 1.088 pu, recorded in H 12 on January on a mild, clear day, where the load in the system was low and the generation was close to its maximum value. The minimum voltage registered was 0.96 pu. In addition, from the data obtained, one calculates that the average voltage presented was 1.017 pu, with a standard deviation of 0.018 pu.

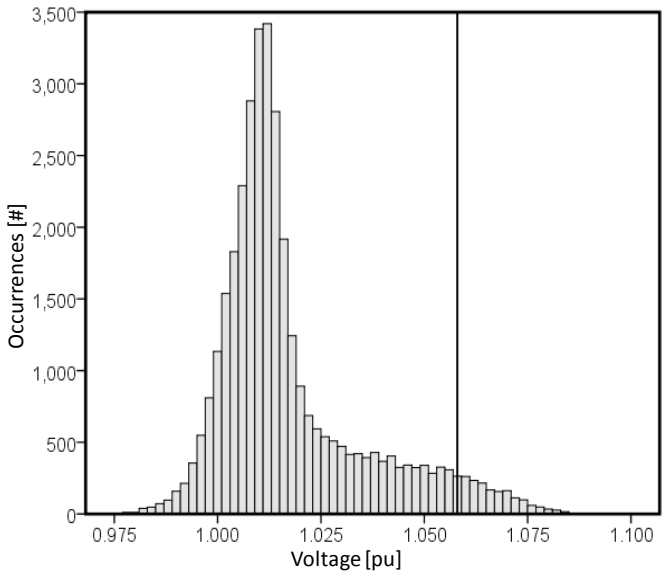

Figure 3.20. Histogram of the voltage in the last house – number of occurrences in a one-year period at a certain voltage [pu] - Base Case.

Figure 3.21 shows the percentage of time that overvoltage happened in each even house [%] when the event occurred. Houses 1 to 4 did not present any overvoltage during the year under study. The results for the odd houses are similar, so they are omitted. An overvoltage is seen for 5% of the samples (voltage above 1.058 pu) at the last house of the feeder (H 12) and as the houses get closer to the transformer, the occurrence of overvoltage at their buses is reduced.

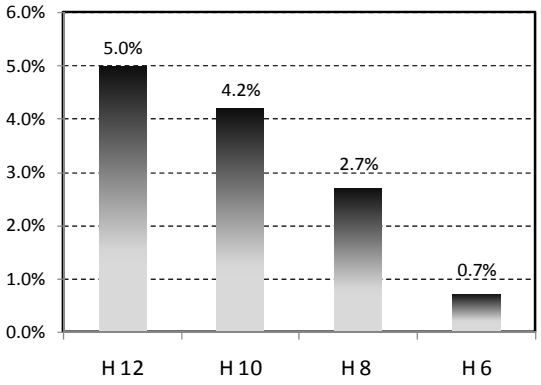

Figure 3.21. Overvoltage occurrences in each even house [%] where the event happened.

Figure 3.22 shows the percentage of the occurrences of overvoltage by month. There, one sees that overvoltage will occur in 7.9% of the samples in February, the worst month of the year in this regard. Note that the ANZH is a non-electric heated house, so winter does not necessarily increase the electrical power demand. For the whole year, overvoltage will occur in 5% of the total samples.

Figure 3.23 presents the histogram for the power flow in the primary of the transformer. It shows the number of occurrences at a certain power level. Negative values mean that

power flows from the grid to the houses. The range for the power flow in the transformer goes from -60 kW to 84 kW.

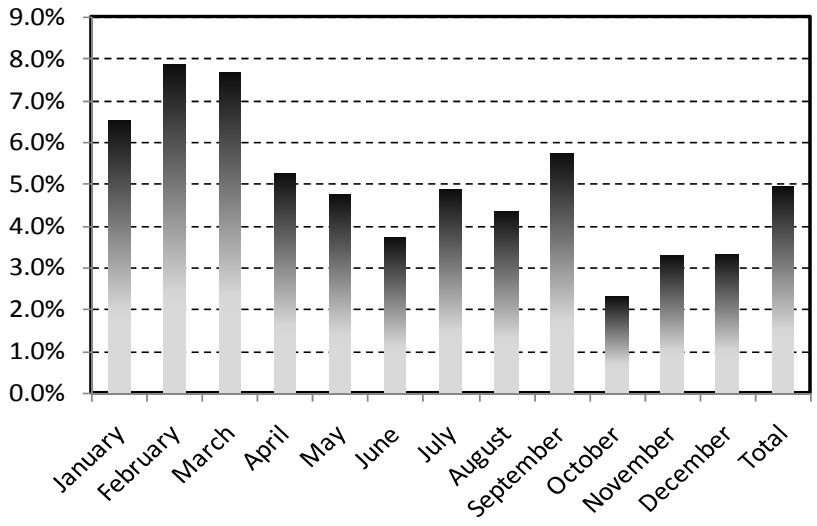

Figure 3.22. Overvoltage occurrences by month [%].

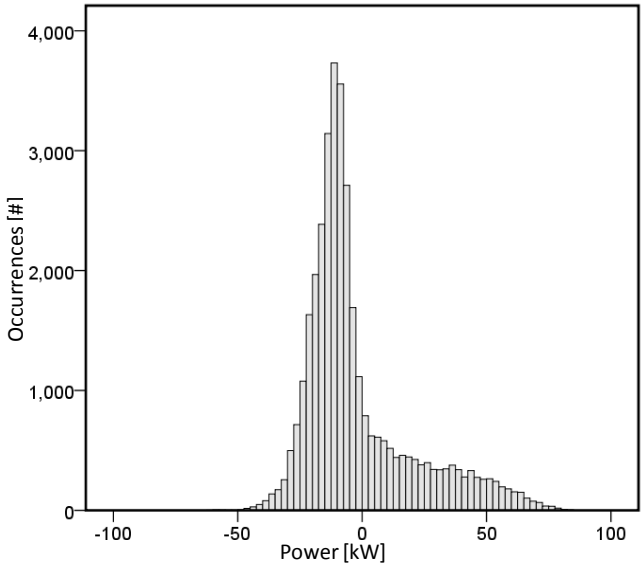

Figure 3.23. Histogram of the power flow in the primary of the transformer – number of occurrences of a certain power [kW] - Base Case.

In addition, from the data obtained, one calculates that the transformer is on average loaded to about -2 kW; thus, the houses consumed more power than they generated, with a standard deviation of 22 kW.

3.5.2.2. Reducing the Installed PV Capacity (Red. PVCap)

The second case considers that the installed PV capacity was reduced from 8.4 kWp to 5 kWp per house. This reduction was defined based on the sensitivity matrix of this system presented in Section 3.3.3 and it was calculated in order to prevent overvoltages, considering that the maximum voltage found in the feeder in the previous case was 1.088 pu.

Figure 3.24 presents the histogram of the voltage in the last house. No cases of overvoltage are seen in this bus or in the feeder. The maximum voltage found was 1.058 pu, as expected by the design approach, and also recorded in H 12 in January. The minimum voltage registered was 0.96 pu. In addition, from the data obtained, one calculates that the average voltage presented was 1.013 pu, with a standard deviation of 0.012 pu.

Figure 3.25 presents the histogram for the power flow in the primary of the transformer. It varied between -60 kW and 47 kW. In addition, from the data obtained, one calculates that the transformer is, on average, loaded to about -8 kW, with a standard deviation of 14 kW.

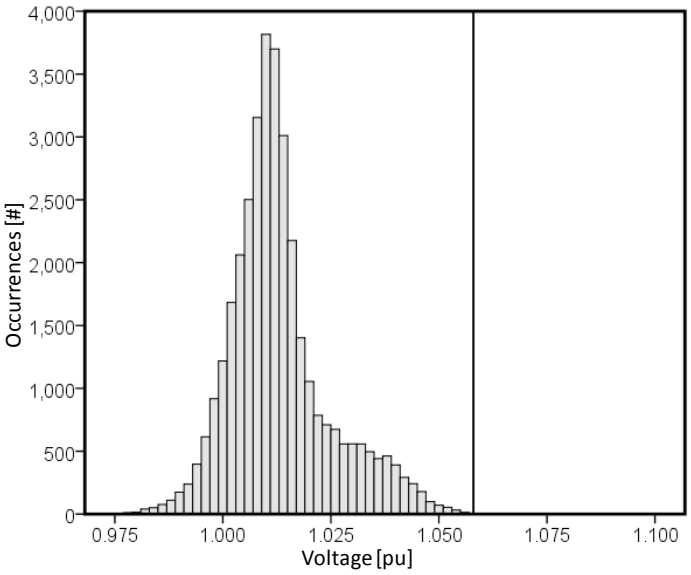

Figure 3.24. Histogram of the voltage in the last house – number of occurrences at a certain voltage [pu] - Red. PVCap.

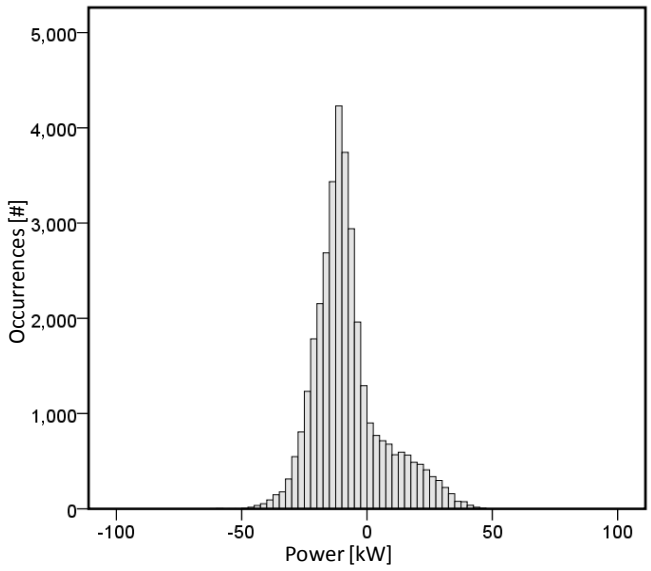

Figure 3.25. Histogram of the power flow in the primary of the transformer – number of occurrences of a certain power [kW] - Red. PVCap.

3.5.2.3. Droop-based APC Results

The third case considers that all PV inverters are controlled with droop-based APCs and present the same droop coefficients as shown in Section 3.3.2.

Figure 3.26 presents the histogram of the voltage in the last house. No cases of overvoltage are seen in this bus or in the feeder and the maximum voltage was 1.052 pu, also recorded in H 12 in January. The minimum voltage registered was 0.96 pu. Note that, as power curtailment occurs for voltages between 1.042 pu and 1.058pu, the voltage occurrences that were above 1.058 pu in Figure 3.20 moved to the region where the APC operates in Figure 3.26. The occurrences for voltages below 1.042 pu are the same in Figure 3.20 and in Figure 3.26. In addition, from the data obtained, one calculates that the average voltage was 1.016 pu, with a standard deviation of 0.015 pu.

Figure 3.27 presents the histogram for the power flow in the primary of the transformer. It varied between -60 kW and 53 kW. Note that, due to the use of APC, the maximum power injected by the PV neighborhood into the MV grid decreased from 84 kW, without APC, to 53 kW. This is the "cost" of preventing overvoltage when the net power produced by the PV neighborhood is high. In addition, from the data obtained, one calculates that the transformer is, on average, loaded at about -3.0 kW with a standard deviation of 19.3 kW.

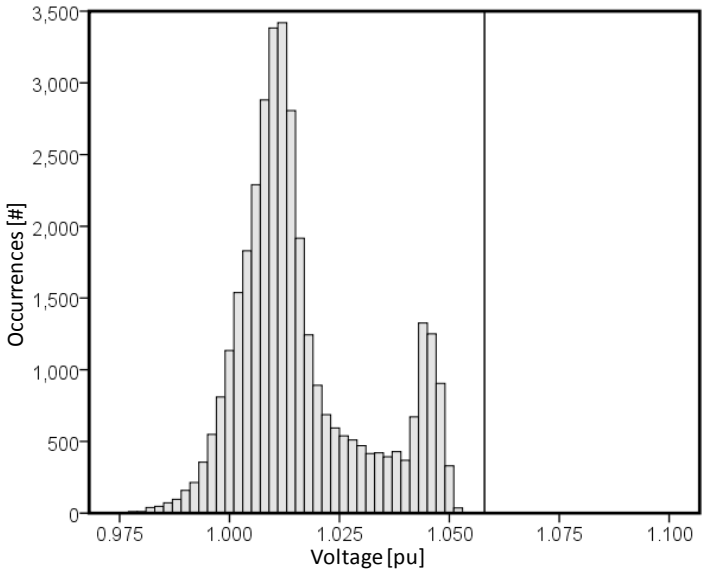

Figure 3.26. Histogram of the voltage in the last house – number of occurrences at a certain voltage [pu] - APC.

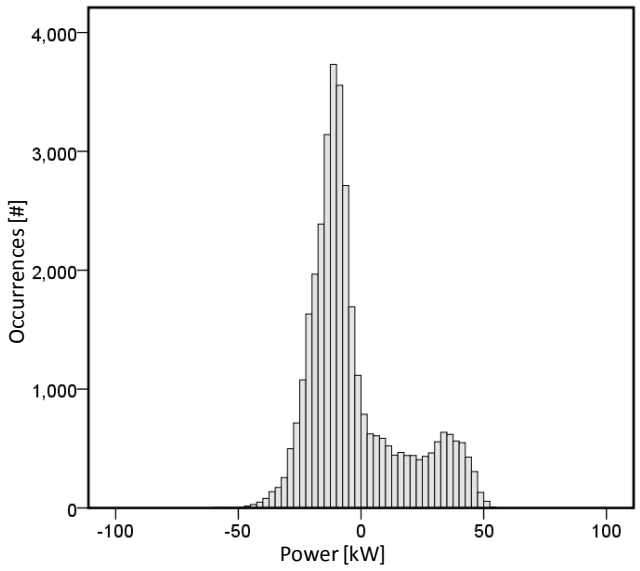

Figure 3.27. Histogram of the power flow in the primary of the transformer – number of occurrences of a certain power [kW] - APC.

3.5.2.4. Droop-based APC Designed for OPL Sharing (APC-OPLS)

Assuming a maximum voltage without curtailment of 1.088 pu (261 V) and using the design approach presented in Section 3.3.3, the coefficients for the APC-OPLS droop function of each PV inverter are obtained and shown in Table IV.

TABLE IV - DROOP COEFFICIENTS FOR EACH PV INVERTER

House	***V_{cri} [pu]***	***m [kW/V]***	***House***	***V_{cri} [pu]***	***m [kW/V]***
1/2	1.026	3.51	***7/8***	1.039	0.99
3/4	1.031	1.73	***9/10***	1.041	0.88
5/6	1.036	1.22	***11/12***	1.042	0.82

Figure 3.28 presents the histogram of the voltage in the last house. No cases of overvoltage occur either in this bus or in the feeder and the maximum voltage found was 1.058 pu, also recorded in H 12 in January. The minimum voltage registered was 0.96 pu. Note that as the power curtailment operates from 1.042 pu of voltage to 1.058 pu, the voltage occurrences that were above 1.058 pu moved to the region where the APC operates. As in the previous case, the occurrences for voltages below 1.042 pu are the same for Figure 3.20, Figure 3.26, and Figure 3.28. In addition, from the data obtained, one calculates that the average voltage presented was 1.016 pu, with a standard deviation of 0.015 pu.

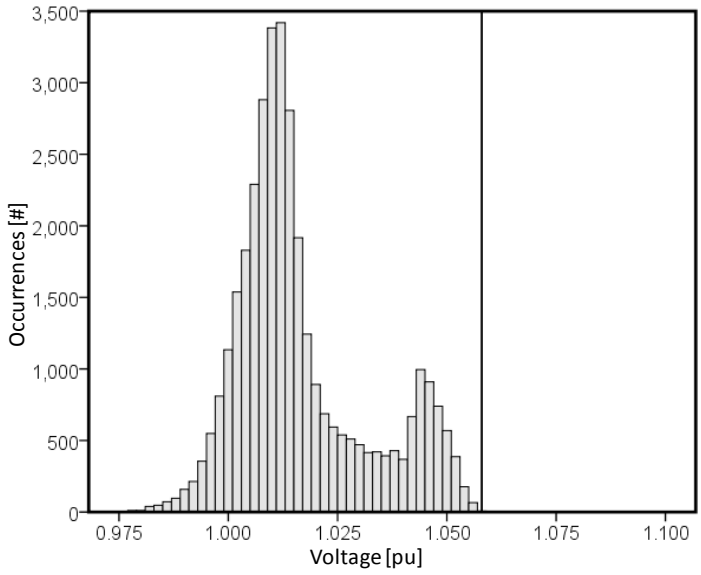

Figure 3.28. Histogram of the voltage in the last house – number of occurrences at a certain voltage [pu] - APC-OPLS.

Figure 3.29 presents the histogram for the power flow in the primary of the transformer. It varies between -60 kW and 47 kW. Note that the maximum power injected by the PV neighborhood into the MV grid decreased using APC-OPLS. This is smaller than the 53 kW obtained with APC. This is the "cost" of sharing the OPL required for preventing overvoltage among all inverters/houses. In addition, from the data obtained, one calculates that the transformer is in average loaded about -3.4 kW with a standard deviation of 18.6 kW.

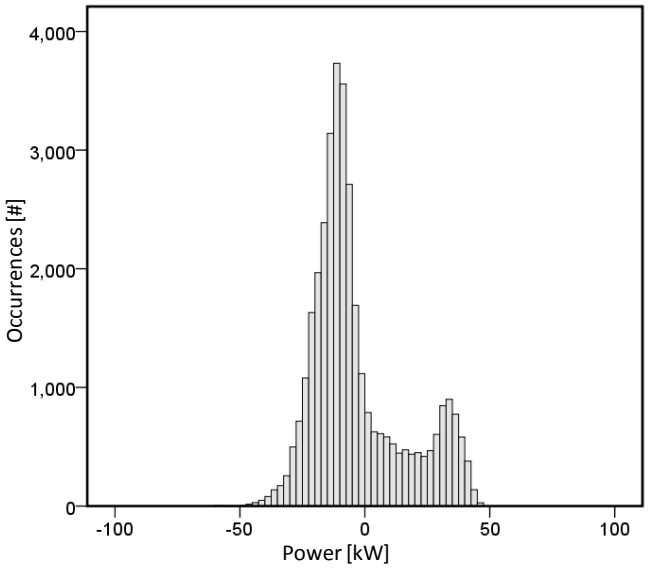

Figure 3.29. Histogram of the power flow in the primary of the transformer – number of occurrences of a certain power [kW] - APC-OPLS.

3.5.3. Yearly Energy Yields

For each of the four cases considered in this study, the energy generated and consumed by each house and by the PV neighborhood as a whole was obtained, together with overvoltage occurrences.

Table V shows the energy produced and the overvoltage occurrences in the feeder for each month. The months between March and September are the ones with the largest energy generation. The base case has the highest overall energy production, but creates overvoltage in the feeder.

Comparing the approaches for preventing overvoltage, simply reducing the installed PV capacity in each house, from 8.4 kWp to 5 kWp, results in a decrease of 41% in PV power generation.

TABLE V - PV INVERTERS ENERGY GENERATED AND CURTAILED BY MONTH

	Energy Generated [MWh]				*Overvoltage Occurrences [%]*			
Month	*Base*	*Red. PV_{Cap}*	*APC*	*APC-OPLS*	*Base*	*Red. PV_{Cap}*	*APC*	*APC-OPLS*
January	8.2	4.8	7.2	6.9	6.5	0.0	0.0	0.0
February	9.7	5.7	8.7	8.3	7.9	0.0	0.0	0.0
March	12.2	7.2	11.0	10.5	7.7	0.0	0.0	0.0
April	11.3	6.7	10.4	10.1	5.3	0.0	0.0	0.0
May	11.6	6.8	10.8	10.5	4.7	0.0	0.0	0.0
June	11.7	6.9	11.1	10.9	3.7	0.0	0.0	0.0
July	12.2	7.2	11.5	11.2	4.9	0.0	0.0	0.0
August	12.1	7.1	11.3	11.1	4.4	0.0	0.0	0.0
September	10.9	6.4	10.0	9.7	5.7	0.0	0.0	0.0
October	8.2	4.8	7.8	7.6	2.3	0.0	0.0	0.0
November	6.3	3.7	5.7	5.6	3.3	0.0	0.0	0.0
December	6.9	4.1	6.3	6.2	3.3	0.0	0.0	0.0
Total	121.2	71.6	111.8	108.6	5.0	0.0	0.0	0.0

Using the APC techniques, one can prevent overvoltage in the feeder while keeping the original 8.4 kWp/house. The reduction in PV power generation was around 7.7% when

all inverters presented the same droop parameters. In that case, the houses farthest from the transformer have more energy curtailment, as can be seen in Table VI. Houses H 12 and H11 lose about 20% of their energy output by the curtailment, while the houses closer to the transformer can profit from all its production. On the other hand, with the APC-OPLS technique, the energy losses due to power curtailment are shared among all the houses. Every house loses about 10% of its energy, leading to an overall decrease of 2.7% in the energy produced by the PV neighborhood with respect to the original APC.

TABLE VI - PV INVERTERS ENERGY GENERATED AND CURTAILED BY HOUSE FOR ONE YEAR

	Energy Generated [MWh]		*Energy Curtailed [MWh]*	
House	*APC*	*APC-OPLS*	*APC*	*APC-OPLS*
H 1/2	10.1	9.2	0.0	0.9
H 3/4	10.1	9.1	0.0	1.0
H 5/6	9.9	9.0	0.2	1.1
H 7/8	9.2	9.0	0.9	1.1
H 9/10	8.5	9.0	1.6	1.1
H 11/12	8.1	9.0	2.0	1.1
Total	111.8	108.6	9.4	12.6

Table VII presents the net energy in the primary of the LV transformer, sent by the PV neighborhood to the grid, which takes into account the losses in the feeder and in the LV transformer itself. It shows that, in that specific year, the PV neighborhood consumed more electricity than it produced in all cases. When the houses are equipped with 8.4 kWp each, the amount of energy required from the grid is relatively small, 16 MWh, but the feeder is subject to overvoltages. These can be prevented by simply reducing the size of the PV arrays to 5 kWp/house, but the amount of electricity imported increases to 66.3 MWh. Instead, one can have the 8.4 kWp/house PV arrays, producing up to this power when the net generation is not high enough to cause overvoltage. Whenever net power generation tends to become too high, it is curtailed with either APC or APC-OPLS, which allows the reduction of electricity required from the grid to 26.2 MWh and 29.3 MWh, respectively.

TABLE VII - TOTAL NET ENERGY GENERATED TO THE GRID [MWH]

Month	*Base*	*Red. PV_{Cap}*	*APC*	*APC-OPLS*
January	-2.2	-5.6	-3.1	-3.4
February	0.9	-3.1	-0.2	-0.5
March	1.6	-3.4	0.4	0.0
April	1.4	-3.2	0.6	0.3
May	2.4	-2.4	1.5	1.3
June	-2.3	-7.1	-2.9	-3.1
July	-1.8	-6.8	-2.5	-2.8
August	-3.9	-8.9	-4.6	-4.8
September	-1.0	-5.5	-1.9	-2.2
October	-3.8	-7.2	-4.2	-4.3
November	-4.5	-7.1	-5.0	-5.2
December	-3.6	-6.4	-4.2	-4.4
Total	-16.7	-66.3	-26.2	-29.3

3.6. Impact of Azimuth Diversification on the Overvoltage Occurrences and on the Yearly Energy Yields in a Feeder with High-penetration of PV

This Section presents a study to evaluate the impact of azimuth diversification on the overvoltage occurrences and yearly energy yields using APC and APC-OPLS in the PV inverters. In the last Section, the results were obtained through a simulation for one year using PSCAD. That method showed a requirement for large computational resources and multiple simulation runs; however, it can account for variations in the load profiles of each house. Several weeks were required to run, export, and analyze the simulation results. In this chapter, an alternative approach is used to estimate the energy yields and overvoltage occurrences for the same feeder. This method consists of estimating the voltage at each node of the feeder based on the overall net-generation of the feeder. This method uses a second order equation, obtained through a quadratic regression of the results presented in Section 3.3. It showed a reduction in the time required to obtain the simulation results and also to analyze them as analysis can be implemented directly in an IBM PASW©(Predictive Analytics SoftWare) spreadsheet.

As in the previous Section, the seasonal residential load data from [28] was scaled in HOMER; however, the annual average energy demand of 27 kWh/day is used. The day-by-day and hour-by-hour random variability factors of 20% (both) were considered to represent the high variability characteristic of residential loads.

The one-year hourly PV inverter output was estimated for Montreal (Latitude 45°55' N and Longitude 73° W) using HOMER and data taken from the NASA weather information center [78]. Two layouts, shown in Figure 3.30 and Figure 3.31, were considered to investigate the effect of the azimuth diversification of PV panels on the voltage profile and overvoltage problem. In the first case, all houses are considered to be south facing (layout I), while in the second case (layout II), 4 of these houses are considered to be south facing, 4 houses face due southeast, and 4 others face due southwest. In both layouts, all PV panels are tilted with a slope of 45° and are considered to be fixed on the roof. The efficiency of each inverter was assumed to be around 96%, and the derating factor of the panels equal to 80%.

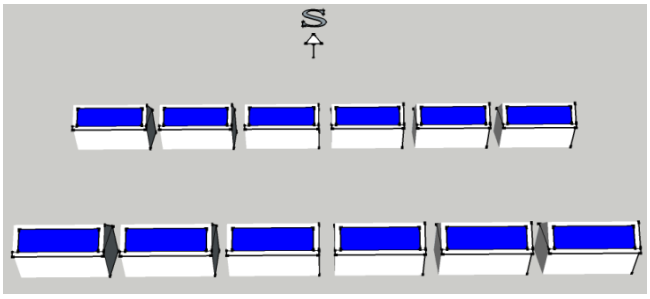

Figure 3.30. Layout I, where all the 12 houses face due south.

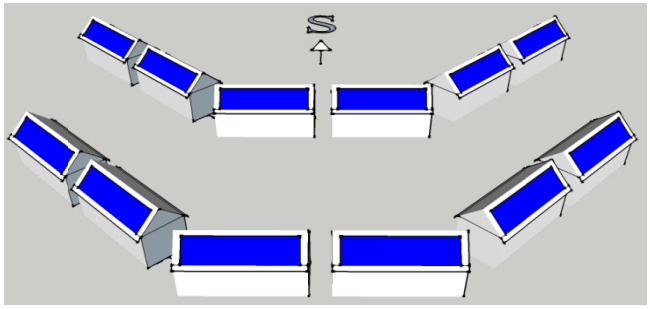

Figure 3.31. Layout II, where 4 of the houses face due southeast, 4 due southwest and 4 due south.

Three studies are presented to investigate the system's voltage profile and energy yields of the original net-zero energy PV neighborhood considering the two different layouts and the proposed droop-based APC schemes.

3.6.1. Base Case and Azimuth Diversification

The first set of results corresponds to systems where the PV inverters do not present any sort of active scheme to prevent overvoltage in the feeder. They operate with MPPT until, if ever, the voltage at their point of connection reaches 1.1 pu, when the inverters shut down. In the first case, all rooftop PV arrays are arranged to obtain maximum energy yield (layout I) while in the second, they are arranged with different azimuth angles to avoid the large excesses of PV power generation that results in overvoltage.

Figure 3.32 presents the histogram of the voltage level in the last house, assuming all the houses are south facing (layout I). Basically, it shows the number of occurrences at a certain voltage level. The vertical line indicates the 1.058 pu threshold where overvoltage occurs. There one sees that a number of cases of overvoltage occur in this bus. The maximum voltage found was 1.082 pu, recorded on a mild clear day, where the load in the system was low and the generation was close to its maximum value.

Figure 3.33 presents the histogram of the voltage level in the last house of the feeder with layout II (Figure 3.31). There, one sees that a number of overvoltage cases still occur in this bus. However, they are fewer in number than for the previous layout. The maximum voltage was 1.075 pu, which was lower than for layout I.

Figure 3.34 shows the percentage of the time that overvoltages happened in each even house for the two layouts. Houses 1 to 4 did not present any overvoltage problems during the year under study. The results of the odd houses are similar to the even ones due to the symmetry of the layouts; therefore, they are omitted.

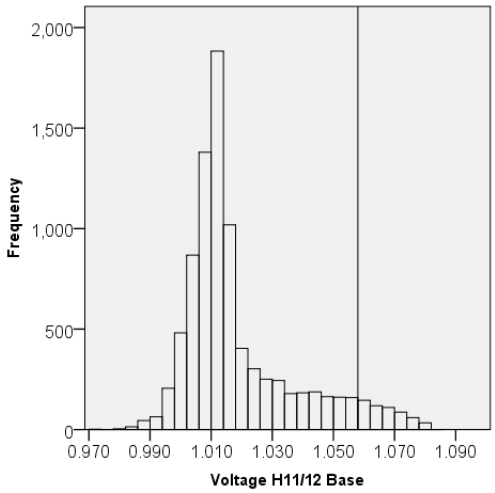

Figure 3.32. Histogram of the voltage level in the last house – number of occurrences in a one-year period at a certain voltage [pu] - Base Case layout I.

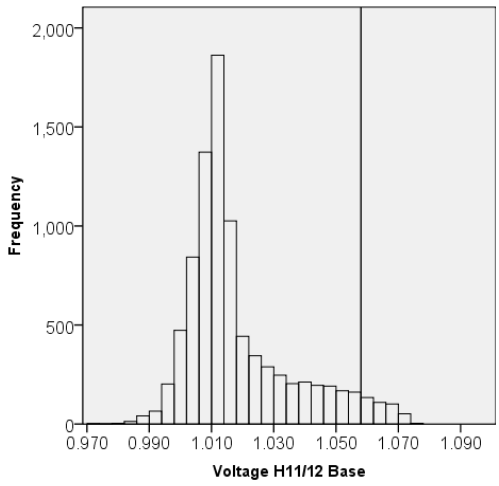

Figure 3.33. Histogram of the voltage in the last house – number of occurrences in a one-year period at a certain voltage [pu] - Base Case layout II.

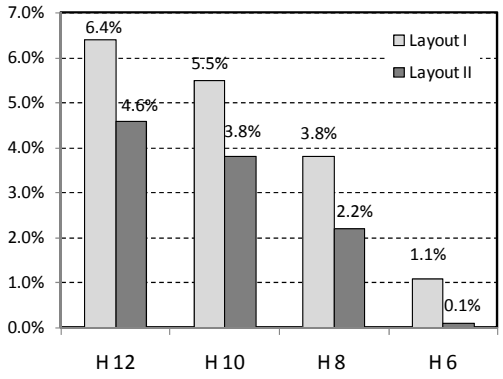

Figure 3.34. Overvoltage occurrences in each even house [%] where the event happened.

For 6.4% of the time, overvoltages (voltage above 1.058 pu) occurred in the last house/bus of the feeder (H 12), when all the houses' PV panels were south facing. As the houses got closer to the transformer, the occurrence of overvoltage problems was significantly reduced. When the houses did not have the same azimuth (layout II), the occurrence of overvoltage problem in the feeder was reduced. Therefore, distribution of the panels into different azimuths could indeed reduce the occurrence and severity of overvoltage in the feeders, but it could not eliminate it for sure, at least with the basic design approach used in this chapter. The impact of the variation of the azimuth on the energy yield of the feeder is shown in Table VIII, along with for the cases shown in the following Sub-Sections.

3.6.2. Effect of Using the APC Scheme

This Section shows the impact of having all PV inverters controlled with droop-based APC and with the same parameters as calculated in Section 3.3.2.

Figure 3.35 shows the histogram of the voltage level in the last house, assuming layout I. No cases of overvoltage occur in this bus or in the feeder and the maximum voltage was 1.052 pu. Note that, as power curtailment occurs for voltages between 1.042 pu and 1.058 pu, the voltage occurrences that were above 1.058 pu in Figure 3.32 moved to the region where the APC operates in Figure 3.35. The occurrences for voltages below 1.042 pu are the same in Figure 3.32 and in Figure 3.35. Similar results were obtained for layout II. No cases of overvoltage occurred and the maximum voltage was 1.051 pu.

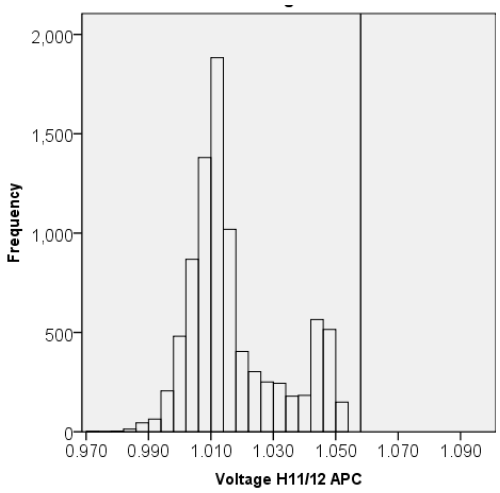

Figure 3.35. Histogram of the voltage in the last house – number of occurrences at a certain voltage [pu] - APC layout I.

3.6.3. Effect of Using the APC-OPLS Scheme

In this study, the droop parameters of the PV inverters are different, calculated as described in Section 3.3.3 for sharing the OPL equally among all the houses.

Figure 3.36 presents the histogram of the voltage levels at the last house, considering layout I. No cases of overvoltage occur in this bus or anywhere else in the feeder and the

maximum voltage was 1.058 pu. As in the previous case of operation with APC, the voltage occurrences that were above 1.058 pu moved to the region where the APC operates. The occurrences for voltages below 1.042 pu were also the same for Figure 3.32, Figure 3.35, and Figure 3.36. Again, no major differences were noted between the results obtained with APC-OPLS for layouts I and II. The most noticeable difference was the maximum voltage for layout II, which was equal to 1.056 pu.

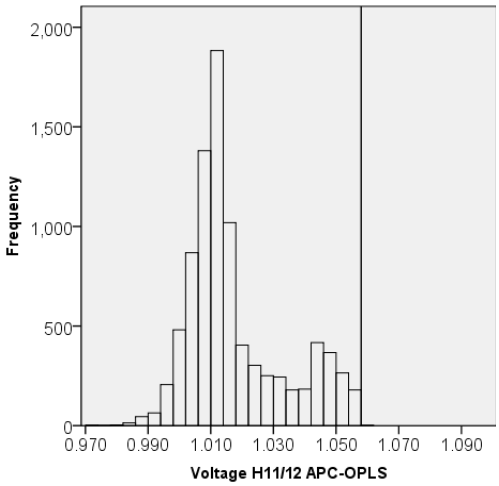

Figure 3.36. Histogram of the voltage levels of the last house – number of occurrences at a certain voltage [pu] - APC-OPLS layout I.

3.6.4. Yearly Energy Yield

This Section presents the energy yields obtained in one year for each of the 12 houses equipped with 8.4 kWp of PV in a 75 kVA LV feeder, and the total for the feeder, when using different strategies for preventing overvoltage. A summary of the results obtained for the various cases is shown in Table VIII.

The maximum energy yield is obtained for the base case, where all PV arrays face south and no APC schemes are used. However, this approach results in overvoltage in some buses. The use of azimuth variation, which did not solve the overvoltage problem with the simplistic design approach used, resulted in lower energy yield for the feeder due to the lower energy yield of the houses with the non-ideal azimuth angle.

TABLE VIII - ENERGY GENERATED BY PV INVERTERS FOR ONE YEAR

House	*Energy Generated [MWh]*					
	Layout I			*Layout II*		
	Base	*APC*	*APC-OPLS*	*Base*	*APC*	*APC-OPLS*
H 11/12	10.0	7.1	8.8	9.2	7.0	8.4
H 9/10	10.0	7.6	8.8	9.2	7.4	8.3
H 7/8	10.0	8.6	8.8	10.0	9.0	9.1
H 5/6	10.0	9.6	8.8	10.0	9.8	9.2
H 3/4	10.0	10.0	8.6	9.2	9.2	8.2
H 1/2	10.0	10.0	8.6	9.2	9.2	8.2
Total	120.0	105.6	105.3	113.6	103.4	102.8

Using the APC techniques, one can prevent overvoltage in the feeder while having the desired 8.4 kWp installed per house, for net-zero energy operation. The reduction in the energy yield of the feeder with layout I was around 7.7% when all inverters presented the same droop parameters. In this case, the houses farthest from the transformer have more

energy curtailed, as can be seen in Table VIII. Houses numbered as H11 and H12 lose about 20% of their energy output due to the power curtailment, while the ones closer to the transformer can profit from all of their production. On the other hand, when the APC-OPLS technique is used, the energy losses due to power curtailment are shared among all the houses almost equally. Each house loses about 10% of its energy, leading to an overall decrease of 2.7% in the energy yield of the feeder, with respect to the original APC scheme. A similar result is obtained for layout II with APC, but in this case, the energy yield is lower than for layout I and sharing of the OPL among all PV inverters is not as good as for layout I. This could be improved with an appropriate approach for selecting the APC parameters, but there would be no significant gains regarding either the energy yield or overvoltage prevention.

3.7. Conclusion

This chapter discussed the use of droop-based APC schemes for overvoltage prevention in LV feeders with high-penetration of distributed PV. Two design approaches were proposed and verified using a benchmark developed based on typical parameters found in a Canadian suburban residential feeder with 12 net-zero energy solar houses connected to a 75 kVA LV transformer. In the basic APC scheme, all inverters/houses use the same droop coefficients but the contribution, in terms of APC required from each inverter for overvoltage prevention, was different. Inverters more downstream along the feeder were required to curtail more power than the others, which affects their revenues. An approach that resulted in approximately equal sharing of the output power losses (OPL) among inverters (APC-OPLS) was proposed and its effectiveness was demonstrated. However,

this feature came at the expense of increased OPL with respect to the basic APC scheme. The choice of either technique should be done based on the importance of sharing the overvoltage prevention "costs" among all houses or maximizing the energy exported by the entire feeder.

As PV system owners are particularly interested in the energy yield (revenue) they will get from their systems, a one year simulation study was performed to evaluate the impact of the APC techniques on the overall energy yields of the feeder and individually for the customers, using yearly load and PV generation profiles. Installation of the desired PV capacity for yearly net-zero energy operation, in a particular year, indicated that the energy import of the neighborhood would be about 13% of its needs, but there would be overvoltage occurrences in the feeder. Reducing the installed PV capacity can prevent overvoltages; however, the solar neighborhood had to import around 50% of its electricity needs. Arranging the rooftop PV systems with different azimuth angles (4 houses south, 4 houses southeast, and 4 houses southwest) marginally reduced the occurrences as well as the degree of overvoltages in the feeder, but could not eliminate the problem. Using the basic APC with the proposed design approach, allowed complete avoidance of overvoltages and the electricity import from the MV grid was limited to around 20% of its needs. This was closer to yearly net-zero energy than in the case where the PV installed capacity was reduced. The contribution of each house/inverter, in terms of APC for overvoltage prevention, also differed based on the location of the feeder. All PV inverters used the same droop coefficients, but houses located downstream on the feeder were required to curtail more energy than were the others (closer to transformer), which affected their revenues. This problem was eliminated with the proposed APC-

OPLS method that shares the output power losses (OPL) among all inverters. The difference in energy curtailment between houses located downstream and upstream became negligible. However, this feature came at the expense of a smaller (~3%) energy yield for the residential PV feeder with respect to the basic APC scheme.

4. ACTIVE POWER CURTAILMENT OF PV INVERTERS IN DIESEL HYBRID MINI-GRIDS

The fluctuating and intermittent power characteristics of non-dispatchable RETs, such as PVs, can lead to a number of issues in distribution systems with high-penetration of RETs, as previously discussed. The general overvoltage issue was discussed in chapters 2 and 3. Other issues in diesel-dominated mini-grids involve frequency regulation and the operation of the diesel genset(s) at low load conditions, leading to reduced fuel displacement and increased maintenance costs. Typically, for the operation of multiple generation units, droop-based governors are used in order to provide load sharing among the units. This means that the mini-grid's frequency is proportional to the loading level of the units. Thus, the increase in the overall power variations in the mini-grid load due to the introduction of non-dispatchable RETs will also increase the frequency variations in the mini-grid. Diesel gensets should also not operate below a certain minimum load for extended periods in order to prevent carbon build-up in the diesel engine.

A common solution for these problems in storage-less systems is the use of a dump load to increase the loading level when the load is low. This can also reduce the frequency rise, which is a global quantity, but not necessarily the voltage rise, particularly if the electrical distance between dump load and the point of common coupling (PCC) of the RETs is long. Demand side management and storage units could be used; however, these require a significant investment. Alternatively, one can employ active power curtailment (APC) of RETs based on locally measured variables (frequency), which has the potential to address the low loading condition of the genset – overfrequencies as well as

overvoltages. Recall that diesel power plants in mini-grids are usually composed of a number of gensets operating with power vs. frequency droop control. Reducing the power injected by the RETs can reduce overvoltages and also increase the power demanded from the gensets, which reduces the frequency rise. Therefore, APC can, in principle, simultaneously address the low loading of gensets and overfrequency.

This chapter discusses the potential of active power curtailment of RETs during periods of energy surplus in a diesel-dominated mini-grid for improving the steady-state performance. The output power of PV inverters is varied using the well-known frequency x power droop control. A 75 kVA PV-diesel residential mini-grid benchmark is developed to verify, by means of simulations, the suitability of the technique. The effect of using active power curtailment is evaluated for a one-year case study and compared with the standard method (dump load) regarding reduction in the genset's supplied energy and fuel consumption.

Section 4.1 introduces the basic concepts for using APC in diesel-based mini-grids for improving the steady-state behavior of the system. Section 4.2 presents the benchmark developed to validate the technique. The design of the droop coefficients for the frequency x power APC of PV inverters and preliminary simulation results to investigate the effect of the solar irradiance variation with and without APC on the mini-grid operation are presented on Sections 4.3 and 4.4, respectively. Section 4.5 presents a one-year simulation study looking into the impact on fuel consumption and energy profile of the mini-grid. Finally, the conclusions are stated in Section 4.6.

4.1. Basic Concepts

An elementary PV-diesel hybrid mini-grid is shown in Figure 4.1. It consists of a grid-forming diesel power plant, which can include one or more droop-controlled gensets operating in parallel. The PV inverter(s) are rated at a fraction of the diesel plant and are distributed across the mini-grid. They supply a non-controllable lumped load representing the customers' loads. Although not shown in Figure 4.1, an on-off dump (controllable) load is often employed in such a system to provide a minimum load to the genset(s), thus preventing operation of the genset(s) at light load. This is usually placed close to the diesel power plant and is dispatched by the supervisory control system of the diesel plant. No energy storage units are used in this particular case study.

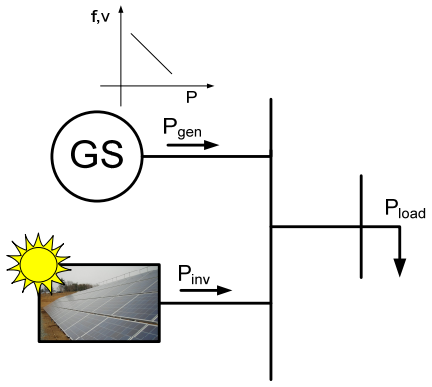

Figure 4.1. Main components of a PV-diesel hybrid mini-grid.

4.1.1. Frequency x Power Droop Controlled PV Inverter

Grid-tie inverters are typically controlled with MPPT as current sources. Alternatively, the power injected by the inverter can be controlled (reduced) as a function of the system frequency according to:

$$P_{inv} = P_{MPPT} - m\left(f - f_{cri}\right) \tag{4.1}$$

for $f \geq f_{cri}$. This is valid as long as $P_{inv} \geq 0$, if the inverter is connected directly to the PV array (no battery storage in an intermediate dc bus) as assumed in this analysis. There, P_{MPPT} is the maximum power available in the PV array for a given solar irradiance (kW), m is a slope factor equivalent to s_p and f_{cri} is the frequency (Hz) above which the power injected by the inverter is decreased with a droop factor. For $f < f_{cri}$ the inverter injects P_{MPPT}, as most PV inverters do. For enhanced performance, this value should be selected based on the genset droop characteristics, load and generation profile, in order to limit the frequency rise and, consequently, the reduction in genset loading. This strategy can also be used to support isolated systems with droop-based gensets to keep operating between the frequency operational limits that are required in European standards for non-interconnected systems [79].

4.1.2. Diesel PV Hybrid System Characteristics

The droop characteristics of the diesel PV hybrid system can be obtained by substituting (1.6) and (4.1) in (1.7). After some manipulations, one obtains:

$$P_{load} - P_{MPPT} = s_p\left(f_{nl} - f\right) + m\left(f_{cri} - f\right) \tag{4.2}$$

for $f_{cri} \leq f \leq f_{nl}$. In the left hand side, one sees a "frequency independent" load and a "frequency independent" source. On the right hand side are two "frequency dependent" (droop controlled) elements. One is a source (genset) and the other is a load (power curtailed from the PV inverters). Although these have the same format, they have opposite signs since the system frequency (f) is always below f_{nl} and PV inverter power

curtailment only occurs for $f \geq f_{cri}$. For $f < f_{cri}$, the frequency dependent element is not active (zero) and the inverter supplies as much power as available in the PV array.

A numerical example is used to illustrate these two operating regions. The key parameters of the system are shown in Table IX. Figure 4.2 shows the droop curve of a 75 kW genset and also the frequency vs. power curve of the diesel PV hybrid system, which is divided into two segments. In the first, for $f < f_{cri}$, the PV inverter operates with MPPT and the grid forming genset supplies the difference between the load, assumed to be 31 kW in this example, and the PV inverter power that varies with the solar irradiance. Any increase in the power supplied by the PV system will result in an equivalent decrease in the genset output power. The system frequency increases according to the droop curve of the genset. As the solar irradiance increases, or load power decreases, the system frequency tends to increase and when it becomes larger than f_{cri}, the output power of the PV inverter begins to be curtailed. In this second segment, the system frequency will vary according to a new curve defined by the droop characteristics of the genset and of the APC of the PV inverter. The diesel PV hybrid droop curve presents a smaller slope than that of the genset. For instance, for $m = s_p$, it is half the slope of the diesel genset curve. Note that the slope is numerically equal to the inverse of the s_p and m parameters when the frequency vs. power droop characteristics is shown with the parameter frequency in the vertical axis.

Figure 4.2 shows that when the solar irradiance is at its rated value (P_{MPPT} = 24 kW) the system frequency, according to the diesel PV hybrid droop curve (4.6), is equal to 60.87 Hz. At this frequency, using (4.2), the genset load is equal to 11 kW (~ 0.15pu) and the power curtailed from the PV inverter (P_{droop}) is around 4 kW. Alternatively, if the PV

inverter was allowed to inject maximum power into the system, the genset load would be reduced to 7 kW (~0.09pu), which should have a significant impact on the carbon buildup in the diesel engine and on its maintenance costs. Note that for the droop parameters selected for the APC of the PV inverter and the load level considered in this case (31 kW), no power curtailment would occur until P_{MPPT} reaches 15 kW and f reaches f_{cri} = 60.75 Hz. Beyond this point, PV power would be curtailed, as the frequency increases at the same rate as the genset power is reduced, since they present the same droop factor (slope). Mathematically, for this case, one can say that the power curtailed from the PV inverter (P_{droop}) is:

$$P_{droop} = \frac{P_{MPPT} - P_{MPPT\_cri}}{2} = P_{gen\_cri} - P_{gen} \tag{4.3}$$

PV powers (P_{MPPT}, P_{MPPT_cri} and P_{inv}) are shown from right to left in Figure 4.2, starting at the load power level (P_{load}). As mentioned in previous Sections, a dump load is often used in practice to prevent operating the genset below ~0.15 pu. Another approach suggested by genset manufacturers is that when required to operate at low loading conditions, gensets should run at full load for 1-2 hours to get rid of the carbon accumulated along the day. This leads to high costs in fuel and offsets part of the gains with the installation of renewable energy sources. A compromise between maintenance costs and the cost of power curtailment should be established in order to design optimum APC parameters for a specific mini-grid. However, this is beyond the scope of this analysis.

TABLE IX - MAIN PARAMETERS OF THE DIESEL PV HYBRID SYSTEM.

	Diesel genset	*PV*
Rated power	75 kW	24 kW
Droop factor	33.2 kW/Hz	33.2 kW/Hz
No-load frequency	61.2 Hz	-
Critical frequency	-	60.75 Hz

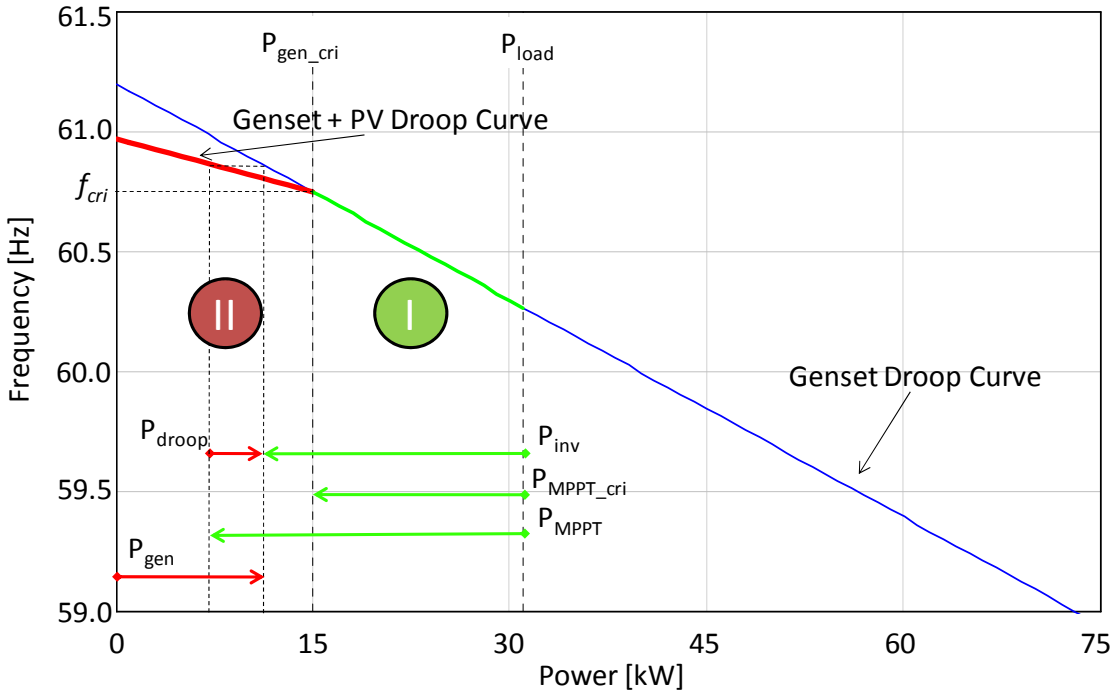

Figure 4.2. Diesel-PV hybrid system frequency variation.

4.2. PV-Diesel Hybrid Mini-grid Benchmark

To verify the performance of the proposed technique in terms of fuel consumption and energy yields, a benchmark of a rural isolated system based on [54] was adapted to study mini-grid operation and implemented in PSCAD©. The benchmark scheme is presented in Figure 4.3.

A 600 V-75 kW genset is used to feed a single phase feeder. The frequency and voltage curves of the diesel genset are shown in Figure 1.7 and Figure 1.8. A 10 kW dump load, located nearby the genset, is active when the genset load is below 10 kW and disconnected when the load reaches 12 kW in order to prevent low load operation and reverse power flow in the diesel unit.

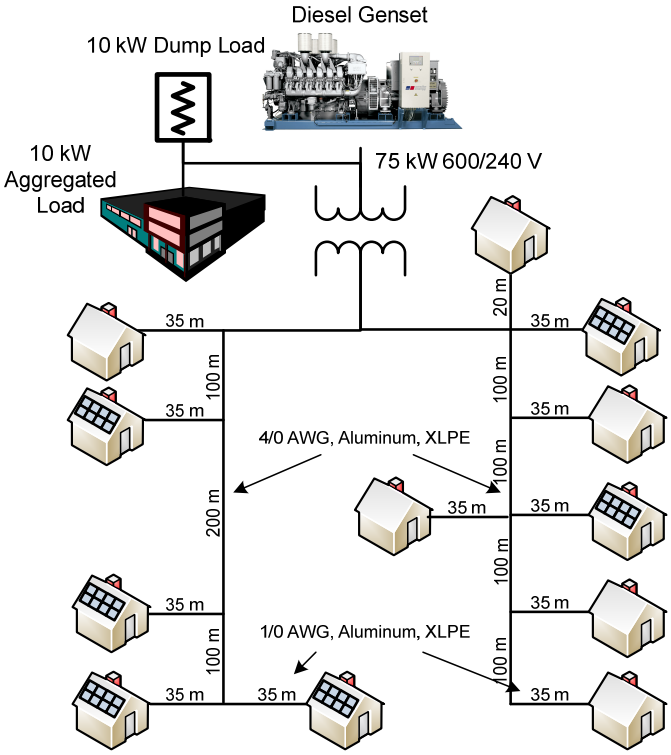

Figure 4.3. Rural mini-grid benchmark.

The power distribution is accomplished through low-voltage single-phase overhead lines. The voltage is brought from 600 V to 240 V using a standard 75 kVA distribution transformer next to the diesel power plant. A 10 kW aggregated load is considered to be always connected in the feeder, representing a commercial load and other miscellaneous loads.

The 240 V line is a typical wood pole line. It is wired using 4/0 AWG Aluminum, XLPE for both line and ground and the drop lines are wired with 1/0 AWG Aluminum, XLPE. The cable and transformer parameters are presented in Table X and Table XI. They were chosen based on system planners' guidelines. Twelve houses are connected in the 240 V line. Six of them have 4 kWp PV systems installed in the rooftop facing south and with a slope of 45°.

TABLE X - SINGLE-PHASE PI SECTION LINES PARAMETERS (PER LINE CONDUCTOR)

	Drop Lines	*Pole-Pole Lines*
R	0.549 Ω/km	0.27 Ω/km
L	0.23 mH/km	0.24 mH/km
C	0.055 μF/km	0.072 μF/km

TABLE XI - TRANSFORMER'S SIMULATION PARAMETERS

Rated Power	75 kVA	*Copper Losses*	0.045 pu
Primary Voltage	600 V	*No Load Losses*	0.002 pu
Tap	0.95:1	*Leakage Reactance*	0.045 pu
Secondary Voltage	240 V		

4.3. Design of Droop-based APC

The droop-based APC is designed so that power curtailment starts, based on local frequency measurements, when the genset load falls below 0.2 pu (15 kW). Until this

point, no curtailment is used and all the PV power is injected into the mini-grid. The output power of the PV inverter is reduced linearly by the APC as the frequency increases and when the genset load reaches 0.05 pu (3.75 kW), the PV inverter does not allow any amount of power to be injected into the system. The design of the PV droop coefficients uses these two set points as reference. The value of f_{cri} is obtained by manipulating equation (1.6) and considering the frequency as the APC starts to act. Equation (4.4) presents the design for the 75 kW genset:

$$f_{cri} = f_{gen0.2\,pu} = f_{nl} - \frac{P_{gen0.2\,pu}}{s_p} = 60.75\ Hz \tag{4.4}$$

The coefficient m is obtained from equation (4.5). Considering that all the installed PV power capacity (P_{PVcap}) should be curtailed linearly when the genset is operating between 0.2 pu and 0.05 pu, the m coefficient is obtained by dividing the power to be curtailed in this period by the frequency variation.

$$m = \frac{P_{PVcap}}{f_{gen0.2\,pu} - f_{gen0.05\,pu}} = 11.8\ {}^{kW}\!/_{Hz} \tag{4.5}$$

4.4. Simulation Results

In all the simulations shown below, the load is assumed to be constant at around 31 kW (0.42 pu) and is equally distributed among the twelve houses of the system (2.6 kW each). In total, 6 houses have installed 4 kWp PV systems, for a total of 24 kWp of PV, as shown in Figure 4.3. The objective of the simulations is to investigate the effect of the solar irradiance variation with and without APC on the mini-grid operation. The fuel consumption rate was estimated from the information provided by one manufacturer of a

75 kW genset employed in [54] and using an exponential regression. The equation obtained is:

$$Fuel\ Rate = 6.105\, e^{0.015P} \left[l/h \right] \tag{4.6}$$

Two case studies are considered, assuming that the power available in each PV system (P_{PV}) varies from 1.5 kW to 4 kW.

Case #1 presents the simulation results for the system operating with MPPT and variable solar irradiance. A 36 Ω dump load (about 10 kW connected at the 600 V side of the transformer) is used to compensate for the decrease in genset load. The genset load starts at 23 kW (0.31 pu) for a total PV generation of 9 kW (37.5% of total PV capacity). After that, the genset load decreases when the PV penetration increases. In Figure 4.4, the PV generation goes from 9 kW to 24 kW in t = 5 s. The genset load falls until the dump load acts. Instantaneously, just after the dump load is connected, the genset loading goes to about 19.3 kW and is decreased by the PV generation increase to 17.6 kW (0.23 pu). This is above the 0.15 pu minimum load recommendation for newer gensets. This happens as dump loads mostly operate in steps and would hardly match the desired genset load condition. The frequency of operation increases from 60.52 Hz (9 kW of total PV capacity) to 60.67 Hz (24 kW of total PV capacity) as shown in Figure 4.5. The voltage in the farthest house of the left feeder reaches 1.051 pu (Figure 4.6). At t = 17.5 s, the solar irradiance and PV generation start to decrease, reaching 37.5% of their rated value at t = 25 s.

In Case #2, the droop-controlled inverters provide the power curtailment to regulate the genset operation. The dump loads are still present in the system, but they are not activated because of APC operation. The parameters used in the droop controllers are f_{cri} = 60.75 Hz and m = 11.8 kW/Hz. The power curtailment is done proportionally to the frequency rise above f_{cri}, in order to make the genset to operate above 0.15 pu for a 31 kW load and at rated solar irradiance. Figure 4.4 shows that when the PV generation reaches 100% of its capacity, the genset load reaches 12.1 kW (0.16 pu). Compared to the dump load case, the power curtailment operates linearly, preventing sudden load and frequency variations and also adapting to a new condition of genset load. The frequency increases linearly to 60.81 Hz, curtailing 0.75 kW per PV inverter (Figure 4.7). The voltage rise in the farthest house in the left feeder (Figure 4.6) was also limited to 1.047 pu, below the dump load case (1.051 pu), which also helped to prevent overvoltages in the feeder. This is due by reducing the reverse power flow in the left feeder, as compared with the dump load case. The impact of APC addressing the low loading of gensets on systems with overvoltage issues is reported in [80].

Figure 4.8 presents the fuel consumption rate for both cases. The fuel consumption rate when the dump load is connected is higher than when APC is used. The APC provides overall better fuel consumption performance and still keeps the genset load level closer to the minimum loading. This is clearly seen by comparing performances in Figure 4.8, just after the dump load is connected. At that moment, with APC, the fuel consumption is about 7.4 l/h, whereas with the dump load it goes to 8.1 l/h, burning unnecessary fuel.

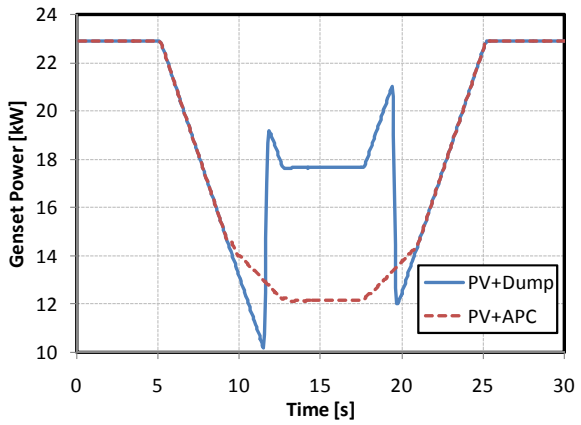

Figure 4.4. Diesel genset output power.

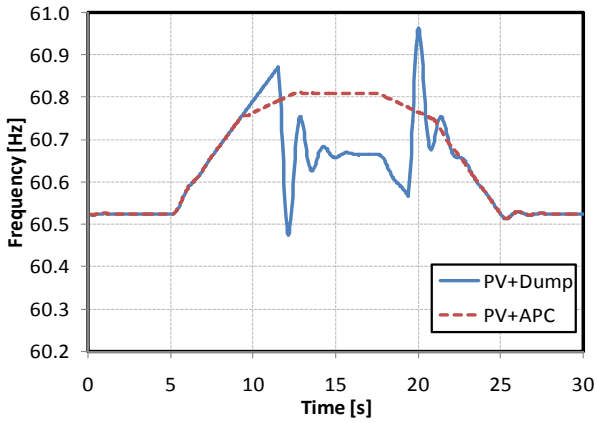

Figure 4.5. Mini-grid frequency.

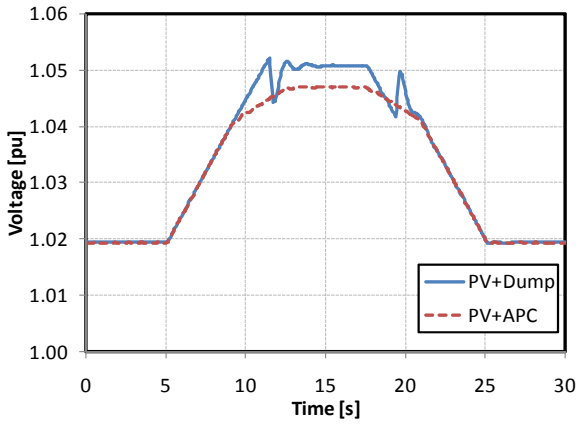

Figure 4.6. Voltage in the last house of the left feeder.

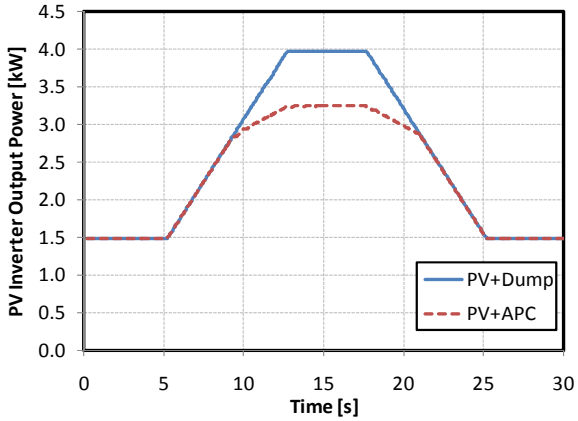

Figure 4.7. PV inverter output power.

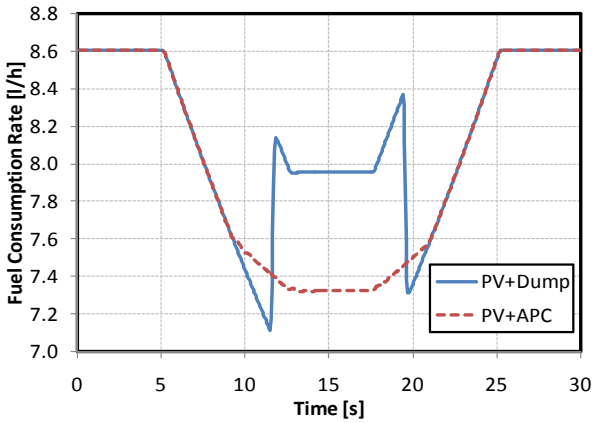

Figure 4.8. Diesel genset fuel consumption rate.

4.5. Yearly Load Profile, Energy and Fuel Consumption

This Section presents the genset load profile, PV systems energy yields, and fuel consumption in a one-year study for the mini-grid.

The software package HOMER was used to estimate the PV panel and inverter's power output levels for each hour of one year. The one-year hourly PV inverter output was estimated for Montreal (Latitude 45°55' N and Longitude 73° W) using HOMER and data taken from the NASA weather information center [78]. The PV panels were considered to

be fixed on the roofs facing south and with a slope of 45°. The efficiency of each inverter was assumed to be around 96%, and the derating factor of the panels equal to 80%.

The average daily load data for a non-electric heated residence was taken from [81] for different seasons as well as weekdays and weekends (Figure 3.16 and Figure 3.17 respectively). They were used as reference data for HOMER to generate hourly load values for a whole year period. Winter was considered from December until February, spring from March to May, summer starting from June to August, and fall from September to November.

The seasonal data were then scaled in HOMER to have an annual average energy demand of 23 kWh/day. The day-by-day and hour-by-hour random variability factors of 40% were considered to represent the high variability characteristic of residential mini-grid loads.

Three case studies are presented to investigate the genset's load and energy profiles for the original mini-grid considering the system without the integration of PV systems and with the PV systems, with and without the use of APC.

4.5.1. Base Case

The first set of results corresponds to system where no PV systems are used in the feeder. In this case, a dump load is not required to prevent reverse power flow in the genset as no additional means exist for generating energy in the system besides the diesel genset and a minimum load is always present in the feeder. Figure 4.9 presents the histogram of the load profile of the genset. It essentially shows the number of occurrences at a certain

power level. One sees that the genset power varies from 10 kW to 71 kW (min and max load, respectively). For about 5% of the time, the genset is under loaded (operating with a load below 0.15 pu/11.25 kW). Recall that operation below 15% of the rated capacity for long periods leads to carbon build-up in the internal combustion engine (newer gensets). In this analysis, operation of this genset below 0.15 pu for more than 10% of the time is assumed to be detrimental.

Figure 4.10 presents the histogram of the frequency in the mini-grid. The frequency varies from 59.07 Hz to 60.89 Hz at maximum and minimum load respectively. As a reference, this frequency variation is within EN 50160 [79], which requires that, for a non-interconnected power system (i.e., mini-grid), the frequency should be within the rated value ± 2% (for a 60 Hz system, 58.80 Hz $\leq f \leq$ 61.20 Hz) for 95% of a week.

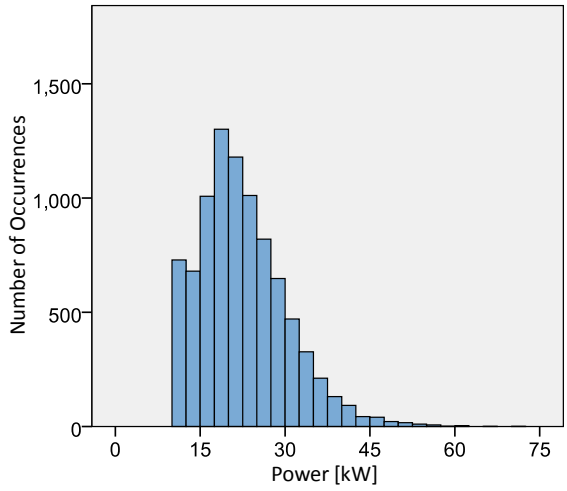

Figure 4.9. Histogram of the genset power supplied to the mini-grid – number of occurrences in one-year period at a certain power [kW] - Base.

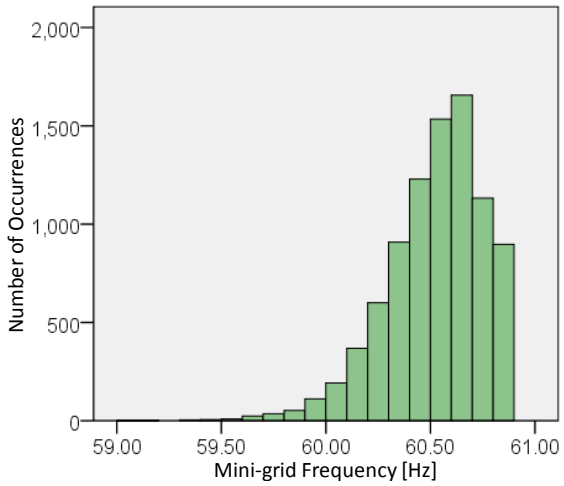

Figure 4.10. Histogram of the mini-grid frequency – number of occurrences in a one-year period at a certain frequency [Hz] - Base.

4.5.2. Integration of PV System in the Mini-grid (PV+Dump)

The second set of results corresponds to the case where 24 kW of PV panels operating with MPPT were integrated into the feeder. Figure 4.11 shows the histogram of the total power generated by the PV systems. For about 50% of the time, the PV systems are generating a certain amount of power, with an average hourly power generation of 3.26 kW and a peak generation of 23 kW. For 13% of the time, the dump load is activated due to the decrease in the load by the integration of the PV system. The average power dumped was 1.3 kW. On average, 40% of the PV power generated is lost in the dump load, with a net average of 1.96 kW of power actually supplied to the mini-grid loads apart from the dump load.

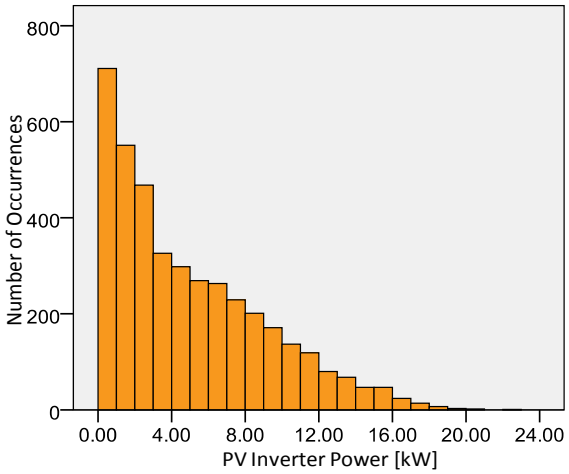

Figure 4.11. Histogram of the PV power generated – number of occurrences in a one-year period at a certain power [kW] - PV+Dump.

Figure 4.12 presents the histogram of the load profile of the genset. For about 8% of the time, the genset is loaded below 0.15 pu (11.25 kW). This value is not higher because the dump load is acting. Compared to the base case, a 3% increase occurs in the time that the generator is operating under loaded. Nevertheless, the 10 kW dump load was able to keep the system above 0.15 pu for most of the time (more than 90% of the time). However, one sees that the minimum genset power was 0.1 kW. This means that the PV system is generating enough electricity to fully supply all the loads and the dump load, reaching an almost no load state. The peak load was 71 kW, which was not reduced since it happens at nighttime.

Figure 4.13 presents the histogram of the frequency in the mini-grid. The frequency varies from 59.07 Hz to 61.20 Hz, still within EN 50160 limits. The frequency variation is increased compared with the base case. This is due to the reduction in the loading range of the genset when the PV systems are integrated.

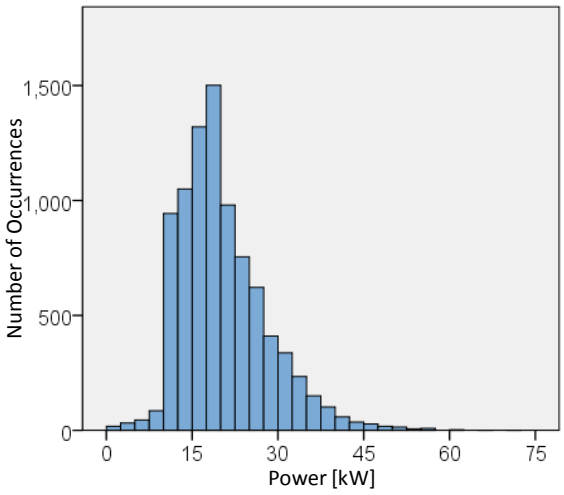

Figure 4.12. Histogram of the genset power supplied to the mini-grid – number of occurrences in a one-year period at a certain power [kW] - PV+Dump.

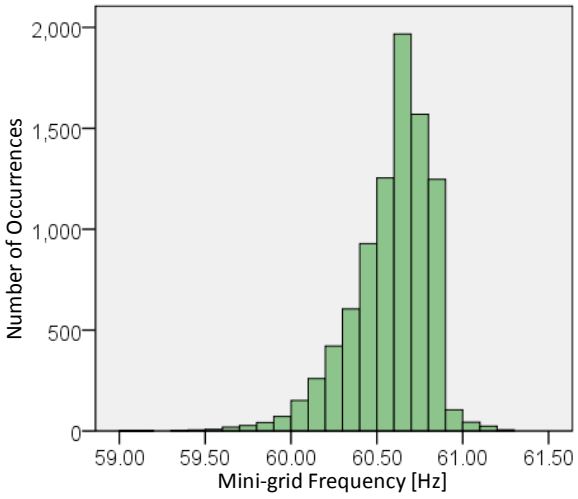

Figure 4.13. Histogram of the mini-grid frequency – number of occurrences in a one-year period at a certain frequency [Hz] - PV+Dump.

4.5.3. Inverters with Active Power Curtailment (PV+APC)

This Section presents the impact of having all PV inverters controlled with droop-based APC and with the same parameters as calculated in Section 4.3. Figure 4.14 shows the histogram of the total power generated by the PV systems. For about 46% of the time, the

PV inverters are injecting a certain amount of power into the mini-grid. This amount is lower than in the previous case (50% for PV+Dump) since, with APC, PV inverter's power that was instantaneously available (P_{MPPT}) in 4% of all cases was totally curtailed and the dump load now was just active for 1.1% of the time with an average power dump of 0.11 kW. This shows that both techniques can coexist in the feeder; however, the dump load could be removed without harm to the system operation, as the APC would warranty a minimum load level. The average hourly power generation was 2.28 kW, which is 1 kW less than in the previous case. However, in the previous case, the losses due to the dump load were not computed in the average hourly power generation, as in this case with the losses from the curtailment. If compared with the average net power generated (power injected consumed by the mini-grid loads), it shows an increase of 0.22 kW on the hourly average. This corresponds to a 16% increase in the average power from the PV systems consumed by the loads using APC.

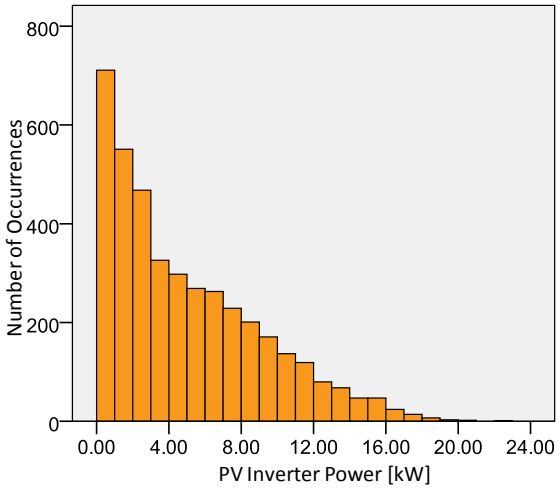

Figure 4.14. Histogram of the PV power generated – number of occurrences in one year period at a certain power [kW] - PV+APC.

The histogram of the total power curtailed in the PV systems is presented in Figure 4.15. The maximum amount of power curtailed was 12 kW. This shows that curtailment of the whole capacity of the PV system was never necessary during peak operation. Power curtailment occurred for 22% of the time, with an hourly average of 0.97 kW. This is lower than the 1.3 kW hourly average power dumped in the previous case.

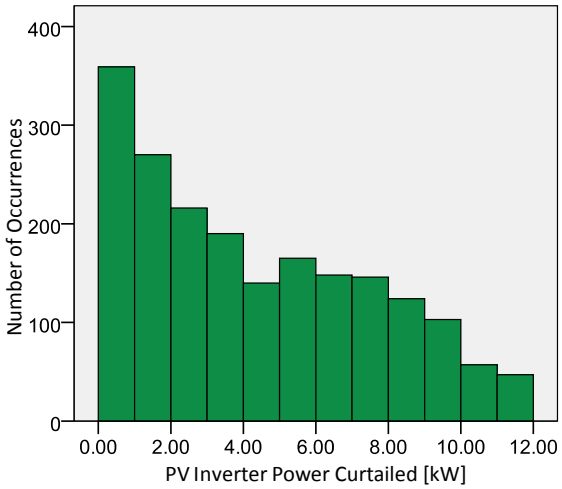

Figure 4.15. Histogram of the PV power curtailed – number of occurrences in a one-year period at a certain power [kW] - PV+APC.

Figure 4.16 presents the histogram of the load profile of the genset. One sees that the genset power varies from 10 kW to 71 kW. If compared with the previous case, the minimum loading is increased. For about 7% of the time (1% more than with dump load), the genset is loaded below 0.15 pu (11.25 kW), which shows that APC was able to keep the system active for most of the time (more than 90% of the time) above 0.15 pu, preventing excessive carbon build-up in the engine. Figure 4.17 presents the histogram of the frequency in the mini-grid. The frequency varies from 59.07 Hz to 60.90 Hz, similar to the base case, where no PV systems were integrated into the mini-grid.

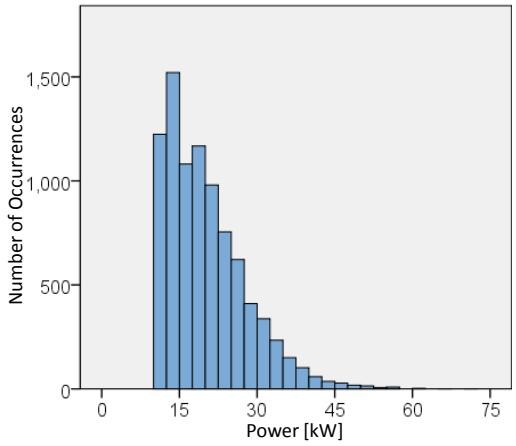

Figure 4.16. Histogram of the genset power supplied to the mini-grid – number of occurrences in a one-year period at a certain power [kW] - PV+APC.

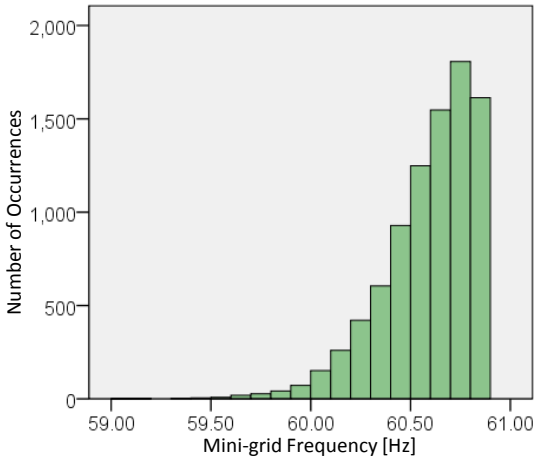

Figure 4.17. Histogram of the mini-grid frequency – number of occurrences in a one-year period at a certain frequency [Hz] - PV+APC.

4.5.4. Energy Yields and Fuel Consumption

The integration of PV systems will certainly reduce the amount of energy needed to be supplied by the genset, reducing its fuel consumption and consequently the operational costs of the diesel system. However, the relationship between energy displacement and fuel consumption is not linear, as the genset is more efficient at higher loads. This

Section presents the total energy supplied by the genset and the impact on the fuel consumption for the one year under study in the mini-grid. The amount of energy curtailed using APC is also discussed. Most of the time, the correlation between load and generation is not known a priori. Monitoring the energy curtailment can be used to reassess the economics of inclusion of a given number of PV systems into a mini-grid. It can also give an indication for designing storage units that could be integrated with the PV inverters, to store the energy that would be curtailed for later use.

A summary of the results obtained for the various cases is shown in Table XII. One can see that the energy supplied by the genset is reduced by 9.4% with the integration of the 6 x 4 kWp PV system (PV+Dump). This is reflected in the fuel consumption; however, the reduction was only 3.1%, due to the increase in the occurrences of low load operation that makes the dump load present more frequently in the system.

TABLE XII - GENSET YEARLY ENERGY SUPPLIED, YEARLY ENERGY GENERATED BY PV SYSTEMS AND YEARLY FUEL CONSUMPTION

Case	*Energy Supplied by the Genset [MWh]*	*Energy Generated by PV Systems [MWh]*	*Fuel Consumption [kl]*
Base	196.8	0.0	75.4
PV+Dump	178.4	28.5	73.1
PV+APC	176.8	20.0	72.9

In addition, the genset has a lower efficiency under low load. Using the APC technique, the reduction in the energy supplied by the genset was around 10.1% if compared to the

base case, although the energy generated by the PV systems was about 30% smaller than in the PV+Dump case. Regarding fuel consumption, the reduction was 3.4%, also compared to the base case, which is expected to have a direct impact on reducing the diesel genset's operational costs.

The frequency and magnitude with which APC occurs are important factors to be considered when reassessing the ideal number of PV systems in a certain feeder. Figure 4.18 presents the total daily energy curtailed in the PV inverters. For 92% of the days, the APC reduces the PV inverter's energy output from as little as 0.15 kWh. For 50% of these days, the curtailment was below 22 kWh per day with an average of 25.4 kWh per day. The maximum daily energy curtailment was 84 kWh during a full day of sun and low energy consumption from the houses.

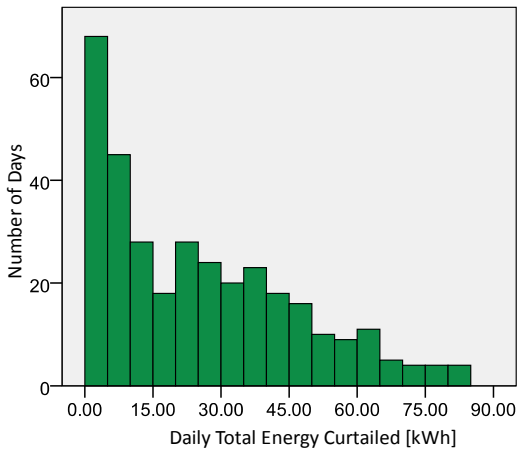

Figure 4.18. Histogram of the daily energy curtailed – number of days in a one-year period that a certain energy curtailment occurs [kWh] - PV+APC.

4.6. Conclusions

This chapter discussed means for reducing part of the load operation of the diesel genset(s) and fuel consumption in a storageless PV-diesel hybrid mini-grid, which can affect the maintenance costs and even the lifespan of the genset. A benchmark was used to evaluate the impact of each method on the load level of the diesel genset and on the fuel consumption, by means of a simulation study with PSCAD©. The mini-grid under study consisted of a 75 kW diesel genset feeding a mostly residential LV feeder with 12 houses, six of them with 4 kWp rooftop PV systems. The utilization of a dump load and the APC of PV inverters during periods of energy surplus in the mini-grid were compared regarding effectiveness for reducing partial load operation of the diesel genset, fuel consumption reduction, and the voltage rise in the feeder. A design approach for a frequency x power droop APC was proposed and the operation was analyzed in detail in this chapter. The voltage rise in the mini-grid was significantly reduced using APC as compared with the case where a dump load was used, when there was excess PV power generation. The results for a one-year period showed that APC leads to a slight reduction in the amount of energy being supplied by the genset, and, consequently, a reduced fuel consumption, which is expected to have a direct impact on reducing the diesel genset's operational costs. For each MWh of energy displaced with the integration of PV systems in the mini-grid, 125 l of fuel were saved in both cases. Both methods were also able to keep the genset operating, most of the time, above the minimum load threshold recommended by the manufacturers.

5. CONCLUSIONS AND FUTURE WORK

5.1. Summary

Renewable energy technologies will play an important role in helping meet the increased demand for electricity without having to expand the transmission and distribution network. The residential rooftop PV system has a great potential to help fill this need; however, its non-dispatchable, fluctuating, and intermittent characteristics can have detrimental impacts on the PQR of distribution feeders. Rooftop PV systems can usually be installed without the need for impact-assessment studies that are required for larger units. In actual electricity grid, the power is expected to flow downstream from the large power plants to the consumers. If large amounts of non-dispatchable PV sources are integrated in a distributed way, power may flow upstream (reverse power flow) in some sections of the feeder. With today's technologies, PQR cannot be ensured, given this scenario. In addition, sudden variations in reasonable amounts of power generation/consumption may also deteriorate the PQR of isolated systems. This problem is even more critical in diesel-based autonomous systems with high-penetration of PVs, operating with reduced amounts of load, which can significantly increase the wear and tear on the diesel gensets. As a result, relatively modest amounts of PV are currently allowed to be connected at the LV distribution level. In order to increase the allowed penetration level of PV systems that can be installed without an impact-assessment study, new techniques are required to minimize their impact on the PQR of LV distribution feeders.

The current PhD thesis focused on the detrimental impact of high-penetration of PVs on LV systems. Techniques capable of increasing PQR and increasing the displacement of fossil fuels in diesel based autonomous systems, thereby reducing operational costs, were investigated and assessed in LV feeders in the presence of a high penetration of PV systems. A brief review regarding the overvoltage issue in LV feeders with high-penetration of PV and operational aspects of diesel-based mini-grids with high-penetration of PV was presented in this thesis. The likelihood of overvoltage is higher in weak residential suburban and rural feeders, especially those with net-zero energy PV neighborhoods that use large PV systems. The integration of non-dispatchable RETs in diesel-based mini-grids will reduce the load seen from the genset in diesel-based autonomous systems for remote communities with high penetration of PV. This can also increase the operation at low load conditions (part load operation). Diesel gensets should not operate below a certain minimum load for extended periods of time, as this can significantly affect the maintenance costs and even the lifespan of the genset. Therefore, balancing the system in the quasi-steady-state using a control scheme for active power sharing of controllable DGs must be envisaged. These two scenarios were considered in this thesis.

The first scenario examined the impact of high penetration of PV systems in LV grid connected systems in which the reverse power flow resulted from the high penetration of non-controllable PV systems, which can create overvoltages during periods of high generation and low load. The well-known solutions used in medium-voltage (MV) feeders needed to be revisited considering the fact that the impedance of LV feeders is mostly resistive, with large R/X ratios. A method was proposed to analyze the impact of

varying active power and reactive power on the voltage and losses of a radial LV distribution feeder with uniformly distributed loads and non-dispatchable (active power) sources based on the sensitivity analysis of the feeder. The feeder impedance characteristic plays an important role in the choice of the most effective approach. The voltage in feeders with large *R/X* ratios, common in LV feeders, can be regulated with lower variation of active power than reactive power. In other words, voltage regulation with reactive power is less effective in LV feeders than in MV ones.

Next, a method was developed to obtain the feeder loss sensitivity to active and reactive power control that are candidate means to prevent overvoltage. The use of reactive power control results in more losses in the feeder, which can possibly offset the additional active power injected by the PV inverters, if no active power is curtailed. On the other hand, with active power control, one can achieve both voltage regulation and feeder loss reduction. Reactive power control is more indicated for MV feeders, which typically present a smaller *R/X* ratio. The net power factor of the buses can change the behavior of the sensitivity matrix, but the effect of line characteristics is stronger in the definition of the voltage regulation strategy.

The use of droop-based APC schemes was discussed for overvoltage prevention in LV feeders with high-penetration of distributed PV. Two design approaches were proposed and verified using a benchmark developed based on typical parameters of a Canadian suburban residential feeder with 12 net-zero energy solar houses connected to a 75 kVA LV transformer. In the basic APC scheme, all inverters/houses used the same droop coefficients, but the contribution, in terms of APC required from each inverter for overvoltage prevention, differed. Inverters more downstream on the feeder were required

to curtail more power than were the others, which affects their revenues. An approach that resulted in approximately equal sharing of the output power losses (OPL) among inverters (APC-OPLS) was proposed and its effectiveness was demonstrated.

A one-year simulation study was performed to evaluate the impact of the APC techniques on the overall energy yields of the feeder and individually for the customers, using yearly load and PV generation profiles. Use of the basic APC with the proposed design approach completely avoided overvoltages and the electricity import from the MV grid was limited to around 20% of its needs, reaching closer to yearly net-zero energy than when the PV installed capacity was reduced. The contribution of each house/inverter, in terms of APC for overvoltage prevention, differed depending on the location of the feeder. With the proposed APC-OPLS method, the energy losses due to the OPL of PV inverters were similar in all houses; however, the energy yield for the residential PV feeder was smaller (~3%) than for the basic APC scheme.

The second scenario considered the impact of high penetration PV systems in LV diesel-based autonomous systems. A benchmark evaluated the impact of each method to reduce low load operation of the diesel genset and on the fuel consumption, using a simulation study with PSCAD©. A method for APC of PV inverters in diesel-based autonomous power systems, typical of remote communities, was presented as a means of reducing frequency variation and ensuring minimum loading of the diesel genset. A design approach for a frequency x power droop APC was proposed and the operation was analyzed in detail. When excess PV power was generated, the voltage rise in the mini-grid was significantly reduced using APC compared with the case where a dump load was used. The results for a one-year period showed that APC leads to a slight reduction

in the amount of energy supplied by the genset, and, consequently, to a reduction in fuel consumption, which is expected to have a direct reduction in the diesel genset's operational costs. Both methods were able to keep the genset operating, for most of the time, above the minimum load threshold recommended by the manufacturers.

5.2. Future Work Suggestions

Some suggestions for future studies related to this thesis topic are presented, based on observed needs revealed by this research.

5.2.1. Impact of Distribution System Architecture in the Overvoltage Prevention Choice

This thesis primarily considers the characteristics of Canadian (North American) LV distribution feeders. The main differences between them are their layouts, ratings, and configurations. European feeders use larger transformers and they have more customers connected to each transformer. This can impact the overall feeder impedance and, consequently, the choice of overvoltage prevention scheme. As a suggestion, an analysis of the differences of both systems and the impact that this could have in the overvoltage prevention scheme can identify the applicability of each method.

5.2.2. Design of Retrofit Neighborhoods to Net Zero Energy PV Neighborhood and Reassessment of Overvoltage Prevention Approach in Weak Feeders

Retrofitting buildings by installing PV systems to reach net zero energy operation can support the energy self-sustainability of certain regions. The existing methods allow the installation of PV systems until the thermal limits of the line are met. However, there will

be losses when the voltage reaches a certain value due to the overvoltage prevention approach used. This will impact the energy output of the feeder and net zero energy operation can be compromised. A suggestion for future study is to investigate a design approach for recommending the appropriate installed PV capacity to reach net zero energy operation for a certain existing neighborhood and that considers the APC of PV inverters in weak LV feeders, where overvoltages might happen often. Guidelines to suggest when to strengthen the feeder, considering load and generation growth models, could also provide the tools necessary to plan upgrades in these systems.

5.2.3. Sensitivity of the APC-OPLS Approach for Variations in Grid Parameters

The APC-OPLS method uses information about the characteristics of the LV feeder to estimate the voltage rise in each bus to which the inverters are connected and also the impact of varying active power in that bus to make the APC similar in all inverters. A possible future study would be to identify the possible "error" regarding the actual and the estimated impedance values and its impact on the APC-OPLS performance. The results would identify the robustness of the method.

5.2.4. Optimization of the Voltage x Power APC Droop Coefficients to Increase the Yearly Energy Output Considering Stability Analysis

The design procedures proposed in this thesis for the droop-based APC coefficients focused on guaranteeing that the PV inverters would not contribute to overvoltages in the feeders. If m and V_{cri} are increased, the APC would operate closer to the overvoltage limits. This would reduce the amount of OPL. The main limitation to the increase in these parameters is the impact on system's stability. A method that would include the impact of

the droop-based APC in the stability of the feeder would be able to reduce the OPL and increase the penetration of PV in the feeder.

5.2.5. Optimization of the Frequency X Power APC Droop Coefficients to Improve Fuel Consumption and to Reduce Operation under Low Load Conditions.

Using a stochastic approach and statistical information about the load and generation, the frequency x power APC droop coefficients could be optimized to operate closer to the minimum load limit of the diesel genset and, consequently, reduce the amount of APC. The impact on system stability should be also considered in this analysis, as the tendency to reach better results is related to the increase in the values of the droop coefficients. Reduction in the APC can increase the fuel displacement of the diesel genset and reduce operational costs.

5.2.6. Secondary Control of Multi Genset Autonomous Systems and APC Droop Parameter Re-scheduling to Optimize System Operation

Another option to improve the fuel displacement of a PV-diesel hybrid autonomous system would be to readjust the droop parameters of the diesel genset and/or of the APC during the day in order to match the load and also to consider the best genset to operate at a given time in multi-genset systems. Figure 1.9 shows that if the load level is low, a genset with reduced capacity would consume less power than a larger one. A control approach that considers statistical and real time data of the genset load to dispatch the units could improve the fuel displacement. If the genset is expected to operate near its full load for a couple of hours in a certain day, the droop-based APC coefficients could also be readjusted as the temperature of the genset is expected to be high for a couple of

hours, and it would be able to get rid of the carbon build-up of that day. This would reduce the APC of the system and, consequently, increase the fuel displacement in the mini-grid due to the integration of PV.

6. REFERENCES

[1] T. Newcombe. (2009, Jan 10th). *Stimulus Bill Has Billions for Smart Grids*. Available: http://www.govtech.com/gt/620183

[2] H. Farhangi, "The Path of the Smart Grid," *IEEE Power and Energy Magazine,* vol. 8, no. 1, pp. 18-28, 2010.

[3] N. Hatziargyriou, H. Asano, R. Iravani, and C. Marnay, "Microgrids," *IEEE Power and Energy Magazine,* vol. 5, no. 4, pp. 78-94, 2007.

[4] K. Mauch, "Off-grid PV Systems - Technological Advancements," in *Intersolar USA*, San Francisco, 2009, pp. 1-19.

[5] K. Ah-You and G. Leng, "Renewable Energy in Canada's Remote Communities," Natural Resources Canada, Varennes, June 10th 1999.

[6] K. Mauch, G. Bopp, M. Vandenbergh, and J.-C. Marcel, "PV Hybrids in Mini-Grids - New IEA PVPS Task 11," in *17th Photovoltaic Solar Energy Conference*, Fukuoka, Japan, 2007, pp. 1-4.

[7] S. Cobben, B. Gaiddon, and H. Laukamp, "WP4 – Deliverable 4.3 - Impact of Photovoltaic Generation on Power Quality in Urban Areas with High PV Population," EIE/05/171/SI2.420208, 2008.

[8] R. Tonkoski and L. A. C. Lopes, "Voltage Regulation in Radial Distribution Feeders with High Penetration of Photovoltaic," in *IEEE Energy 2030 Conference*, Atlanta, 2008, pp. 1-7.

[9] Y. Ueda, K. Kurokawa, T. Tanabe, K. Kitamura, and H. Sugihara, "Analysis Results of Output Power Loss Due to the Grid Voltage Rise in Grid-Connected Photovoltaic Power Generation Systems," *IEEE Transactions on Industrial Electronics,* vol. 55, no. 7, pp. 2744-2751, 2008.

[10] Y. Ueda, T. Oozeki, K. Kurokawa, T. ltou, K. Kitamura, Y. Miyamoto, M. Yokota, H. Sugihara, and S. Nishikawa, "Analytical Results of Output Restriction Due to the Voltage Increasing of Power Distribution Line in Grid-Connected Clustered PV Systems," in *31st IEEE Photovoltaic Specialists Conference*, Lake Buena Vista, 2005, pp. 1631-1634.

[11] F. Katiraei, K. Mauch, and L. Dignard-Bailey, "Integration of Photovoltaic Power Systems in High-Penetration Clusters for Distribution Networks and Mini-Grids," *International Journal of Distributed Energy Resources,* vol. 3, no. 3, pp. 207-223, 2007.

[12] K. De Brabandere, A. Woyte, R. Belmans, and J. Nijs, "Prevention of Inverter Voltage Tripping in High Density PV Grids," in *19th European Photovoltaic Solar Energy Conference*, Paris, 2004, pp. 1-4.

[13] P. McNutt, J. Hambrick, M. Keesee, and D. Brown, "Impact of SolarSmart Subdivisions on SMUD's Distribution System," NREL/TP-550-46093; TRN: US200915%%252, 2009.

[14] J. M. Guerrero, J. Matas, V. Luis Garcia de, M. Castilla, and J. Miret, "Decentralized Control for Parallel Operation of Distributed Generation Inverters Using Resistive Output Impedance," *IEEE Transactions on Industrial Electronics,* vol. 54, no. 2, pp. 994-1004, 2007.

[15] J. Ayoub, L. Dignard-Bailey, and Y. Poissant, "Exchange and Dissemination of Information on PV Power Systems - National Survey Report Canada 2009," Varennes, 2010.

[16] Ontario Power Authority. (2011, Feb. 24th). *Bi-weekly microFIT Program reports*. Available: http://microfit.powerauthority.on.ca

[17] The Shpigler Group, "Gearing Up for Electric Vehicles: Tackling the EV Challenges to the Smart Grid - April 2011," Montebello, 2011.

[18] A. Woyte, V. Van Thong, R. Belmans, and J. Nijs, "Voltage fluctuations on distribution level introduced by photovoltaic systems," *IEEE Transactions on Energy Conversion,* vol. 21, no. 1, pp. 202-209, 2006.

[19] S. Papathanassiou, N. Hatziargyriou, and K. Strunz, "A Benchmark Low Voltage Microgrid Network.," in *Proceedings of the CIGRE Symposium: Power Systems with Dispersed Generation*, Athens, 2005, pp. 1-8.

[20] CSA, "C22.2 No. 257-06 Interconnecting Inverter-based Micro-distributed Resources to Distribution Systems," 2006.

[21] CSA, "CAN3-C235-83 Preferred Voltage Levels for AC Systems, 0 to 50 000 V," R2006.

[22] CSA, "C22.2 No. 107.1-01 General Use Power Supplies," 2001.

[23] Underwriters Laboratories Inc., "UL-1741 Inverters, Converters, Controllers and Interconnection System Equipment for Use with Distributed Energy Resources," 2005.

[24] A. Elmitwally and M. Rashed, "Flexible Operation Strategy for an Isolated PV-Diesel Microgrid Without Energy Storage," *IEEE Transactions on Energy Conversion,* vol. 26, no. 1, pp. 235-244, 2011.

[25] M. Thomson and D. G. Infield, "Impact of Widespread Photovoltaics Generation on Distribution Systems," *IET Renewable Power Generation,* vol. 1, no. 1, pp. 33-40, 2007.

[26] Y. Ueda, K. Kurokawa, T. Itou, K. Kitamura, K. Akanuma, M. Yokota, H. Sugihara, and A. Morimoto, "Advanced Analysis of Grid-Connected PV System's Performance and Effect of Batteries," *Electrical Engineering in Japan,* vol. 164, no. 1, pp. 247–258, 2008.

[27] R. Tonkoski, D. Turcotte, and T. El-Fouly, "Voltage Profile Variations in Residential Sub-urban Feeders with High PV Penetration," in *4th International*

Conference on Integration of Renewable and Distributed Energy Resources, Albuquerque, 2010, p. 1.

[28] R. Tonkoski, L. Lopes, and T. El-Fouly, "Coordinated Active Power Curtailment of Grid Connected PV Inverters for Overvoltage Prevention," *IEEE Transactions on Sustainable Energy,* vol. 2, no. 2, pp. 139-147, 2011.

[29] R. Tonkoski and L. Lopes, "Overvoltage Prevention in Residential Feeders with High Penetration of Photovoltaics," *IEEE Canadian Review,* no. 66, pp. 12-16, 2011.

[30] J. Runmin, M. H. Nehrir, and D. A. Pierre, "Voltage Control of Aggregate Electric Water Heater Load for Distribution System Peak Load Shaving Using Field Data," in *39th North American Power Symposium*, 2007, pp. 492-497.

[31] T. Ericson, "Direct Load Control of Residential Water Heaters," *Energy Policy,* vol. 37, no. 9, pp. 3502-3512, 2009.

[32] J. A. Duffie and W. A. Beckman, *Solar Engineering of Thermal Processes*, 3rd ed. Hoboken: Wiley, 2006.

[33] R. A. Shayani and M. A. G. de Oliveira, "Photovoltaic Generation Penetration Limits in Radial Distribution Systems," *IEEE Transactions on Power Systems,* vol. PP, no. 99, pp. 1-7, 2010.

[34] C. L. Masters, "Voltage Rise: The Big Issue When Connecting Embedded Generation to Long 11 kV Overhead Lines," *Power Engineering Journal,* vol. 16, no. 1, pp. 5-12, 2002.

[35] S. Toma, T. Senjyu, Y. Miyazato, A. Yona, T. Funabashi, A. Y. Saber, and K. Chul-Hwan, "Optimal Coordinated Voltage Control in Distribution System," in *IEEE Power and Energy Society General Meeting*, 2008, pp. 1-7.

[36] M. R. Salem, L. A. Talat, and H. M. Soliman, "Voltage Control by Tap-Changing Transformers for a Radial Distribution Network," *IEE Proceedings - Generation, Transmission and Distribution,* vol. 144, no. 6, pp. 517-520, 1997.

[37] D. N. Gaonkar, P. C. Rao, and R. N. Patel, "Hybrid Method for Voltage Regulation of Distribution System with Maximum Utilization of Connected Distributed Generation Source," in *2006 IEEE Power India Conference*, 2006, pp. 1-5.

[38] A. H. Rafa, O. Anaya-Lara, and J. R. McDonald, "Power Factor Control for Inverter-Interfaced Microgeneration," in *43rd International Universities Power Engineering Conference*, 2008, pp. 1-5.

[39] J. C. Vasquez, R. A. Mastromauro, J. M. Guerrero, and M. Liserre, "Voltage Support Provided by a Droop-Controlled Multifunctional Inverter," *IEEE Transactions on Industrial Electronics,* vol. 56, no. 11, pp. 4510-4519, 2009.

[40] M. H. J. Bollen and A. Sannino, "Voltage Control with Inverter-based Distributed Generation," *IEEE Transactions on Power Delivery,* vol. 20, no. 1, pp. 519-520, 2005.

[41] P. M. S. Carvalho, P. F. Correia, and L. A. F. Ferreira, "Distributed Reactive Power Generation Control for Voltage Rise Mitigation in Distribution Networks," *IEEE Transactions on Power Systems,* vol. 23, no. 2, pp. 766-772, 2008.

[42] P. Bousseau, E. Monnot, G. Malarange, and O. Gonbeau, "Distributed Generation Contribution to Voltage Control," in *19th International Conference on Electricity Distribution (CIRED 2007)*, Vienna, 2007, pp. 1-4.

[43] E. F. Mogos and X. Guillaud, "A Voltage Regulation System for Distributed Generation," in *IEEE PES Power Systems Conference and Exposition*, 2004, pp. 787-794.

[44] W. Paul, R. S. Kirk, J. Michael, and H. Andrew, "A Global Perspective on Energy: health effects and injustices," *The Lancet,* vol. 370, no. 9591, pp. 965-978, 2007.

[45] F. Katiraei, R. Iravani, N. Hatziargyriou, and A. Dimeas, "Microgrids Management," *IEEE Power and Energy Magazine,* vol. 6, no. 3, pp. 54-65, 2008.

[46] J. A. P. Lopes, C. L. Moreira, and A. G. Madureira, "Defining Control Strategies for MicroGrids Islanded Operation," *IEEE Transactions on Power Systems,* vol. 21, no. 2, pp. 916-924, 2006.

[47] J. B. Malosh, R. Johnson, and S. Bubendorf, "Part-Load Economy of Diesel-Electric Generators," State of Alaska - Department of Transportation and Public Facilities, Fairbanks, 1985.

[48] R. Hunter and G. Elliot, *Wind-Diesel Systems*, 2005.

[49] F. Katiraei, "IEC PVPS Task 11 Subtask 20 Report - Control Strategies in PV Hybrid Mini-Grids - Chapter 5 - Multi-Master Diesel Dominated Control", Unpublished Work.

[50] "ISO 8528-5:2005, Reciprocating internal combustion engine driven alternating current generating sets - Part 5: Generating sets," no., 2005.

[51] Simson-Maxwell. (2009, Nov. 3rd). *Power Generation and Industrial Engines*. Available: http://simson-maxwell.com/website/products_generatorspecs.aspx

[52] L. L. J. Mahon, *Diesel Generator Handbook*. Oxford ; Boston: Butterworth-Heinemann, 1992.

[53] B. Lasseter, "Microgrids [distributed power generation]," in *IEEE Power Engineering Society Winter Meeting*, 2001, pp. 146-149.

[54] D. Turcotte, "Xeni Gwet'in PV/Diesel Minigrid System Documentation," Natural Resources Canada, Varennes, Report, June 2009.

[55] W. A. Omran, M. Kazerani, and M. M. A. Salama, "Investigation of Methods for Reduction of Power Fluctuations Generated From Large Grid-Connected Photovoltaic Systems," *IEEE Transactions on Energy Conversion, ,* vol. 26, no. 1, pp. 318-327, 2011.

[56] R. Tonkoski, L. A. C. Lopes, and D. Turcotte, "Active Power Curtailment of PV Inverters in Diesel Hybrid Mini-grids," in *Electrical Power and Energy Conference (EPEC 2009)*, Montreal, 2009, pp. 1-6.

[57] M. Vandenbergh, R. Geipel, M. Landau, P. Strauss, and S. Tselepis, "Performance Evaluation of the Gaidoroumandra Mini-grid with Distributed PV Generators," in *4th European PV-Hybrid and Mini-Grid Conference*, Athens, 2008, pp. 1-8.

[58] R. Tonkoski, L. A. C. Lopes, and T. H. M. El-Fouly, "Droop-based Active Power Curtailment for Overvoltage Prevention in Grid Connected PV Inverters," in *IEEE International Symposium on Industrial Electronics*, 2010, pp. 2388-2393.

[59] S. Conti, A. Greco, N. Messina, and S. Raiti, "Local Voltage Regulation in LV Distribution Networks with PV Distributed Generation," in *International Symposium on Power Electronics, Electrical Drives, Automation and Motion* 2006, pp. 519-524.

[60] E. Troester, "New German Grid Codes for Connecting PV Systems to the Medium Voltage Power Grid," in *2nd International Workshop on Concentrating Photovoltaic Power Plants: Optical Design and Grid Connection*, Darmstadt, 2009, pp. 1-4.

[61] A. Notholt, "Germany's New Code for Generation Plants connected to Medium-Voltage Networks and its Repercussion on Inverter Control " in *International Conference on Renewable Energies and Power Quality (ICREPQ'09)* Valencia, 2009, pp. 1-5.

[62] J. C. Van Tonder and I. E. Lane, "A Load Model to Support Demand Management Decisions on Domestic Storage Water Heater Control Strategy," *IEEE Transactions on Power Systems,* vol. 11, no. 4, pp. 1844-1849, 1996.

[63] L. Paull, H. Li, and L. Chang, "A Novel Domestic Electric Water Heater Model for a Multi-objective Demand Side Management Program," *Electric Power Systems Research,* vol. 80, no. 12, pp. 1446-1451, 2010.

[64] K. Elamari, L. A. C. Lopes, and R. Tonkoski, "Using Electric Water Heaters (EWHs) for Power Balancing and Frequency Control in PV-Diesel Hybrid Mini-Grids," in *World Renewable Energy Congress 2011* Linköping, 2011.

[65] J. P. Barton and D. G. Infield, "Energy Storage and its Use with Intermittent Renewable Energy," *IEEE Transactions on Energy Conversion,* vol. 19, no. 2, pp. 441-448, 2004.

[66] M. Black and G. Strbac, "Value of Bulk Energy Storage for Managing Wind Power Fluctuations," *IEEE Transactions on Energy Conversion,* vol. 22, no. 1, pp. 197-205, 2007.

[67] C. Abbey and G. Joos, "Supercapacitor Energy Storage for Wind Energy Applications," *IEEE Transactions on Industry Applications,* vol. 43, no. 3, pp. 769-776, 2007.

[68] C. Abbey and G. Joos, "Coordination of Distributed Storage with Wind Energy in a Rural Distribution System," in *IEEE Industry Applications Conference*, 2007, pp. 1087-1092.

[69] A. Kusko and J. Dedad, "Stored energy - Short-term and long-term energy storage methods," *IEEE Industry Applications Magazine,* vol. 13, no. 4, pp. 66-72, 2007.

[70] E. Demirok, D. Sera, R. Teodorescu, P. Rodriguez, and U. Borup, "Evaluation of the voltage support strategies for the low voltage grid connected PV generators," in *Energy Conversion Congress and Exposition (ECCE), 2010 IEEE*, 2010, pp. 710-717.

[71] R. Tonkoski and L. A. C. Lopes, "Impact of active power curtailment on overvoltage prevention and energy production of PV inverters connected to low voltage residential feeders," *Renewable Energy,* vol. 36, no. 12, 2011.

[72] A. Engler, "Applicability of Droops in Low Voltage Grids," *International Journal of Distributed Energy Resources,* vol. 1, no. 1, March 2005.

[73] W. Kaplan, *Advanced Calculus*, 5th ed. Boston: Addison-Wesley, 2003.

[74] S. Vazquez, S. M. Lukic, E. Galvan, L. G. Franquelo, and J. M. Carrasco, "Energy Storage Systems for Transport and Grid Applications," *IEEE Transactions on Industrial Electronics,* vol. 57, no. 12, pp. 3881-3895, 2010.

[75] R. Tonkoski, D. Turcotte, and T. H. M. EL-Fouly, "Impact of High PV Penetration on Voltage Profiles in Residential Neighbourhoods", Unpublished Work.

[76] J. Candanedo and A. Athienitis, "A Systematic Approach for Energy Design of Advanced Solar Houses," in *Electrical Power and Energy Conference 2009 - EPEC 09*, Montreal, 2009, pp. 1-6.

[77] J. A. Candanedo and A. K. Athienitis, "Investigation of Anticipatory Control Strategies in a Net-Zero Energy Solar House," *ASHRAE Transactions,* vol. 116, no. 1, pp. 246-259, 2010.

[78] P. W. Stackhouse Jr. (2010, Dec. 14th). *Surface Meteorology and Solar Energy*. Available: http://eosweb.larc.nasa.gov/sse/

[79] H. Markiewicz and A. Klajn, *Voltage Disturbances: Standard EN 50160 - Voltage Characteristics in Public Distribution Systems*, 2004.

[80] R. Tonkoski and L. A. C. Lopes, "Enhanced Part Load Operation of Diesel Hybrid Mini-Grids with High Penetration of Photovoltaics," in *III Congresso Brasileiro de Energia Solar* Belém, 2010, pp. 1-8.

[81] NorthWestern Energy. (2010, May 20th). *Residential Customer Profile*. Available: http://www.mtenergychoice.com/